PB93108686

CATALYTIC REACTIONS OF SYNTHESIS GAS. PART 1. METHANATION AND CO HYDROGENATION

HELSINKI UNIV. OF TECHNOLOGY, ESPOO (FINLAND). DEPT. OF CHEMICAL ENGINEERING

01 JUN 1992

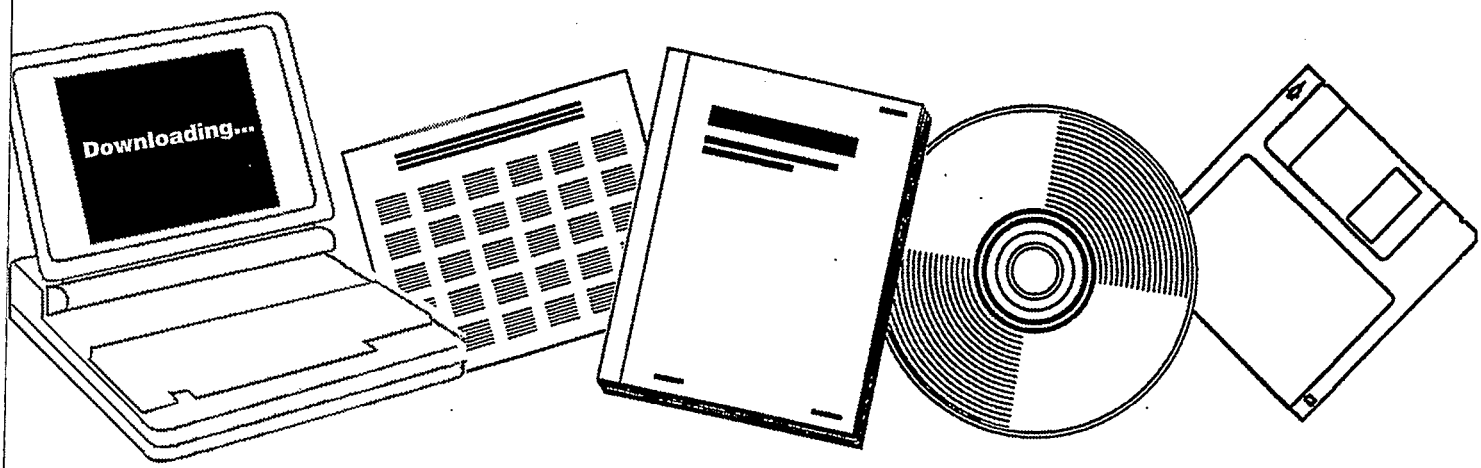

One Source. One Search. One Solution.

NTIS

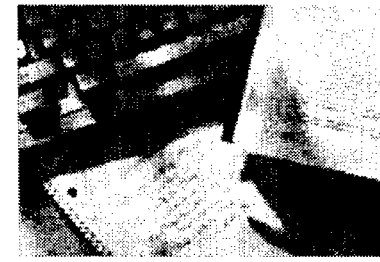

Providing Permanent, Easy Access to U.S. Government Information

National Technical Information Service is the nation's largest repository and disseminator of government-initiated scientific, technical, engineering, and related business information. The NTIS collection includes almost 3,000,000 information products in a variety of formats: electronic download, online access, CD-ROM, magnetic tape, diskette, multimedia, microfiche and paper.

Search the NTIS Database from 1990 forward

NTIS has upgraded its bibliographic database system and has made all entries since 1990 searchable on **www.ntis.gov.** You now have access to information on more than 600,000 government research information products from this web site.

Link to Full Text Documents at Government Web Sites

Because many Government agencies have their most recent reports available on their own web site, we have added links directly to these reports. When available, you will see a link on the right side of the bibliographic screen.

Download Publications (1997 - Present)

NTIS can now provides the full text of reports as downloadable PDF files. This means that when an agency stops maintaining a report on the web, NTIS will offer a downloadable version. There is a nominal fee for each download for most publications.

For more information visit our website:

www.ntis.gov

U.S. DEPARTMENT OF COMMERCE
Technology Administration
National Technical Information Service
Springfield, VA 22161

HELSINKI UNIVERSITY OF TECHNOLOGY
FACULTY OF PROCESS ENGINEERING AND MATERIALS SCIENCE
Department of Chemical Engineering
Marita Niemelä
1.6.1992

CATALYTIC REACTIONS OF SYNTHESIS GAS
PART I: METHANATION AND CO HYDROGENATION

CATALYTIC REACTIONS OF SYNTHESIS GAS

PART I. METHANATION AND CO HYDROGENATION

ABSTRACT

The exothermic, but slow reaction of CO with H_2 is catalyzed by metals of Group VIII, by molybdenum (Group IV) and by silver (Group I). In the present work rhodium and cobalt catalysts are reviewed. Rhodium catalysts provide excellent model systems for studying reactions of synthesis gas. The CO hydrogenation activity of supported rhodium decreases in the order TiO_2 > Al_2O_3 > La_2O_3 and other REO supports > SiO_2 > MgO. Depending on the oxide support, promotors and reaction conditions used the products over supported rhodium may be primarily hydrocarbons or alcohols. Rhodium on acidic oxides, such as SiO_2 or Al_2O_3 produce mainly non-oxygen containing hydrocarbons, whilst on TiO_2, ZrO_2 or La_2O_3 methanol is produced together with ethanol. On the basic oxides, such as ZnO, MgO and CaO, CO is converted mainly to methanol. Additions of promotors, such as alkali, alkali earth, or other metals or metal oxides to the rhodium catalysts have significant effects both on catalyst surface structure and on catalyst activity and selectivity. The role of rhodium catalyst promotors is either to increase catalyst stability or selectivity to oxygenated compounds, particularly C_2-oxygenates.

However, the high cost of rhodium catalysts mitigates against their use. Even a partial replacement of rhodium by cheaper metals, such as cobalt, would be a major economic benefit. Cobalt catalysts are promising candidates for production of fuels and chemicals via CO hydrogenation due to cobalt being one of the most active metals in synthesis gas conversion. The order of decreasing hydrogenation activity of supported cobalt is TiO_2 > SiO_2 > Al_2O_3 > C > MgO. The product selectivity is best correlated with dispersion and extent of reduction, i.e. the molecular weight of hydrocarbon products is lower and the CO_2:H_2O ratio is higher for catalysts having higher dispersions and lower extents of reduction. In the presence of promotors, such as alkali, alkali earth and other metals or metal oxides, cobalt catalysts produce also significant amounts of olefins or oxygenated compounds. The main aim of bifunctional catalysts, namely cobalt supported on or mixed with zeolites, has been to increase the selectivity of the liquid products, especially gasoline.

CONTENTS PAGE

CATALYTIC REACTIONS OF SYNTHESIS GAS
PART I: METHANATION AND CO HYDROGENATION

1. REACTIONS AND THERMODYNAMICS

Methanation refers to hydrogenation of carbon oxides, preferably carbon monoxide, to methane. The importance of research on methanation has increased as the need for high calorific value fuel and the use of methane in chemical syntheses has increased. Concern on methanation has been also due to removal of concentrations of undesirable carbon monoxide in hydrogen-rich gases by methanation (e.g. ammonia production), and undesirable methane formation in the hydrogenation of carbon monoxide to alcohols or hydrocarbons /1/

The methanation reactions are the reverse of those for methane steam reforming, and they are strongly exothermic /2,3/. The methane formation by the conversion of carbon monoxide and hydrogen can be described by the following reaction /4/:

$$CO + 3\ H_2 \longleftrightarrow CH_4 + H_2O \qquad (1)$$

Methane is also formed by hydrogenation of carbon oxides in two other reactions /4/:

$$2CO + 2H_2 \longleftrightarrow CH_4 + CO_2 \qquad (2)$$

$$CO_2 + 4H_2 \longleftrightarrow CH_4 + 2\ H_2O \qquad (3)$$

Reaction (3), the hydrogenation of carbon dioxide, does not occur in the presence of carbon monoxide. Also reaction (2) can be considered to be a combination of reaction (1) and the water gas shift reaction. Although the water gas shift reaction does not produce methane, it is an important reaction in methanation chemistry, altering the H_2:CO ratio with far-reaching effects on reaction products /4/:

$$CO + H_2O \longleftrightarrow CO_2 + H_2 \qquad (4)$$

The free energy values of methanation reactions are negative over a wide temperature range. However, the reactions are relatively slow and catalysts are needed to accelerate them to acceptable commercial rates. In this connection a further reaction is important, since it can lead to a deposition of carbon on the catalyst with eventual resultant fouling of the catalyst /4/:

$$2\ CO \longrightarrow C + CO_2 \qquad (5)$$

At temperatures used in coal gasification (900 °C), methane formation by hydrogenation of carbon occurs /4/:

$$2H_2 + C \longrightarrow CH_4 \qquad (6)$$

However, this and related reactions, such as the steam-carbon reaction, do not occur significantly in commercial catalytic processes, which operate at temperatures of above 280 °C and pressures of 20 - 25 bar /4, 2/.

Thermodynamic values for Reactions (1) - (5) are given in Table 1 /4/. The listed values indicate, that all reactions are exothermic and, indeed, all except reaction (4) are highly exothermic. This heat release makes it difficult to prevent overheating and inactivation of the catalyst. In addition, the heats of reaction are not greatly influenced by temperature, whilst the free energy and equilibrium constants are quite dependent on it.

The composition of methanated gases depends on the number of methanation stages, methanation conditions, i.e. temperature and pressure, and the feed gas composition. Methane yields increase with increasing number of methanation stages, increasing pressure, decreasing temperature and decreasing H_2:CO ratio. The lowest limiting boundary ratio of H_2:CO is determined by the prevention of carbon deposition on catalyst /1, 4/. Usually a slight excess of hydrogen is used in the methanation of CO, i.e. the H_2:CO ratio is > 3 /5/.

Table 1. Thermodynamic values for Reactions (1) - (5) /4/.

Temperature		Reaction				
°K	°C	1	2	3	4	5
Heat of Reaction, $\Delta H_f°$, kcal						
300	27	−49.298	−59.136	−39.460	−9.838	−41.227
400	127	−50.360	−60.070	−40.650	−9.710	−41.434
500	227	−51.297	−60.815	−41.779	−9.518	−41.499
600	317	−52.084	−61.376	−42.792	−9.292	−41.460
700	427	−52.730	−61.780	−43.680	−9.050	−41.350
800	527	−53.248	−62.047	−44.449	−8.799	−41.190
900	627	−53.654	−62.203	−45.105	−8.549	−40.996
1000	727	−53.957	−62.261	−45.653	−8.304	−40.729
Free Energy of Reaction, $\Delta F°$, kcal						
300	27	−33.904	−40.731	−27.077	−6.827	−28.621
400	127	−28.610	−34.451	−22.769	−5.841	−24.385
500	227	−23.062	−27.956	−18.168	−4.894	−20.111
600	327	−17.338	−21.329	−13.347	−3.991	−15.836
700	427	−11.493	−14.620	−8.366	−3.127	−11.574
800	527	−5.567	−7.865	−3.269	−2.298	−7.332
900	627	+0.594	−1.079	+1.921	−1.500	−3.108
1000	727	+6.444	+5.715	+7.173	−0.729	+1.090
Equilibrium Constant, Log K_p						
300	27	24.698	29.670	19.724	4.973	20.849
400	127	15.630	18.822	12.44	3.191	13.322
500	227	10.080	12.219	7.940	2.139	8.790
600	327	6.314	7.768	4.861	1.453	5.768
700	427	3.588	4.564	2.611	0.976	3.613
800	527	1.521	2.148	0.893	0.628	2.003
900	627	−0.144	0.261	−0.466	0.364	0.755
1000	727	−1.408	−1.248	−1.568	0.159	−0.238

In addition to methane the direct conversion of synthesis gas offers many routes to industrial chemicals. The direct conversion deals with the straight hydrogenation of carbon monoxide to paraffins, olefins and heteroatom containing products as shown in Table 2. CO hydrogenation is best known as the Fischer-Tropsch synthesis involving a stepwise hydrocarbon chain growth. The particular carbon number distribution of the products is determined by the probability of chaingrowth, α, according to Schultz-Flory distribution shown in Figure 1. Three considerations influence the economics and process feasibility, namely the ratio of $CO:H_2$, the loss of oxygen as a byproduct water or CO_2, and the interrelation of chemicals/fuels. The product distribution has been tailored by various catalyst modifications /6/.

Table 2. CO and H_2 usage /6/.

			ratio $CO:H_2$	reactant loss (%) as H_2O
Direct conversion				
$CO + 2\ H_2$	$\longrightarrow$	methanol	1:2	-
$2\ CO + 2\ H_2$	$\longrightarrow$	acetic acid	1:1	-
$2\ CO + 2\ H_2$	$\longrightarrow$	methyl formate	1:1	-
$2\ CO + 4\ H_2$	$\longrightarrow$	ethanol	1:2	28
$3\ CO + 6\ H_2$	$\longrightarrow$	propanol	1:2	38
$2\ CO + 3\ H_2$	$\longrightarrow$	ethylene glycol	2:3	-
$4\ CO + 8\ H_2$	$\longrightarrow$	isobutanol	1:2	50
$2\ CO + 4\ H_2$	$\longrightarrow$	ethylene	1:2	56
$8\ CO + 34\ H_2$	$\longrightarrow$	n-octane	1:2.1	57
Indirect conversion				
$CH_3OH + CO$	$\longrightarrow$	acetic acid	-	-
$CH_3COOCH_3 + CO$	$\longrightarrow$	acetic anhydride	-	-
$2\ CH_3OH$	$\longrightarrow$	ethylene	-	56

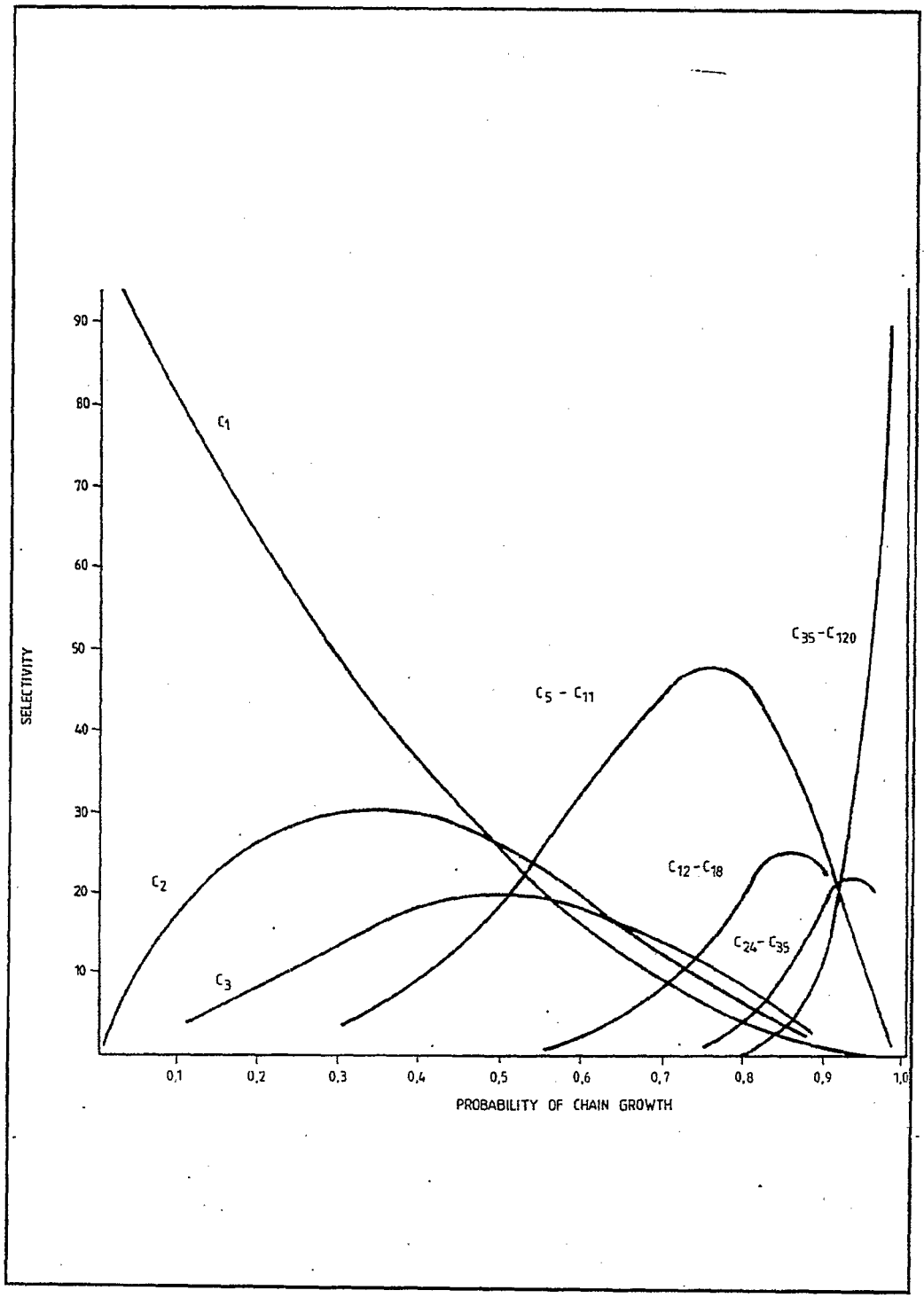

Figure 1. Product selectivity of CO hydrogenation as a variable of the probability of chain growth /6/.

2. CATALYSTS

The exothermic, but slow reaction of CO with H_2 is catalyzed by metals of Group VIII, by molybdenum (Group IV) and by silver (Group I). The specific activities of Group VIII metals were determined by Vannice /7/ at 1 bar pressure. The observed order of decreasing activity was ruthenium > iron > nickel > cobalt > rhodium > palladium > platinum and iridium. However, some of these supported metals (Ru, Fe, Co, Ni) had large average crystallite sizes and others (Rh, Pt, Ir, Pd) were more highly dispersed. In the present work rhodium and cobalt catalysts are reviewed. Rhodium catalysts provide excellent model systems for studying reactions of synthesis gas. Depending on the oxide support, promoters and reaction conditions used the products over rhodium may be primarily hydrocarbons or alcohols /8/. Nevertheless, the high cost of rhodium catalysts mitigates against their use. Even a partial replacement of rhodium by cheaper metals, such as cobalt, would be a major economic benefit. Cobalt catalysts are promising candidates for production of fuels and chemicals via CO hydrogenation due to cobalt being one of the most active metals in synthesis gas conversion. In terms of commercial applications, however, the methanation catalysts are mainly in the form of nickel metal dispersed on a support consisting of various oxide mixtures /3/.

In practice, a good methanation catalyst is one which is physically strong, reducible at 300 °C and has high activity /1/. Consequently, the form of the methanation catalyst is invariably a result of a compromise between physical properties and effective activity /3/. The desired combination can be achieved by careful attention to the formulation and manufacture of the catalyst. To provide a long life, the properties obtained must be retained in use. Lives of 8 - 10 years are commonly obtained from charges of ICI catalysts, depending on the temperature of operation and on the poisons in the synthesis gas /3/.

Commercial methanation catalysts contain between 15 % and 35 % metal oxide and are made either by precipitation, or by impregnation of a metal solution onto a preformed support. There is generally no correlation between metal content and catalyst activity if catalysts are prepared in different ways. Moreover, under normal operation conditions the activity of a methanation catalyst may be to some extent

dependent on total geometric surface area of the catalyst particle, i.e. smaller particles can display higher apparent activity. However, if particle size is too small the pressure drop across the bed is too high and the process power requirement excessive. In practice, catalyst particles such as pellets with a diameter of about 5 mm are suitable, although in special situations smaller particles may be used /3/.

Methanation catalysts are usually manufactured and transported in oxidized form. Therefore reduction is necessary to make them active. The reduction is usually carried out in process gas and it occurs by the following two reactions:

$$MeO + H_2 \text{--->} Me + H_2O \qquad (7)$$

$$MeO + CO \text{--->} Me + CO_2 \qquad (8)$$

The gas used for reduction should contain as little carbon monoxide and carbon dioxide as possible, and preferably not more than 1 % in total to avoid excessive temperature rise in the catalyst bed. Progress of the reduction can be monitored by following the rapid fall in the exit carbon monoxide and dioxide to the design level which is normally less than 5 ppm $CO + CO_2$.

All active methanation catalysts are poisoned by sulphur /1/. The action of sulphur is undoubtedly through the reaction of hydrogen sulphide with metal according to:

$$Me + H_2S \text{<--->} MeS + H_2 \qquad (9)$$

Hydrogen sulphide is either present in the feed gas or formed by hydrogen reduction of any sulphur bearing compound over the catalyst. The thermodynamic data suggest that, under conditions typical of those expected in commercial operation, as much as about 4 ppm H_2S could be tolerated in the feed. However, sulphide poisoning has been observed even at levels as low as 0,3 ppm H_2S. Hence sulphide poisoning likely occurs in active centers.

If all materials which adversely affect the performance of catalyst were classified as poisons, the carbon laydown, and under extreme conditions, water vapour would be

included as methanation catalyst poisons /1/. Steam is a potential poison of methanation catalysts under extremely high steam concentrations and low hydrogen concentrations:

$$Me(active) + H_2O \longleftrightarrow MeO + H_2 \qquad (10)$$

2.1 Supported rhodium catalysts

Rhodium catalysts of various formulations have been explored for use in both heterogeneous and homogeneous carbon monoxide hydrogenation processes. The selectivity of heterogeneous rhodium catalysts has been verified to depend on the nature of the support, rhodium deposition method, pretreatment method and added promoters. Rhodium foil and alumina-supported rhodium have been reported to produce no oxygen containing hydrocarbon products, in contrast with results obtained for rhodium on silica producing acetaldehyde and acetic acid, and for rhodium on MgO or ZnO with high yields of ethanol and methanol /9/. Hence, the nature of the reaction products obtained with rhodium has been quite sensitive to the environment of the catalyst, making an understanding of its structure and its adsorptive properties imperative in understanding the behaviour of the catalyst in these reactions.

The interaction of CO with supported Rh catalysts has been a subject of quite a few infrared studies. The chemisorption of CO on Rh has been found to exert a dramatic influence on the state of Rh dispersed on a support. Van't Blik et al /10/ studied the structure of rhodium by extended X-ray absorption fine structure spectroscopy (EXAFS). They found that CO adsorption at 25 °C caused significant disruption of the Rh crystallites, leading to isolated Rh^{1+} sites and formation of the species I, commonly referred to as the gem-dicarbonyl, $Rh(CO)_2$. This observation was confirmed by the IR studies of Solymosi and Pasztor /11/. These gem-dicarbonyl species have been the only CO species observed for catalysts of a very low rhodium loading (e.g. 0,5 %) /12/ and/or a highly dispersed state /13/. The properties of these gem-dicarbonyl species have been found to be significantly influenced by the support, i.e. the IR stretching parameter, k(CO), was found to increase in the order NaX < Al_2O_3 < NaY < TiO_2 indicating a decreasing back-bonding ability of the

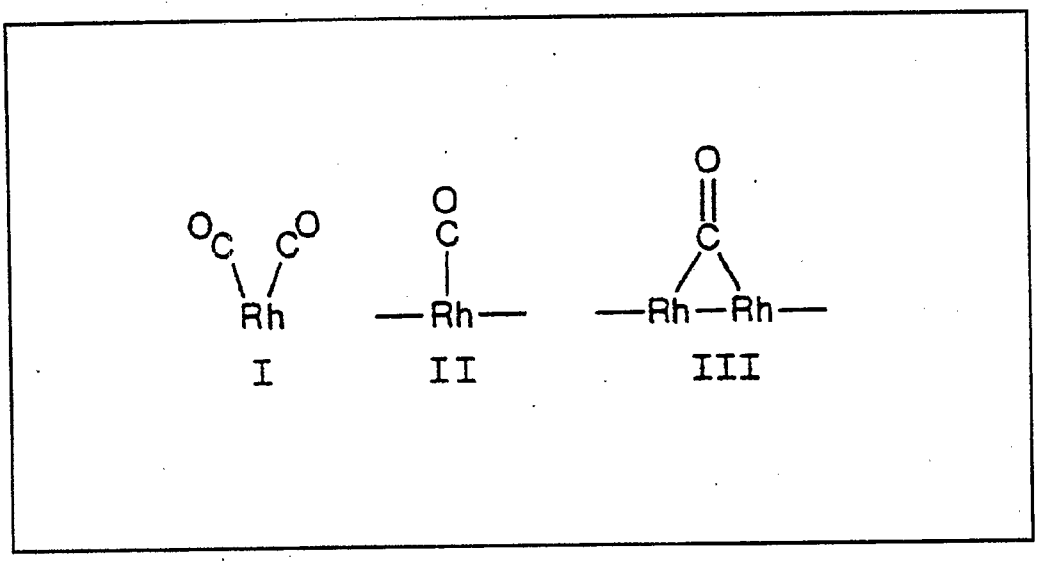

Figure 2. CO surface species on supported rhodium catalysts /12/.

supported rhodium in the same order. The increase of the stretching parameter was accompanied by a weaker Rh-C bond and, therefore by a desorption of CO from the dicarbonyl species at lower temperatures /14/. Catalysts of higher rhodium loading (> 1 %) have adsorbed molecular CO by forming species II, the linear CO species, and species III, the bridged carbonyl species (see Figure 2), both of which contain clusters of Rh atoms in the zero oxidation stage /12,13/. The appearance of linear and bridged CO species has been enhanced also by an increase in temperature /11/; above 150 °C the adsorption of CO led to the formation of Rh crystallites compared with the production of isolated sites at 27 °C. The practical significance of the relative presence of these three species is evident: it refers to the degree of dispersion, and to the proportion of ionic Rh and metallic Rh present on the catalyst surface.

In addition to molecular adsorption of CO, dissociative adsorption has been found to occur on supported Rh to a small extent above 200 °C. The dissociation was influenced by the support; it was the largest on Rh/TiO_2, followed by Rh/Al_2O_3, Rh/SiO_2 and Rh/MgO. However, the extent of dissociation increased considerably with increasing temperature /15,16/. At the temperature of dissociation (200 ... 301 °C) only the linearly bonded and bridged CO were present on the surface; the

gem-dicarbonyl species desorbed before this temperature. Considering the stability of these species, it was proposed that dissociation of CO mainly occurred in the bridged form /17/. Yin-Sheng and Xiao-Le /18/ stated that before dissociation CO must have been tilted from the upright bridged adsorption state to the horizontal state, which is the transition state for CO dissociation. The calculated energies of these transition states indicated that the dissociation activity of the supported rhodium decreased in the order TiO_2 > Al_2O_3 > SiO_2 consistent with the experimental results. Moreover, Solymosi et al /17/ found that at 275 °C the CO dissociation was clearly promoted by H_2, which was envisaged to occur through the formation of the Rh-carbonyl-hydride H-Rh-CO species. Some of the surface carbon formed was hydrogenable already at room temperature or at 100 °C. In spite of the high reactivity of the surface carbon formed in dissociation, substantial amounts of it accumulated on the catalyst blocking the active sites and resulting in less reactive aged form of carbon. Consistently, Efstathiou and Bennett /19,20/ also observed the presence of two forms of carbon on Rh/Al_2O_3 during the CO/H_2 reaction at temperatures in the range 180 ... 260 °C. The reactivity of the very small amount of highly active carbon, C_α, rose sharply with temperature. The inactive carbon, C_β, accumulated on the metal at relatively long times on stream and high temperatures. However, Mochida et al /21/ found that the surface carbon formed at 250 °C did not exhibit any reactivity with H_2 at 200 °C whereas at 250 °C it reacted readily on Rh/TiO_2, and required more than 1 h for complete conversion on Rh/Al_2O_3. On Rh/SiO_2 the surface carbon production was so low, that its reactivity could not be measured. Nevertheless, the fastest conversion rate obtained was much lower than the conversion rate of irreversibly adsorbed CO at 200 °C and that of the catalytic reaction at 250 °C.

2.1.1 Rhodium on alumina

The selectivity of the Rh catalyst is closely related to the metal oxides used for its support. Furthermore, Rh catalysts are very sensitive to the addition of various promoters, which improve the activity, selectivity or the stability of the catalyst. The key to tailor-made rhodium catalysts lies in the fundamental understanding of the adsorptive and reactive properties of the Rh catalyst systems and how these properties

are altered with changes in preparation, and concentration of promotor species.

The general CO adsorption characteristics of supported Rh catalysts were briefly described previously in section 2.1.1. Duprez et al /22/ studied the effect of partial reduction on the carbon monoxide chemisorption on 2 w-% and 4 w-% Rh/Al_2O_3. They observed, that in the presence of an unreduced phase of rhodium the gem-di/linear carbonyl ratio increased, i.e partially reduced catalysts behaved as if they were both totally reduced and better dispersed. Worley et al /23/ studied the effect of precursor on 2,2 w-% Rh supported on Al_2O_3. They found that $RhCl_3$ as a precursor gave more gem-dicarbonyl adsorption than $Rh(NO_3)_3$ or $Rh_6(CO)_{16}$. They concluded, that $Rh(NO_3)_3$ and $Rh_6(CO)_{16}$ were more easily reduced than $RhCl_3$. Moreover, $Rh(OCOCH_3)_2$ and $Rh_2(SO_4)_3$ were reported to poison the catalyst surface for CO adsorption. Vis et al /24/, however, claimed based on their own results that the systems of Worley et al /23/ must have been fully reduced. Hence they suggested that the reason for the observed higher gem-dicarbonyl adsorption in the case of $RhCl_3$ was in fact the better dispersion as a result of disruption of Rh particles upon CO adsorption.

The addition of alkali metal promoters on Rh supported on alumina has been found to significantly alter the catalyst. Dai and Worley /12/ and Solymosi et al /25/ examined the influence of potassium additive on 2,2 w-% $Rh\text{-}K/Al_2O_3$ with K:Rh ratio of 2,5 and 1-1 w-% $Rh\text{-}K_2O/Al_2O_3$ respectively. Dai and Worley /12/ observed that the presence of potassium decreased the temperature of disappearance of gem-dicarbonyl and linear CO species, and enhanced the bridged carbonyl species on supported rhodium. They concluded, that potassium (i) enhanced CO dissociation through an electronic effect, (ii) sterically blocked active methanation sites and caused formation of an increased amount of bridged carbonyl species, and (iii) formed cluster complexes with CO or exhibited either short or long range interactions with CO on transition metals. However, a portion of potassium might have been located on the support rather than on the Rh atoms or ions. Also Solymosi et al /25/ found the potassium additive, very likely by an electronic effect, to promote the CO-induced reductive agglomeration of isolated Rh^{1+} sites, i.e. the reformation of Rh_x clusters. Blackmond et al /26/ studied the effects of Cs promotion on reduced 3 w-% Rh/Al_2O_3 catalysts by IR at ambient temperature. Their results indicated that a

significant fraction of the added Cs interacted directly with the support rather than with the Rh crystallites. Upon increasing Cs addition the amount of gem-dicarbonyl species and bridged CO species decreased. Hence, the primary effect of increasing Cs promotion on coimpregnated Rh/Al_2O_3 was either to perturb adsorption on the isolated Rh atoms interacting with the support, or to prevent the redispersion of Rh crystallites as $Rh(CO)_2$ clusters upon CO adsorption. In addition, alkali appeared to break up ensembles for bridged CO adsorption on larger crystallites.

The promoting effect of CeO_2 has been relevant particularly for the performance of automobile catalytic converters. The adsorbed states of carbon monoxide on a 0,5-10 w-% $Rh\text{-}Ce/Al_2O_3$ catalyst were investigated by IR by Dictor and Roberts /27/. They emphasized, that the qualitative behaviours of ceria-promoted Rh/Al_2O_3 was very similar to that of the unpromoted catalyst; the notable exception was that the promoted catalyst maintained a high dispersion during CO-induced sintering at 200 °C. The sintered Rh particles of the non-ceria catalyst were 3-dimensional and much bigger than the flat small Rh particles of the promoted catalyst. Hence ceria promoted Rh dispersion by covering the alumina and interacting with Rh, or simply provided a physical barrier between Rh deposits on the alumina surface.

In recent years also bimetallic catalysts have received considerable attention. Such systems can contain metals from early and late transition metals. DeCanio and Storm /28/ studied the amounts of CO chemisorbed by reduced samples of 1-X w-% $Rh\text{-}Mo/Al_2O_3$ with X = 3, 6 and 12. Supporting rhodium on 3 w-% Mo/Al_2O_3 or 6 w-% Mo/Al_2O_3 reduced the chemisorption capacity of rhodium by a factor of 4 or 8, respectively. In case of 12 w-% Mo/Al_2O_3 as a support, the chemisorption decreased a small amount more. Paralleling these chemisorption results, the IR intensities of the linear and bridged carbonyls were reduced in 1-3 w-% $Rh\text{-}Mo/Al_2O_3$ compared to 1 w-% Rh/Al_2O_3. The intensities of gem-dicarbonyl were not reduced, however. When 6 w-% Mo/Al_2O_3 was the support, there was an additional decrease in intensities, and the intensity ratio of the gem-dicarbonyl to linear carbonyl increased. Increasing the Mo loading to 12 w-% caused only a small further decease in IR intensity. Foley et al /29/ studied reduced 3-2,8 w-% $Rh\text{-}Mo/Al_2O_3$, which had a dispersion of at least 70 % based on hydrogen chemisorption. The XPS data indicated that the rhodium was not fully reduced. Molybdenum was apparently in fully oxidized form, which

may interact with highly dispersed rhodium. The TEM and STEM-EDS results showed, that two particle sizes were present: large rhodium rich (Rh:Mo < 1,6) particles of 1,0 ... 1,5 nm in diameter and molybdenum enriched (Rh:Mo<0,9) particles of apr. 0,5 nm in diameter. Kip et al /30/ studied V_2O_3 promoted 1,5 w-% Rh/Al_2O_3 catalysts with V:Rh ratio of 7. The IR spectra at 25 °C indicated, that the bridged and linear CO species were suppressed by the presence of vanadium oxide, whilst the gem-dicarbonyl species were favoured. A minor extra peak was attributed to CO bonded to Rh(III) in vanadium promoted system. Hence the presence of either molybdenum or vanadium favoured the CO adsorption in gem-dicarbonyl form, which is associated with high dispersion. Kraus et al /31/ studied the influence of oxide modifiers ZrO_x, TiO_x and NbO_x with final promotor P to metal Rh atomic ratio P:Rh of 3:1 and 1:1 on the state of rhodium supported on alumina by CO adsorption and IR spectroscopy. The IR spectra obtained with promoted catalysts with P:Rh of 1:1 were qualitatively very similar to those of unmodified Rh/Al_2O_3. However, NbO_x seemed to have a detectable effect with Nb:Rh of 1:1 and a more pronounced effect with Nb:Rh of 3:1 probably due to geometrical blocking of the metal particles for CO adsorption. This presumably consisted of an encapsulation of Rh_x^0 particles by a niobium suboxide NbO_x and of the protection of Rh^{x+} ions anchored onto the Al_2O_3 support surface by a spread layer of NbO_x.

Hydrogen chemisorption has been used through the years by many workers to characterize metal surfaces. A hydrogen metal stoichiometry of 1 has been generally used when metal surface areas have been calculated from hydrogen chemisorption data. However, the results of Vis et al /24/ indicated clearly, that H:Rh values can exceed unity. For Rh/Al_2O_3 prepared by impregnating the support with $RhCl_3$ this occurred for metal loadings up to 5 %. They suggested that when H:Rh exceeded unity, the hydrogen chemisorbed did not exceed a monolayer and it was all bound to the metal. Hence, calculation of particle size from chemisorption data was impossible for highly dispersed systems. Crucq et al /32/ suggested, however, that chlorine in an unknown chemical form was responsible for the observed high H:Rh values. They broke down the adsorption of H_2 into a fast (1 min) and slow process (>1 h) and studied it with 1,6 w-% Rh/Al_2O_3 prepared from $Rh(NO_3)_3$ and with 4,8 w-% Rh/Al_2O_3 containing 1,1 w-% chlorine before washing and 0,05 w-% after it. They observed, that the presence of chlorine was certainly largely responsible for the slow

form of adsorption whereas fast adsorption was related to the pure metal. Similarly they suggested, that the slow adsorptions of hydrogen on the Rh catalyst prepared using a nitrate precursor might be due to presence of some residual NO_x on the surface. Also Kip et al /30,33,34/ obtained a high H:Rh ratio of 1,6 for 1,5 w-% Rh/Al_2O_3 prepared by incipient wetness method using aqueous $Rh(NO_3)_3$ or $RhCl_3$. In the case of vanadium promotion the H:Rh value remained constant up to V:Rh = 1. The systems with high V:Rh ratio of 7,0 and 8,4 increased the H:Rh ratio to 3,3 and 3,1, respectively. These high ratios, however, could not be explained by the assumption that all hydrogen was bonded to the metal. Hydrogen was apparently adsorbed also on the support, whereas it was not adsorbed on vanadium oxide itself. Thus the presence of metal was necessary to reach such high H:Rh values.

Temperature programmed reduction (TPR) and oxidation (TPO) studies of Rh/Al_2O_3 catalysts have been carried out to obtain (semi)quantitative information about the rate and ease of reduction as well as the rate and ease of oxidation. The TPR and TPO measurements of Vis et al /24/ showed, that 2,3 ... 20 w-% of Rh on Al_2O_3 was easy to reduce to the metal, giving a reduction peak in TPR around 67 °C. Rh was oxidized via chemisorption at -50 °C, followed by formation of an oxide skin around 357 °C. Kip et al /33/ obtained the TPR profiles for alumina supported rhodium catalysts prepared from nitrate and chloride precursors. The results indicated, that the nitrate also reduced during the TPR-run causing a huge hydrogen consumption. The reduction at 350 °C for 0,5 h in pure hydrogen was found sufficient to completely reduce the dried Rh catalysts. Kip et al /30/ studied the reduction profiles of $Rh-V_2O_3/Al_2O_3$ catalysts with V:Rh ratios in the range 0 ... 8,4. For catalysts with V:Rh $<$ 1 no intimate contact between Rh_2O_3 and V_2O_5 in the form of a mixed oxide existed, and the particles were located separately on the support. Reduction started at 25 °C and had a maximum at 142 ... 169 °C; the hydrogen consumption matched with reduction of Rh^{3+} to Rh^0 and of V^{5+} to V^{3+}. For catalysts with V:Rh of 7,0 and 8,4, there was clearly an influence of the V_2O_5 on the reduction behaviour of Rh_2O_3. The resulting higher reduction temperature pointed to the formation of a mixed oxide, $RhVO_4$, which was formed only after oxidation at 625 °C. The schematic illustration of vanadium-promoted rhodium alumina catalyst is shown in Figure 3.

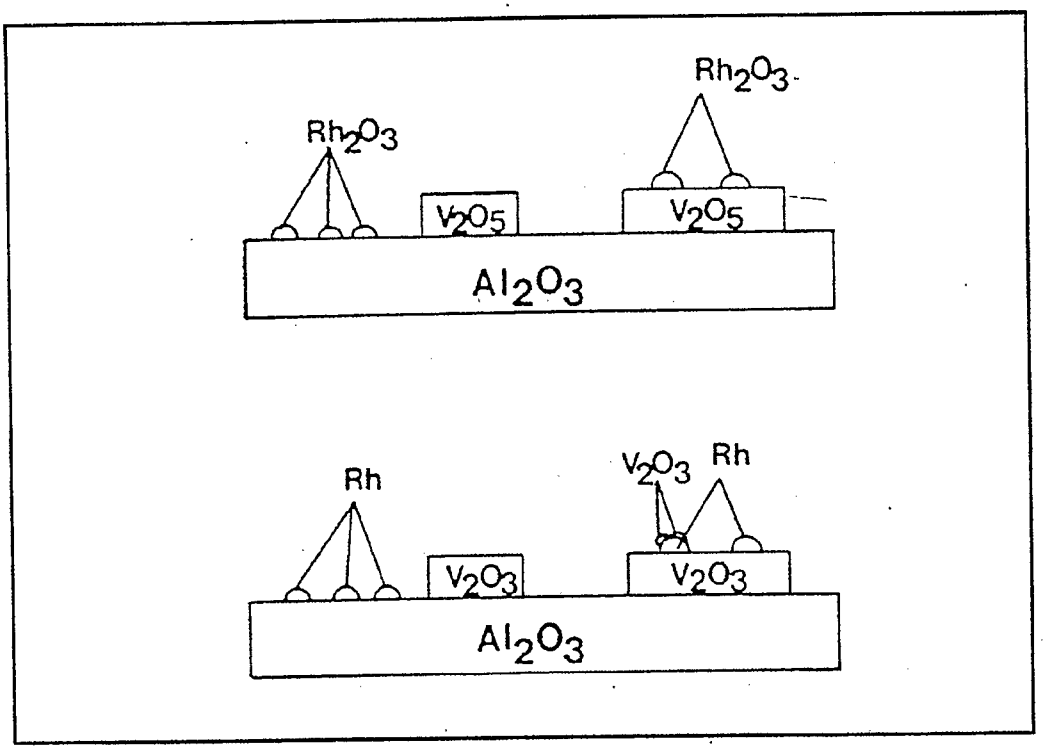

Figure 3. Schematic illustration of the model for the alumina supported, vanadium oxide-promoted rhodium catalyst after calcination at 450 °C above and after reduction at 250 °C below /30/.

Hydrogenation on alumina supported Rh has been investigated to identify the surface species during the reaction as well as the effect of catalyst preparation and composition on the activity and selectivity of the reaction. Erdöhelyi and Solymosi /16/ and Solymosi et al /17/ carried out *in situ* IR spectroscopic measurements during the hydrogenation of CO on Rh/Al_2O_3. They observed the presence of both linear and bridged CO species together with formate ion. They suggested, that the formate ion was not located on the Rh, but rather on the support. They proposed, that the hydrogen activated on the Rh migrated onto the support, where it reacted with CO producing formate ion ($OH^- + CO \longleftrightarrow HCOO^-$). Gopal et al /35/ discovered, that CO reacted directly with alumina surface at temperatures between 102 and 302 °C. The temperature at which CO reacted to produce surface formate was dependent upon the hydroxyl concentration on the oxide surface; the greater the degree of dehydroxylation the higher the temperature needed to produce formates. Hence the rehydroxylation of the surface by H_2 or H_2O exposure facilitated formate

production. In spite of the location of the formate group, it was not a totally inactive surface species, as evidenced by Solymosi et al /17/ by isotope substitution experiments. Nevertheless, they postulated that the production of CH_4 and other hydrocarbons in the hydrogenation of CO on supported Rh occurred only to a negligible extent through the formation and reactions of surface formate. However, Efstathiou and Bennett /19,20/ obtained results supporting the presence of formate as a spectator species, which did not exchange with ^{13}CO nor participated in the methanation reaction.

The activity and selectivity studies of CO hydrogenation carried out with Rh supported on alumina differ considerably from each other, thus no direct comparison of the results obtained is possible. CO hydrogenation at atmospheric pressure has been studied by Duprez et al /22/ and Van't Blik et al /36/. Duprez et al /22/ carried out their experiments with 2 w-% and 4 w-% Rh/Al_2O_3 at 200 ... 260 °C with H_2:CO molar ratio of 1 keeping the conversion below 5 %. They observed, that the proportion of methane was best correlated with the particle size, i.e., it was highest for the best dispersed catalyst. The same tendency was observed for C_2 hydrocarbons. On the other hand, the selectivities towards higher hydrocarbons followed an opposite trend and were conspicuously favoured on the largest particles. The yields of oxygenated compounds depended on the dispersion state of the catalyst; the formation of alcohols appeared particularly favoured on particles 30 ... 40 Å. Van't Blik /36/ et al studied the catalytic activity of 2,3 ... 11,6 w-% Rh/Al_2O_3 for CO hydrogenation at 250 °C with H_2:CO:N_2 of 2:1:1. With increasing metal loading, the catalyst dispersion decreased and the turnover frequency (TOF) increased. In fact, the rate of hydrogenation increased by about a factor of 2,5 with decreasing dispersion. Moreover, the increase in activity was accompanied by an increase in the olefin to paraffin ratio. Neither the selectivity to methane (aver. 62 %) nor the probability of chain growth was greatly affected. Medium pressure hydrogenation of CO over Rh/Al_2O_3 has been carried out by Gilhooley et al /37/ and Mori et al /38/. Gilhooley et al /37/ performed CO hydrogenation in a flow reactor at 250 °C and 10 bar with CO:H_2 ratio of 1:2 using a catalyst containing 1,2 w-% Rh. They obtained a methane, C_2-C_4 and ethanol selectivity of 55 %, 17 % and 13 % respectively at steady state. Mori et al /38/ carried out the experiments at 280 °C and 20 bar using H_2:CO ratio of 1 with 0,5 ... 20 w-% Rh/Al_2O_3 catalyst. The increase of metal

loading from 0,5 to 20 w-% increased the conversion from 1,7 % to 89,2 %. The methane selectivity varied within range 68 ... 100 %. However, the largest turnover frequency together with highest methane selectivity was obtained with a metal loading of 10 w-%. Kip et al /33/ studied the catalytic behaviour of alumina supported rhodium catalysts, reduced *in situ* in pure hydrogen at 1 bar with 5 °Cmin^{-1} 25 ... 350 °C, in synthesis gas reaction at 40 bar with H_2:CO ratio of 3 and GHSV of 4000 ll^{-1}h^{-1}. The results obtained are shown in Table 3 for illustrative purposes. The results indicated, that chlorine content and pretreatment method of the catalyst affected particularly the oxoselectivity. They postulated that chlorine, trapped by vacancies on the alumina surface formed by dehydroxylation of OH-groups, disfavoured the formation of oxygenates in the hydrogenation of CO. High water vapour pressure during the reduction of the metal chloride on alumina prevented the trapping. Moreover, calcination of the $RhCl_3/Al_2O_3$ system caused removal of the chlorine, resulting in high oxoselectivities. The negative influence of chlorine on the activity was not completely understood. Possibly it enhanced the coke formation or alternatively it covered part of the active metal area. Kieffer et al /39/ studied the catalytic behaviour of 2,5 w-% Rh/Al_2O_3 at 320 °C, 70 bar using CO:H_2 ratio of 1. After 24 h of reaction they obtained a conversion as low as 3 % with 50 % methane and 27 % oxygenates selectivities.

Table 3. CO + H_2 reaction over various 1,5 w-% rhodium catalysts supported on Al_2O_3 and SiO_2 /33/.

no.	catalyst system[b]	H/Rh	Activity[c]	Selectivity (%)[d]				
				CH_4	C_2^+[e]	tot.C_1-OH[f]	tot.C_2-OH[g]	tot. oxo[h]
1	$RhCl_3/Al_2O_3$[i], 1.8 mol % Cl	1.6	2.3	72.0	16.3	3.5	3.7	11.1
2	$RhCl_3/SiO_2$[j], 0.1 mol % Cl	0.6	0.6	48.0	11.3	26.7	14.0	40.7
3	$Rh(NO_3)_3/Al_2O_3$	1.3	0.6	45.4	14.4	27.5	11.1	38.6
4	$Rh(NO_3)_3/Al_2O_3$, calcined at 723 K	1.6	1.8	50.8	11.9	19.5	14.1	35.3
5	$Rh(NO_3)_3/Al_2O_3$, calcined at 723 K. HCl treated, 1.4 mol % Cl	1.4	0.9	61.3	24.9	9.3	0.0	11.7
6	$Rh(NO_3)_3/SiO_2$[k]	0.4	1.1	44.2	7.1	35.6	13.1	48.6
7	$RhCl_3/Al_2O_3$, 4% H_2O	1.6	2.6	63.9	4.1	14.7	14.8	29.5
8	$RhCl_3/Al_2O_3$, 1% H_2O[l], 1.8 mol % Cl	1.6	1.5	72.8	15.3	4.9	4.9	11.9
9	$RhCl_3/Al_2O_3$, 1% H_2O, heating rate during reduction 30 K min^{-1}, 1.5 mol 5 Cl	1.6	2.2	60.1	7.3	16.0	12.6	30.8
10	$RhCl_3/Al_2O_3$, H_2O injection during reduction, 0.9 mol % Cl	1.3	4.0	57.0	5.8	9.5	17.0	29.6
11	$RhCl_3/Al_2O_3$, calcined	1.6	3.1	65.7	4.7	13.1	12.1	26.4
12	$RhCl_3/Al_2O_3$, calcined, reduction at 723 K	1.6	1.9	60.1	14.7	8.5	11.9	22.0

(a) T_{react}= 523 K, unless stated otherwise. (b) standard reduction (see experimental). (c) Activity in mmole CO (mole Rh)$^{-1}$s^{-1}. (d) calculated by carbon efficiency. (e) $C_2^+ = C_2+C_3+C_4$ hydrocarbons. (f) tot.C_1-OH = C_1-OH + C_1-O-C_1 + 1/3 C_2-O-C_1. (g) tot.C_2-OH = C_2-OH + 2/3 C_2-O-C_1. (h) tot.oxo = tot.C_1-OH + tot.C_2-OH + C_2=O. (i) dried in-situ at 383 K, 16 h before reduction. (j) T_{react} = 623 K. (k) T_{react} = 628 K. (l) T_{react} = 506 K.

Mori et al /38/ studied the effect of potassium addition on the activity and selectivity of 2 w-% Rh/Al_2O_3 catalyst under conditions described on page 16. With increasing amount of potassium in the range 0 ... 2 w-% the TOF decreased; the TOF of a 2 w-% promoted catalyst was 4 times lower than that of an unpromoted catalyst. The activity decrease was accompanied by a decrease in methane selectivity and an increase in the selectivity of C_2-oxygenates. Blackmond et al /26/ studied the effect of Cs addition on 3 w-% Rh/Al_2O_3 with Rh:Cs ratios of 1:0, 1:2 and 1:5 at 253 °C, 1 bar with equimolar mixture of CO and H_2 after 16 h on stream. The rates of formation for all products were suppressed with increasing addition of alkali species. However, the hydrogenation selectivity to methane decreased more than that to higher hydrocarbons, whereas the selectivity to oxygenated compounds increased. Hence, in both studies the alkali metal addition on Rh/Al_2O_3 decreased both the catalyst activity and selectivity to methane, whilst it increased the selectivity to higher hydrocarbons and oxygenates.

The activity of bimetallic 3-2,8 w-% Rh-Mo and 3-1,6 w-% Rh-W on alumina was studied by Foley et al /29/ at steady state conditions both at 250 °C and 300 °C using pressures of 1 bar and 4 bar, and at 250 °C using pressures of 17,2; 34,5; 51,7 and 66,9 bar with H_2:CO ratio of 0,75:1,0. At low pressures Rh-Mo catalyst was more active than Rh-W, and their activation barrier to carbon monoxide reduction was similar to that of Rh catalyst. Due to the demonstrated low-pressure selectivity for the production of alcohols, the Rh-Mo catalyst was tested at high pressures determined above. The TOFs were found to increase with increasing pressure. When the product distributions were compared at 17,2 bar and 66,9 bar the observed change in activity was paralleled by a change in selectivity. At 17,2 bar the major products were methane and dimethylether, and the minor products light hydrocarbons and methyl ethyl ether. At 66,9 bar the major product was dimethyl ether and the minor products were methane, methyl ethyl ether together with methanol, and light hydrocarbons. The bimodality of the product distribution was linked to the proposed bimodality in the size and type of particles present on the support surface as described previously. This led to a two-site model - one site on the larger rhodium-rich particles for hydrocarbon synthesis and one site on the smaller molybdenum-rich particles for oxygenate synthesis as described in Figure 4. The former site was more electron rich, and sintered more readily, whilst the latter was slightly more electron deficient, and

thus more stable towards sintering. Kip et al /34/ investigated the effect of vanadium oxide as a promoter of 1,5 w-% Rh/Al_2O_3 on the hydrogenation of CO at 1,5 and 40 bar, 220 °C and 228 °C with H_2:CO ratio of 3. Low amounts of vanadium oxide (V:Rh < 1) had a negligible influence on the activity, and a slight influence on selectivity. This observation was consistent with the minor change of properties of the respective catalyst surface described previously. At both pressures, increasing the V:Rh ratio to 7,0 or 8,4 caused an increase in the activity by a factor of three. Consequently, the selectivities to C_2-oxygenates and higher hydrocarbons increased, whereas the selectivities to methane and methanol were diminished. Hence large amounts of vanadium oxide were required to promote the Rh/Al_2O_3 catalyst due to the strong interaction with alumina; first part of vanadium oxide was scavenged by the alumina support. In fact, high vanadium loading suppressed the formation of dimethyl ether indicating that vanadium oxide had covered the alumina sites responsible for the dehydration of methanol.

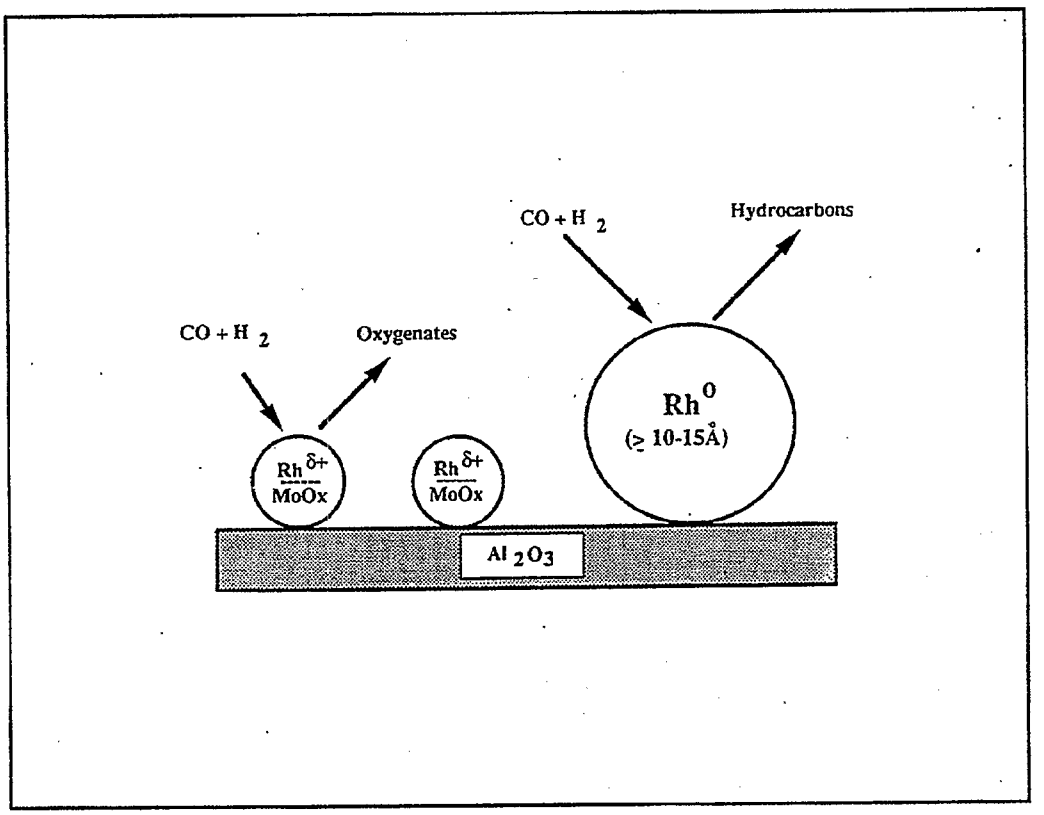

Figure 4. Two-site model for reduced $Rh\text{-}Mo/Al_2O_3$ /29/.

2.1.2 Rhodium on silica

Synthesis gas conversion over rhodium supported on a slightly acidic support, such as SiO_2, produces predominantly hydrocarbons. Hence, Rh supported on SiO_2 is active for CO dissociation, but inactive for CO insertion /40/. Additions of other species, such as alkali, alkali earth, lanthanoide or early transition metals, to the basic Rh/SiO_2 catalyst recipe have striking effects on catalyst structure, and its activity and selectivity.

Kesraoui et al /41/ studied the effect of alkali, namely potassium, addition on a catalyst containing 3 w-% Rh on either wide-pore or nonporous SiO_2. They observed, that the only CO species affected by the presence of the alkali on Rh supported on widepore SiO_2 was the gem-dicarbonyl. As the amount of alkali was increased the gem-dicarbonyl IR-peaks decreased. Hence, alkali had very minor effects on the adsorptive properties Rh supported on the widepore SiO_2, and it probably preferentially partitioned to the support. In the case of nonporous silica, the addition of alkali produced intriguing changes in the IR-spectra. The changes depended on the preparation method and level of addition. Hence, they concluded, that on nonporous support coimpregnation of alkalisalt increased dispersion and resulted in a through-metal electronic interaction between the alkali species and metal. Sequential impregnation on nonporous silica resulted in a different effect attributed to a localized interaction between the oxygen end of an adsorbed CO and the alkali species itself.

The effect of lanthana and ceria additions on Rh/SiO_2 structure has been studied by Underwood and Bell /42/, Solymosi et al /25/ and Krause et al /43/. Underwood and Bell /42/ characterized the 4 w-% Rh/SiO_2 catalysts with La/Rh ratios of 0 ... 10. They observed that the influence of lanthana content on IR-spectra was rather dramatic, and the degree of perturbation of the spectrum from that of Rh/SiO_2 increased with increasing lanthana content. The band for linearly adsorbed CO decreased dramatically with lanthana content. Also the bands for $Rh(CO)_2$ and bridged CO decreased with lanthana content. In addition, bands for carbonate groups associated with LaO_x islands, and bands attributed to CO adsorbed by the oxygen end of the molecule on surface Rh atoms near the edge of LaO_x islands appeared. Hence the LaO_x moieties formed reduced the capacity of Rh to adsorb CO, assisted in CO

dissociation, but had little effect on the chemisorption of H_2. Solymosi et al /25/ carried out infrared studies on the effect of 5 w-% addition of CeO_2 on 1 w-% Rh/SiO_2 catalyst. They observed, that the presence of CeO_2 had no effect on the CO adsorption IR spectrum at 27 °C, but had a dramatic effect on it at 150 °C. The gem-dicarbonyl species exhibited a remarkable stability in this case suggesting that CeO_2 greatly retarded the reductive agglomeration of Rh^{1+} into Rh_x clusters. Presumably CeO_2 supplied oxygen to Rh preserving the Rh^{1+} sites. Krause et al /43/ studied the microstructure of Rh-Ce on SiO_2 after heat treatments in H_2 and O_2 using TEM, high resolution electron microscopy (HREM), XPS and electron energy loss spectroscopy (EELS), focusing on the very stable structures formed after heating in H_2. After initial reduction at 600 °C Rh was present as 50 ... 100 Å metal particles whilst Ce formed a thin uniform amorphous film of Ce^{3+} on SiO_2. After oxidation at 600 °C, Rh was oxidized to Rh_2O_3 whilst Ce formed small and large CeO_2 particles. After rereduction Rh metal returned with less uniform particle size distribution, the small CeO_2 particles transformed back to Ce^{3+}, and the large CeO_2 particles reduced to $Ce_2Si_2O_7$. No evidence, that Rh formed compounds with the Ce or Si was observed. Nevertheless, Rh catalyzed the formation of large CeO_2 particles, and thus the formation of $Ce_2Si_2O_7$. Kip et al /44/ studied the effect of thorium oxide promotion on 1,5 w-% Rh/SiO_2 with Th:Rh ratios of 0 ... 4,0. Addition of ThO_2 mainly influenced the bridge-bonded carbon monoxide, which decreased with increasing Th:Rh ratio. Also the amount of linearly adsorbed CO was slightly lower for the promoted catalyst. No evidence was found for an intimate contact between the promotor oxide and Rh_2O_3. Neither the TPR profiles or chemisorption capacities were affected by ThO_2 additions.

Early transition metal promoters have a significant effect on the Rh/SiO_2 catalysts. IR spectra of CO chemisorption on Ti, Zr or Mn promoted Rh/SiO_2 has been studied by Ichikawa and Fukushima /45/, Sachtler and Ichikawa /46/ and Orita et al /47/. They observed, that Ti, Zr and Mn promoters present as Ti^{4+}/Ti^{3+}, Zr^{4+}/Zr^{3+} and Mn^{2+}, respectively, caused a significant decrease of bridged CO species. Ichikawa and Fukushima /45/ explained this effect by a tilted CO chemisorption mode, where the carbon of the chemisorbed CO is bonded to two or more Rh atoms, and the oxygen to the promoter metal ions as depicted in Figure 5. Also Wilson et al /48/ observed strong interaction between the added Mn and the Rh crystallites. Formation

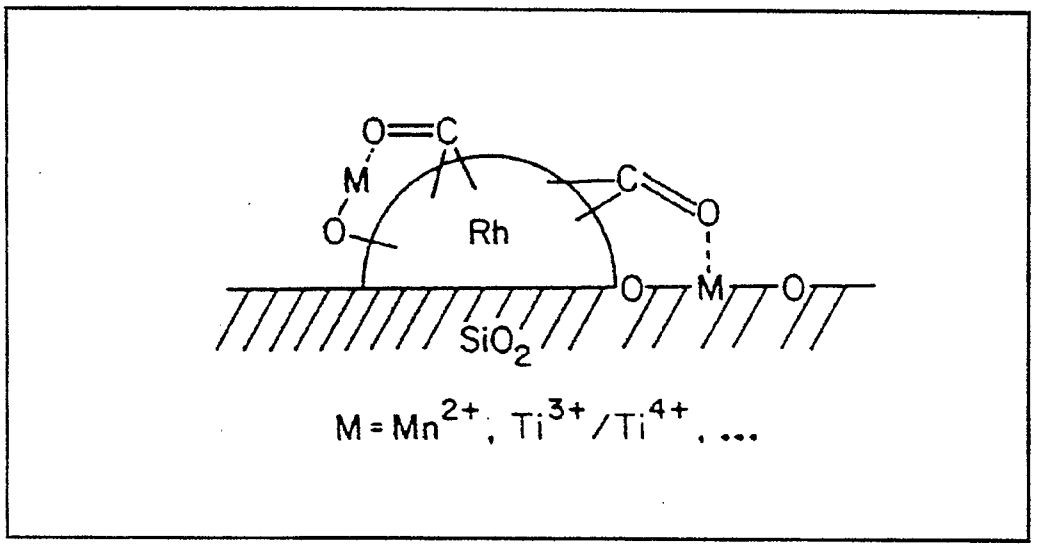

Figure 5. Schematic presentation of tilted CO bonding /45/.

of a stable Mn-O-Rh surface compound during the initial catalyst reduction could have accounted for their observations. Moreover, Lisitsyn et al /49/ reported that some manganese promoted Rh/SiO_2 catalysts studied by low-temperature IR spectroscopy displayed an intense IR band compatible with frequencies of M-C-O-M' species in known organometallic compounds. However, contact with CO at temperatures of -73 °C and above disrupted Mn-O-Rh bonds and partially reconstructed the oxide overlayer, exposing metallic rhodium. The IR studies of CO adsorption by de Jong et al /50/ carried out at ambient temperatures and 200 °C showed, that the presence of MnO increased the intensity of linearly adsorbed CO at the expense of gem-dicarbonyl species at the surface. The results also suggested that the number of sites strongly bonding CO were reduced. The MnO was not found to cover up Rh surface to a measurable extent. The effect of MnO was suggested to be due to either enhancement of interaction between metallic Rh and patches of MnO whereby the surface structure of Rh resembled larger crystallites or it decreased the heat of adsorption of CO. Also van den Berg et al /51/ suggested, that the true function of the poorly reducible promoter oxides, such as MnO, and MoO_2 was to decrease the heat of CO chemisorption via the formation and stabilization of rhodium ions. Trunschke et al /52/ investigated the surface complexes of CO formed on Rh-MoO_3/SiO_2 and Rh-WO_3/SiO_2 catalysts. The addition of promotor metals led to a

reduction temperature dependent decrease in the CO chemisorption ability of the samples. The intensities of the various absorption bands were substantially reduced after *in situ* reduction at 200 °C, where the only surface structure present was $Rh(CO)_2$. *In situ* reduction at 400 °C led to almost total suppression of CO adsorption. They assumed that Rh was covered with a layer of the promotor oxide which resulted in suppression of CO adsorption even after reduction at comparatively low temperatures and exerted an electronic influence on the rhodium surface leading to the stabilization of higher oxidation states of Rh. Kip et al /44/ studied the MoO_3-promoted 1,5 w-% Rh/SiO_2 with Mo:Rh ratios in the range 0 ... 4,0. The IR spectra of CO adsorbed on Rh-MoO/SiO_2 catalysts proved that MoO completely suppressed the carbon monoxide chemisorption capacity of rhodium due to coverage of the rhodium metal particles by patches of MoO. For Mo:Rh > 1,0 almost no CO adsorbed on rhodium in the bridged, linear or gem-dicarbonyl form. Hence, at higher Mo:Rh ratios CO was only adsorbed on MoO, whereas hydrogen was also adsorbed on MoO. TPR results suggested the formation of a mixed oxide of the form Rh_2MoO_6.

The effect of vanadium promotion on 1,5 w-% and 4,2 w-% Rh/SiO_2 catalyst was studied by Kip et al /30/ and Hu et al /53/. Their results proved, that an intimate contact between Rh and vanadium oxide was present. Kip et al /30/ found that the weak interaction between V_2O_5 and SiO_2, and the strong interaction between Rh_2O_3 and V_2O_5 resulted in the formation of a mixed oxide during catalyst preparation (calcination), which after reduction resulted in a vanadium oxide layer on top of the metal particle. As a result up to V:Rh = 1 the hydrogen and carbon monoxide chemisorption was strongly suppressed. Further addition did not change the CO:Rh values and caused a gradual increase in H:Rh values. The suppression of CO chemisorption was evidenced by almost complete disappearance of linear and bridged CO species. The intimate contact between the rhodium metal and vanadium oxide promotor even at a low V:Rh ratio was evidenced also by TPR and IR measurements. A schematic presentation of the interaction is presented in Figure 6. For V:Rh < 1, distinct Rh_2O_3 and $RhVO_4$ particles existed, whilst for V:Rh > 1, V_2O_5 and mixed oxide particles like $RhVO_4$ were present on the support. Consequently, vanadium oxide hampered the reduction of rhodium, whilst rhodium facilitated the reduction of vanadium oxide. Also Hu et al /53/ observed an exclusive formation of $RhVO_4$

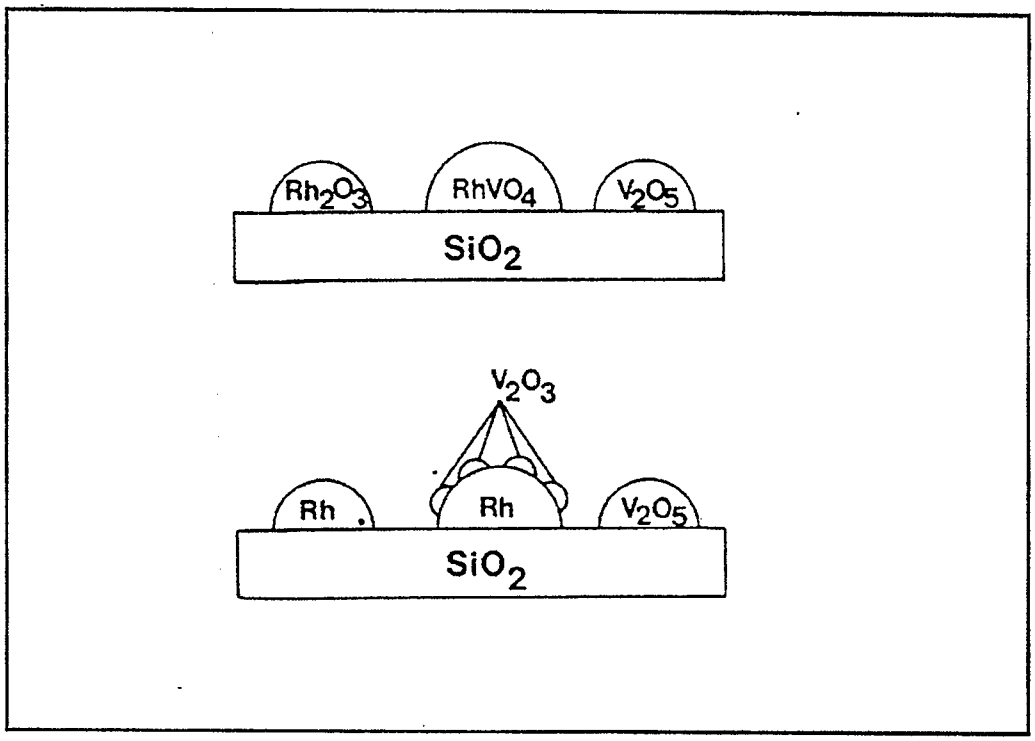

Figure 6. Schematic illustration of the model for the silica-supported, vanadium oxide-promoted rhodium catalysts after calcination at 450 °C on top and after reduction at 250 °C below /30/.

compound by mild calcination at 500 °C, and the formation of larger crystallites by calcination at 700 °C. The silica supported $RhVO_4$ exhibited significant SMSI behaviours through severe suppression of chemisorption capacity after high temperature reduction (HTR) at 500 °C. After HTR $RhVO_4$ was reduced to Rh and V_2O_3, which could cover the Rh surface. A strong interaction between the vanadium and rhodium metal particles was observed also by Koerts et al /54/ and partial coverage of rhodium by V_2O_3 was suggested by Kowalski et al /55/. Hu et al /53,56/ studied the extent of Rh-Nb_2O_5 interaction in the niobia-promoted 4,8 and 4,2 w-% Rh/SiO_2 catalyst with unity Nb:Rh atomic ratio. They observed, that the migration behaviours of Rh and Nb_2O_5 particles depended on the calcination temperatures as described by a model of $RhNbO_4$ formation in Figure 7. The structural changes of the formed $RhNbO_4$ during subsequent reduction and oxidation treatments are also described in Figure 7. They suggested that the strong metal

surface interaction (SMSI) was in fact induced by the formation of NbO_2 species, which blocked the Rh surface resulting in severely suppressed H_2 chemisorption capacity. Hence, in all these studies early transition metal oxide promoters on Rh/SiO_2 have been shown to interact with Rh through a formation of mixed oxide surface compounds.

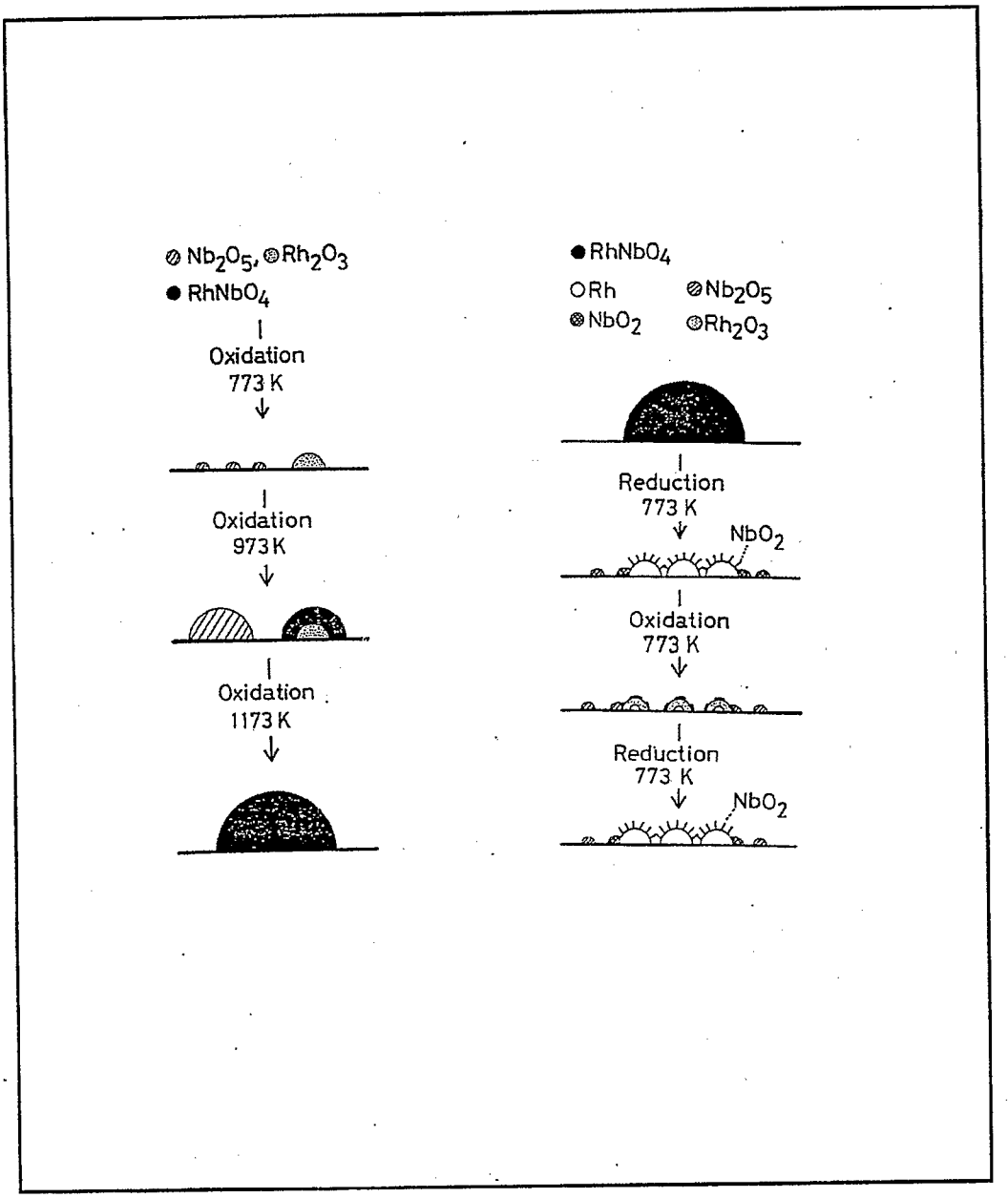

Figure 7. Model for $RhNbO_4$ formation during calcination on the left and structural changes during H_2 or O_2 treatment on the right /56/.

In addition to early transition metals, also other late transition metals and noble metals have been used as Rh/SiO_2 catalyst promoters. Ichikawa and Fukushima /45/ carried out IR studies of iron promoted 4 w-% Rh/SiO_2 catalysts with atomic ratios Fe:Rh in the range 0 ... 1,0. They found that Fe added to Rh highly suppressed the abundance of bridged carbonyl chemisorption on Rh surface resulting in decreased amount of CO adsorption with increasing loading. The multibridged CO chemisorption was preferentially prevented by the formation of Rh-Fe alloy by clustering on the Rh particle surface. Sachtler and Ichikawa /46/ reported that the EXAFS studies have also indicated that Fe is present as Fe^{3+} directly bonded to Rh atoms. Their coordination number, i.e. the average number of nearest neighbors to each Fe^{3+} was 3 ... 4, which suggested that the Fe ions were present on the surface of the Rh particles. Jen et al /57/ studied zinc promoted 4 w-% Rh/SiO_2 catalysts with Zn:Rh ratios of 0 ... 1,1. From the CO and H_2 chemisorption, XPES and IR data they concluded, that the rhodium surface was partly covered with a zinc containing overlayer. This adlayer suppressed the bridging mode of adsorbed CO more than the linear mode. Apparently some atoms of the overlayer blocked the ensembles of surface Rh atoms required for the bridged CO species. However, no Rh^{1+} species were detected. Sachtler and Ichikawa /46/ also noted, that Zn formed an incomplete overlayer, possibly located on the Freundlich sites of the Rh surface. On such surface the bridging sites were blocked with Zn, so CO was confined to the linear mode. Chuang et al /58/ studied the effect of silver addition on 3 w-% Rh/SiO_2 with Ag:Rh ratio in the range 0 ... 1. The adsorption of CO studied by IR indicated that as the ratio of Ag:Rh increased the ratio of bridged CO intensity to linear CO intensity decreased. These results suggested that silver was either interdispersed or it formed patches or islands on the surface of rhodium particle. Hence these metals (Fe, Zn, Ag) added to Rh/SiO_2 either covered Rh or formed intermetallic compounds and decreased the bridged mode of CO adsorption, i.e. suppressed CO dissociation ability.

The identification of surface species formed during the CO hydrogenation reaction on supported rhodium was studied by Erdöhelyi and Solymosi /16/ and Solymosi et al /17/ at atmospheric pressure. They observed that on 1 w-% Rh/SiO_2 (in contrast to 1 w-% Rh/Al_2O_3) there was no indication of the presence of formate ion either during low-temperature interaction (25 ... 152 °C) or during the methanation reactions (152

... 300 °C). Moreover, the dissociation of CO was also less on Rh/SiO_2 than on Rh/Al_2O_3. However, Koerts et al /54/ showed, that CO dissociation on Rh/SiO_2 was enhanced by vanadium promotion due to reduction of the apparent activation energy, which was a strong function of the CO surface concentration. The optimum surface coverage for methanation was found to be of the order of 0,2 ... 0,3. Dissociative CO adsorption at temperatures above 250 °C was found to produce a very reactive carbidic surface species, the formation of which was enhanced by coadsorption of vanadium. Furthermore, vanadium was found to promote the reactivity of this surface carbide to the formation of higher hydrocarbons. Underwood and Bell /42,59/ reported, that a well-defined acyl, formate and acetate bands were generated during the exposure of lanthana promoted 4 w-% Rh/SiO_2 to H_2 and CO at 257 °C. The intensities of these bands increased monotonically with increasing La:Rh ratio. None of these species were observed, though, in the absence of lanthana. The surface intermediated formed on the SiO_2 supported rhodium catalysts under high pressure reaction conditions have been studied by *in situ* high pressure IR by Fukushima et al /60/. The 4 w-% Rh/SiO_2 catalyst formed acyl species together with silyl acetate species, whilst with Fe addition on Rh/SiO_2 three different related oxygenate species, e.g. methoxy, ethoxy and acyl (CH_3CO_{ads}), were proposed as surface intermediates. Sachtler and Ichikawa /46/ also reported that the high pressure IR studies indicated that the highly oxophilic ions Mn, Ti, Zr and Nb, when located at the Rh surface stabilized the acyl species, which were thought to be precursors to C_2-oxygenates. These results were consistent with the observed indication of suppression in the ability of CO dissociation with Fe, Zn and Ag doped Rh/SiO_2.

Sachtler and Ichikawa /46/ suggested a general scheme for the hydrogenation of CO over metal catalysts. This scheme includes the formation of hydrocarbons and oxygenates and consists the following processes depicted in Figure 8. (1) Dissociation of adsorbed CO to form CH_3/CH_2. This step requires the largest ensemble of metal atoms. Hence, Rh^0 is active in this step /40,51/ and the dissociation rate is enhanced by oxophilic metal ions or oxides. (2) Migratory CO insertion in surface-alkyl bonds resulting in acyl species. Their hydrogenation leads to oxygenates, e.g. higher alcohols and aldehydes. This CO insertion is favoured by isolated metal atoms, e.g. Rh. However, recombination of CH_x with CO has been suggested to take place also on Rh^{n+} /61/. (3) The formation of hydrocarbons by hydrogen addition to or β-

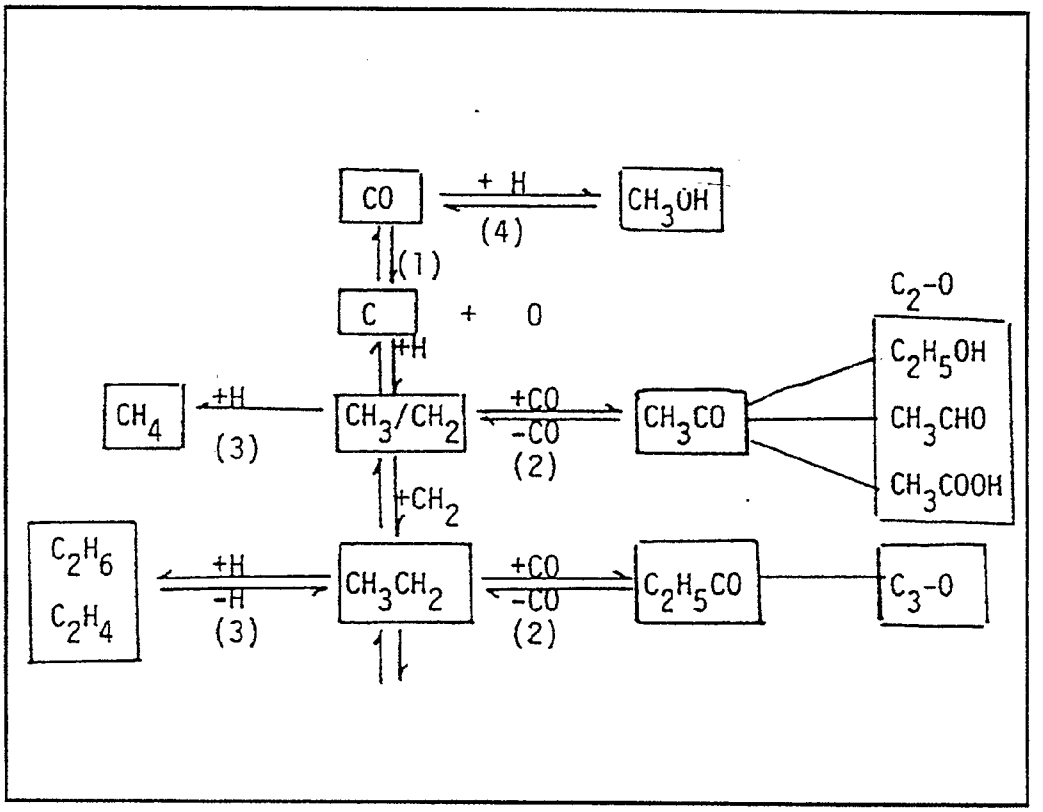

Figure 8. Scheme of elementary steps for syngas conversion to oxygenates and hydrocarbons: (1) CO dissociation, followed with formation of alkyl group; (2) CO migratory insertion in H alkyl group to form acyl species; (3) H addition and β-H elimination of surface alkyl group; (4) CO migratory insertion to metal-H, resulting in methanol /46/.

hydrogen elimination from surface alkyl groups. (4) Nondissociatively adsorbed CO is hydrogenated to methanol possibly via CO insertion in a M-H bond possibly on Rh^{n+} sites /61/. This step is enhanced by the presence of base metals such as Fe and Zn. However, inconsistent with the presented general scheme Orita et al /62/ and Jackson et al /63/ have shown by isotopic labeling that ethanol and ethanal, i.e. acetaldehyde, are produced independently with no common intermediate. A more detailed scheme representing the formation of oxygenates presented by Jackson et al /63/ is shown in Figure 9. Koerts and van Santen /64/ studied the rate of insertion into surface-alkyl species on silica supported Rh and Rh-V catalysts. They observed, that the CO insertion step was fast compared with the hydrogenation steps, and was

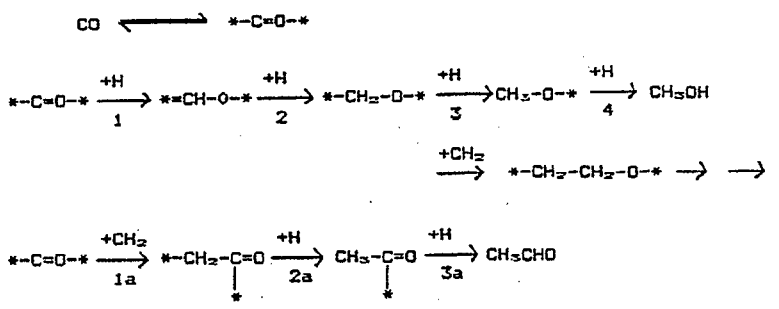

SCHEME

Figure 9. Scheme for the formation of oxygenates in CO + H_2 reaction /63/.

therefore not rate limiting. Vanadium promotion reduced the residence time of ethanol intermediates, whilst it enhanced that of ethanal intermediates. Hence, vanadium promotion stabilized oxygenated reaction intermediates on the catalyst surface and enhanced their hydrogenation activity to ethanol. However, vanadium addition did not promote CO insertion.

A large number of studies has been devoted to examining the influence of support and/or promotor composition on the activity and selectivity of Rh/SiO_2. Gilhooley et al /37/ studied the effect of metal precursor on 1,0 ... 2,0 w-% Rh/SiO_2 at 10 bar with $CO:H_2$ ratio of 1:2 and at 250 °C. Jackson et al /63/ carried out their experiments under similar conditions with Rh/SiO_2 with unspecified Rh loading. The precursors used by Gilhooley et al /37/ were $RhCl_3$, Na_3RhCl_6 , $Rh(acac)_3$ and $Rh(NO_3)_3$, where acac stands for acetonylacetate, whereas Jackson et al /63/ used only $RhCl_3$ and $Rh(NO_3)_3$. They observed profound effects in selectivity, for example loss of ethanal as a product going from $RhCl_3$ to $Rh(NO_3)_3$ or $Rh(acac)_3$. Hence, the residual counter ions affected surface intermediate stability. Mori et al /38/ carried out the experiments at 280 °C and 20 bar using H_2:CO ratio of 1 with 5 ... 20 w-% Rh/SiO_2.

They observed, that with increasing metal loading (decreasing dispersion), the conversion increased and the selectivity to C_2-oxygenates decreased considerably, whereas the methane selectivity increased. Underwood and Bell /65/ studied the influence of Rh particle size on the activity and selectivity of CO hydrogenation over 0,1 ... 29,8 w-% Rh/SiO_2 catalyst at 257 °C using 4 bar flow of CO and 8 bar flow of H_2. They observed that the dispersion of Rh had little effect on the total catalyst activity, but did strongly influence product selectivity. Maximum selectivity to C_2 oxygenates was obtained with high Rh dispersions (small particle size and low loading), whereas high selectivity to hydrocarbons was observed for low Rh dispersions (large particle size and high loading). Kesraoui et al /41/ studied both unpromoted and K-promoted 3 w-% Rh/SiO_2 at atmospheric pressure and 250 ... 340 °C using 1:1 mixture of H_2:CO. The unpromoted Rh on nonporous SiO_2 with large metal particle size, produced more higher hydrocarbons and more olefinic products than that on widepore silica with smaller particle size. K-promotion decreased the activity of all promoted catalysts by at least an order of magnitude compared to unpromoted catalysts. The product selectivities, however, showed less dramatic changes. The highly promoted catalysts with Rh:K ratio of 1:5 produced less higher hydrocarbons and less olefinic products than did the unpromoted ones. Thus, the observed dramatic changes in the adsorptive properties of nonporous SiO_2 catalysts upon promotion were not matched by similar effects in product selectivity. In contrast, the 0 ... 0,1 w-% potassium promotion of 5 w-% Rh/SiO_2 studied by Mori et al /38/ was found to increase the activity at 0,02 w-% level and decrease it thereafter. The effects on selectivity were small. Underwood and Bell /42,59/ reported, that at 257 °C with p_{H2} of 8 bar and p_{CO} of 4 bar the addition of lanthana to 4 w-% Rh/SiO_2 resulted in a higher activity for the formation of all products compared with the unpromoted catalyst. Lanthana promotion also increased the selectivity for the formation of oxygenates and C_{2+} hydrocarbons and decreased the selectivity to methane. Kieffer et al /39/ also obtained a higher total activity and considerably higher selectivity to C_2-oxygenates with 0,25 w-% lanthana promoted 2,5 w-% Rh catalyst compared with the unpromoted one at 320 °C and 70 bar with CO:H_2 ratio of 1. Hence, the observed higher activity with lanthana promotion is consistent with the previously described dissociation enhancement ability of lanthana. Kip et al /44/ studied the CO hydrogenation activity of thorium oxide promoted 1,5 w-% Rh/SiO_2 with H_2:CO ratio of 3 at 1,5 or 40 bar. The conversion was kept

around 2 % by temperature adjustment and the observations were based on 15 h time-on-stream. The promoting effect of thorium oxide was evident already at low pressure; the activity of the promoted catalyst was 38 times larger than that of the unpromoted catalyst. The methane selectivity was high and methanol selectivity low. The increase in pressure from 1,5 to 40 bar did not result in an increased activity. However, at higher pressure the C_2-oxygenate and total oxoselectivities were considerably higher and methane and C_{2+}-hydrocarbon selectivities clearly lower than at lower pressure.

The effect of manganese addition on 2,0 ... 2,5 w-% Rh/SiO_2 at 250 ... 300 °C and 30 ... 200 bar with H_2:CO ratio of unity was studied by de Jong et al /50/, Wilson et al /48/ and Ellgren et al /66/. de Jong et al /50/ observed that the effect of the presence of MnO on the activity depended on Rh dispersion; MnO did not affect to a large extent the activity at high Rh dispersions, whereas at medium dispersions a five- to tenfold increase in the turnover frequency for CO hydrogenation was observed. Highly dispersed Rh catalysts, however, displayed a shift towards methanol as far as product selectivity was concerned. Nevertheless, Wilson et al /48/ found that 0,2 w-% Mn addition increased both overall rate of CO conversion about tenfold and selectivities to C_2-chemicals. Ellgren et al /66/ observed that the addition of 1 w-% Mn raised the synthesis rate of the catalyst about tenfold. The selectivity was not particularly sensitive to additions of manganese. Van den Berg et al /51/ studied the CO and H_2 reaction activity of 2,5-0,3-0,3 w-% $Rh\text{-}Mn\text{-}Mo/SiO_2$ at 100 bar and 210 °C with CO:H_2 ratio of 1 and conversion below 10 %. They observed that the promoted catalyst was about 10 times more active after 24 h of testing. The selectivity to hydrocarbons increased as a function time, mainly at the expense of formation of methanol and C_{3+}-oxygenates in the case of the promoted catalyst, whereas the selectivity to most products decreased in favour of methanol with the unpromoted catalyst. Hence the observed enhanced activity and changed selectivity in the presence Mn was consistent with the observed ability of Mn to enhance CO dissociation and stabilization of acyl-species. Kip et al /44/ and Trunschke et al /52/ studied the effect of molybdenum promotion on CO hydrogenation. Kip et al /44/ carried out their experiments with 1,5 w-% Rh/SiO_2 at pressures of 1,5 bar and 40 bar using H_2:CO ratio of 3. The conversions were kept around 2 % by temperature adjustment. They found that at 40 bar the maximum increase in activity by a factor

of 141 was obtained for a Mo:Rh ratio of 1,0 compared with unpromoted Rh/SiO_2. The molybdenum oxide promoted catalysts had a high methanol selectivity (around 50 %) and a relatively low C_2-oxygenate selectivity (12-20 %). Total oxoselectivity was high (60 - 80 %) and deactivation was low. In the low pressure experiment at 1,5 bar the effect of molybdenum oxide promotion was less effective. The activity of the promoted catalyst with Mo:Rh of 1 was 19 times larger than that of the unpromoted catalyst. The oxoselectivity was lower than with high pressure, 44 % versus 75 %, mainly due to decreased methanol selectivity. Hence the activity and selectivity results supported the previously described intimate contact between the promotor oxide and rhodium metal and suggested that the presence of MoO indeed stabilized Rh^+ ions and thus increased methanol formation rates. Trunschke et al /52/ obtained consistent results on 1,6 w-% and 2,3 w-% Rh/SiO_2 promoted with MoO_3 with molar ratio $n_{Rh}:n_{Mo}$ of 1:2. The experiments were conducted at 10 bar and 200 ... 300 °C using H_2:CO of 2:1. A drastic increase in the catalyst activity by molybdenum addition was evidenced. The small increase in oxoselectivity was again due to the enhanced production of methanol. The results obtained under same conditions with 1,8 w-% Rh/SiO_2 with tungsten promotion ($n_{Rh}:n_W$ = 1:2) showed again increased activity accompanied with a more pronounced formation of ethanol than that of other oxygenated products.

The effect of vanadium promotion on CO hydrogenation over Rh/SiO_2 has been studied by Kip et al /34/, Koerts et al /54/, Kowalski et al /55/ and Bastein et al /67/. Kip et al /34/ carried out their experiments with 1,5 w-% Rh/SiO_2 at 1,5 and 40 bar with H_2:CO ratio of 3 using V:Rh ratio in the range 0 ... 4,5 and adjusting the reaction temperature (228 ... 327 °C) to keep CO conversion around 2 %. In case of low pressure, the presence of vanadium oxide had a remarkable influence on the total oxoselectivity: the total oxoselectivity of unpromoted catalyst was 1 %, whereas that of the promoted catalyst was 36 %. In the high pressure case, a sharp increase in activity with increasing V:Rh ratio was observed. The vanadium oxide promoted catalyst with V:Rh of 4,5 was 40 times more active than the unpromoted one. The total oxoselectivity decreased slightly with increasing V:Rh ratio mainly due to decreased methanol and acetic acid selectivity, but was still around 70 %. Koerts et al /54/ and Kowalski et al /55/ studied the catalytic activity of 2-(0,1...1) Rh-V_2O_5/SiO_2, 3 w-% Rh/SiO_2 with Rh:V molar ratio of 3, and 4,7 w-% Rh/SiO_2 with

Rh:V molar ratio of 2 under differential reaction conditions at 200 °C with H_2:CO of 2. They observed that the total activity was largely enhanced by vanadium promotion. They also found decreased methane selectivity and/or increased oxoselectivity as a result of promotion. The experiments of Bastein et al /67/ were carried out at 1 bar and 200 °C with H_2:CO of 2 over 2 w-% and 4 w-% Rh/SiO_2 promoted with vanadium in the atomic ratio range Rh:V 1:2 ... 1:8. They also obtained an increase in the selectivity of oxygenates. Hence, the results of vanadium promotion on activity and selectivity were consistent with the findings (i) of the enhanced CO dissociation activity due to reduction of apparent activation energy /54/ despite of the reduced CO chemisorption capacity particularly in the form of the bridged CO species /30/, and (ii) the ability of vanadium promotion to increase the surface concentration of oxygenated intermediates /64/.

Chuang et al /58/ investigated the effect of Ag addition on 3 w-% Rh/SiO_2 with Ag:Rh molar ratios of 0,25; 0,5 and 1 at 120 ... 300 °C and 10 bar with CO:H_2 of 1 keeping conversion below 5 %. They observed, that methane, C_{2+}-hydrocarbons and C_2-oxygenates were the major products whilst methanol constituted the minor product with the unpromoted catalyst. Silver was found to suppress the rates of product formation. This inhibiting effect of silver on the product formation rate was more pronounced at high temperature than at low temperature. However, decrease in the rates of formation of methane and C_{2+}-hydrocarbons in the presence of silver was more than in those for C_2-oxygenates. As a result a marked increase in C_2-oxygenate selectivity was obtained by silver promotion.

Herein two examples of multipromoted Rh/SiO_2 catalysts are given for illustrative purposes. Henrion et al /68/ evaluated the catalytic behaviour of a multipromoted 5 w-% rhodium catalysts, $Rh_{1,0}$-$Ir_{0,5}$-$Fe_{0,3}$-$Ti_{1,0}$/SiO_2 with the atomic ratios indicated by the subscripts, in CO hydrogenation at 215 ... 350 °C and 1 ... 60 bar. The effect of the promotors on activity and selectivity of the rhodium catalyst was evident; the reaction rate increase was accompanied with a considerable increase in oxoselectivity, in particular in that of ethanol. Ehwald et al /69/ studied multipromoted 5,0-0,06-0,02 w-% Rh-Mn-Li/SiO_2 and 5,0-1,2-0,06-0,02 w-% Rh-Ir-Mn-Li/SiO_2 catalysts for the selective hydrogenation of CO to oxygenates. The catalytic reaction was performed at 215 ... 300 °C and 11 ... 50 bar with H_2:CO:N_2 of 60:30:10. The results

were compared with Rh/SiO_2 and $Rh\text{-}Ir\text{-}Fe\text{-}Ti/SiO_2$ catalyst presented previously /68/. The effect of promotors was clearly demonstrated. The promoted catalysts showed an enhanced activity together with higher selectivity towards oxygenated products compared with the Rh/SiO_2. Moreover, the rate of CO consumption was enhanced by more than one order of magnitude and the manganese-lithium promoted catalysts were significantly more active than those promoted by iron and titanium. A remarkable difference concerning the selectivity was obtained; whereas mainly ethanol was formed with Rh-Ir-Fe-Ti, whereas the main C_2-oxygenate on manganese and lithium promoted catalysts was acetaldehyde.

2.1.3 Rhodium on titania

The problem of the changes in catalytic properties of small metal particles supported on oxides presents many challenges. The morphology of rhodium supported on TiO_2 has been studied by TEM, TPR and TPO. Fuentes et al /70/ observed, that Rh on TiO_2 formed two kinds of structures, flat platelets with a thickness of two monolayers and atomic rows. Vis et al /24/ also reported, that rhodium on a support can occur either in a dispersed form or in a bulklike form. TEM investigation showed, that the first kind of Rh_2O_3 consisted of flat, raftlike particles and the second kind of spherical particles.

Among the stimulating problems in heterogeneous catalysis, the strong metal-support interaction (SMSI) has received much attention. There is little doubt that the extent of the SMSI depends on the degree of reduction of the support; the more reduced the support the stronger the SMSI. Consequently, after high temperature reduction (HTR), most metals supported on titania loose a large part of their chemisorption ability for H_2 and CO. The chemisorption ability is restored by oxidation at high temperature followed by low-temperature reduction (LTR) /71,72,73/. The recovery of the normal state is achieved also by exposure to $CO{:}H_2$ mixture as a result of produced water /74/. Hence, TiO_2 not only provides a high surface area for the metal, but through SMSI it strongly influences the catalytic behaviour of the metal.

A plausible model for SMSI suggests that titania suboxide, TiO_x, $1<x<2$, species are formed by HTR. These reduced Ti oxide species migrate onto the surface of the metal particles resulting in physical coverage, by which the adsorption sites on the catalyst are blocked /36,72,75,76/. However, Demmin et al /77/ suggested, that the layer also interacts chemically with the metal, because the titania layers on Pt, Rh and Pd were found to have slightly different properties. Moreover, titanium oxide species were found mobile in the bulk of Rh metal. In fact, Resasco and Haller /78/ suggested, that SMSI resulted from a combined geometric effect, i.e. migration of species from the support, and local electronic interaction, i.e. chemical bonding, between the metal and migrated species. Fuentes et al /70/ suggested, that HTR produced O^{2-} vacancies on the support where rhodium incorporated. Merideau et al /73/ also suggested, that HTR produced a high concentration of surface defects, Ti^{3+} ions and oxygen vacancies, resulting in a flow of electrons from the reduced TiO_2 to the metal, and in a negative charge appearing on the metal particles. This electronic charge transfer from reduced Ti cations to the Rh was confirmed by Sadeghi and Henrich /79/. Moreover, Levin et al /80/ attributed the catalytic modification of rhodium by titania to participation of Ti^{3+} species at metal-oxide interface in the CO dissociation step. They proposed, that the influence of titania was based on an ensemble of Ti^{3+} and Rh sites along the TiO_x island periphery. Rh sites consisted of a site pair: a peripheral Rh site and an adjacent non-peripheral Rh site. They obtained a good quantitative agreement between this model and the experimental data.

Buchanan et al /81/ found that CO exposure induced oxidative disruption of metallic Rh clusters at temperatures as low as -113 ... -93 °C leading to gem-dicarbonyl, $Rh(CO)_2$ species. This process apparently involved the isolated OH groups of titania. The surface species detected by Erdöhelyi and Solymosi /16/ and Solymosi et al /17/ during hydrogenation reaction were linear and bridged CO species together with formate ion and surface carbon. However, the stability of the formate species on Rh/TiO_2 was comparatively low, and the amount of accumulated surface carbon was high as a result of a high degree of CO dissociation. Orita et al /82/ observed the adsorbed hydrocarbon species, namely methylene and methyl species, and surface acetate during the $CO + H_2$ reaction at 180 °C and 0,32 bar with $CO:H_2$ of 2. Most of the hydrocarbon species and acetate ions were, however, not reaction

inter-mediates, but were accumulated on the support near Rh metal. The addition of sodium cations was found to increase the intensity of bridged CO species. Also Dai and Worley /12/ found potassium promotion to block active methanation sites and to cause the formation of an increased amount of bridged CO species, the precursors to oxygenated products.

The enhancement of CO hydrogenation on polycrystalline rhodium foil by TiO_x overlayers at atmospheric pressure and 280 °C with H_2 and CO partial pressures of 0,67 and 0,33 bar, respectively, was studied by Levin et al /80/. They observed a threefold enhancement in activity for a TiO_x coverage of 0,15 of a monolayer accompanied by a higher selectivity to olefins. Van't Blik et al /36/ studied the catalytic activity of 0,3 ... 8,1 w-% loaded Rh/TiO_2 at atmospheric pressure and 250 °C. The activities of all catalysts in the H_2 + CO reaction decreased with time on stream. Two deactivation regions could be distinguished. Therefore, initial activity refers to activity obtained by extrapolating from the first region ($t < 4$ h) and steady state activity refers to the activity obtained by extrapolating the second region ($t > 4$h) to zero. The activities of non-SMSI Rh/TiO_2 and Rh/Al_2O_3 hardly differed at equal dispersions. The rate of Rh/TiO_2 activity increased one order of magnitude going from a dispersion of 1,10 to 0,12, i.e. from metal loading of 0,3 to 8,1 w-%. This increase in specific activity was accompanied by an increase in olefin to paraffin ratio, but neither the selectivity to methanol nor the probability for chain growth was affected much. High temperature reduction of the Rh/TiO_2 decreased the initial activity, whereas the steady state activities were hardly affected as shown in Figure 10. This effect on activity was a function of dispersion, and was much more pronounced for small particles indicating that SMSI might be due to covering. Neither the selectivity for methane nor hydrogenation capacity was affected, whereas the probability to chain growth increased somewhat. Taniguchi et al /73/ did not observe an increased activity for hydrogenation of adsorbed CO on titania supported Rh in SMSI state. In contrast, other investigators /17,38,83,131/ obtained higher activities with Rh/TiO_2 than with other carriers. Their comparison was not carried out at similar dispersions, however.

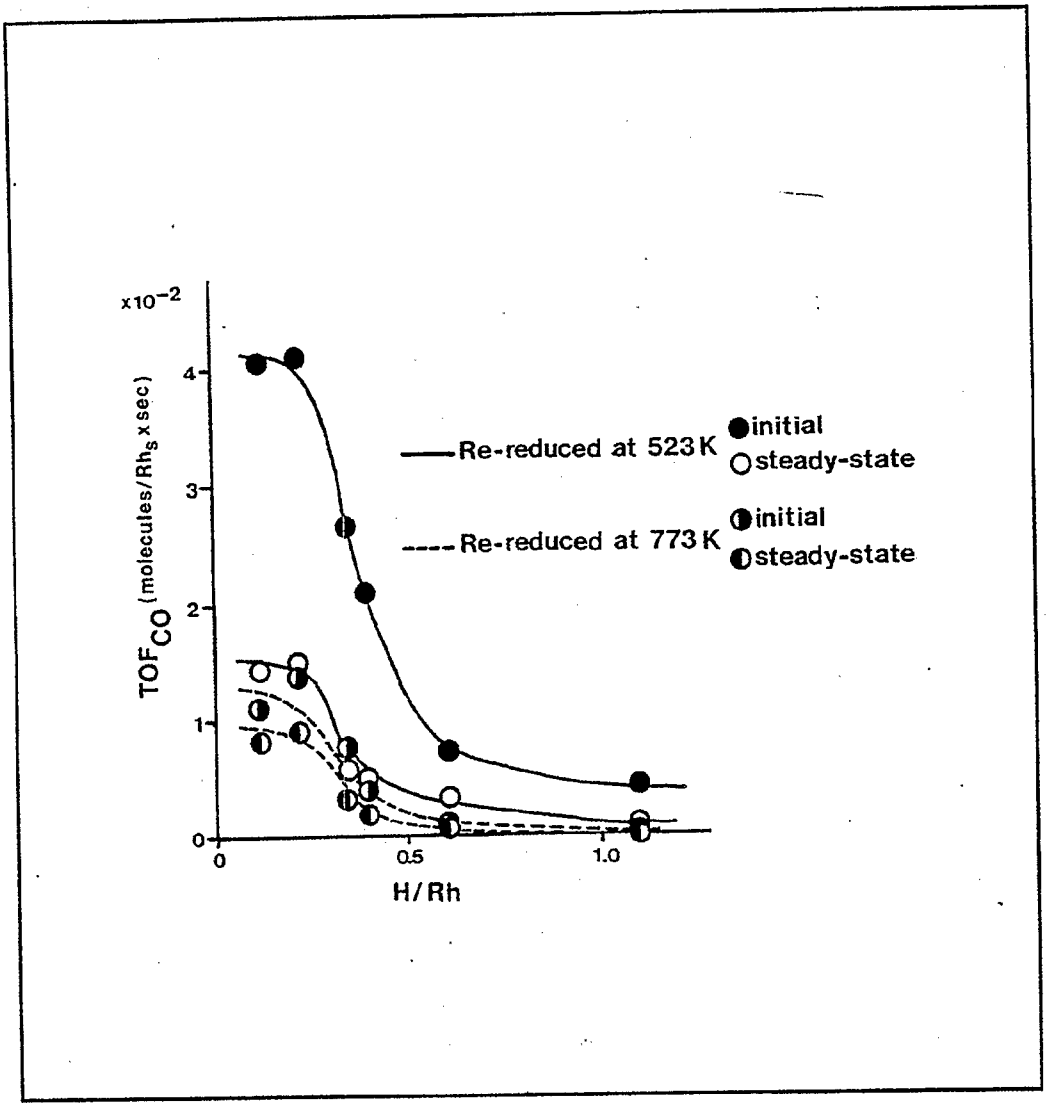

Figure 10. Initial and steady state turnover frequencies in the H_2 + CO reaction versus H:Rh (dispersion) for titania-supported Rh-catalysts re-reduced at 250 °C and 500 °C. P = 1 bar, H_2:CO:N_2 = 2:1:1, T = 250 °C.

Rh/TiO_2 is a useful catalyst for studying alkali promotion effects on product selectivity since it can produce significant quantities of both oxygen containing products and hydrocarbons. Dai and Worley /12/ studied by IR the effects of potassium on CO methanation over 2,2 w-% Rh/TiO_2 films at 0,11 bar and 27 ... 167 °C with CO:H_2 ratio of 1:4. They observed, that the methanation reaction was clearly poisoned by potassium additions (K:Rh = 1), whereas the production of oxygenated compounds was enhanced. The primary oxygenated products obtained

were acetone and acetaldehyde. Hence, the results obtained were consistent with the observed changes in catalyst structure. The effect of Li, K, Na, and Cs addition on Rh/SiO_2 has been studied by Mori et al /38/, Chuang et al /83/, Orita et al /84/ and Inoue et al /85/. Mori et al /38/ carried out the experiments at 280 °C and 20 bar with H_2:CO ratio of 1 over 2 w-% Rh/SiO_2 loaded with 0 ... 2 w-% K. They observed that with increasing amount of potassium added, the turnover frequency and methane selectivity decreased and the selectivities for higher hydrocarbons and C_2-oxygenates increased. Chuang et al /83/ studied the 3 w-% Rh/SiO_2 with alkali:Rh atom ratio of 1:2 in a differential reactor (X < 5 %) at 250 ... 435 °C and 1 ... 10 bar with CO:H_2 ratio of 2. They observed that the rate of CO conversion decreased in the order unpromoted > Li > K > Cs whilst the ability of the alkali species to promote the selectivity for oxygenated compounds increased in the order unpromoted < Li < K = Cs. Orita et al /84/ obtained results consistent results at 180 °C, p_{CO} 0,12 bar, p_{H2} 0,24 bar with 1:3 Rh:alkali atomic ratio and 5 w-% Rh/SiO_2. They noted further, that the formation rate of ethanol was more influenced by alkali promotion than that of acetaldehyde, and it decreased in the order Li > Na > K > Cs. Also Inoue et al /85/ obtained comparable activity with sodium doped (atomic ratio Rh:Na = 1:1,5) and undoped 3 w-% Rh/TiO_2, whereas the selectivity to alcohols, and particularly to ethanol was enhanced by the presence of sodium at 260 - 300 °C and 10 bar with 1:1 ratio of CO:H_2. Hence alkali promotion decreased the CO hydrogenation activity and increased the selectivity to oxygenated products. The effect of 10 ... 20 w-% lanthana promotion on 2 w-% Rh/TiO_2 was studied by Bond and Richards /86/ in a differential fixed bed reactor at 100 bar and 200 °C using H_2:CO of 2:1. The results indicated that La_2O_3 addition led to a significant improvements in formation rates. In particular increased CH_3OH and higher alcohol yields were observed at the expense of methane formation.

2.1.4 Rhodium on basic oxides

Rhodium supported on basic metal oxide supports, such as ZnO, MgO or CaO, in contrast to acidic ones, results in more than 95 % of the CO consumed to be converted into methanol. The electronic state of Rh on ZnO and MgO has been found to correspond with Rh^{1+} state resulting in suppressed CO dissociation reaction and a

greater tendency for CO insertion in the case of these catalysts /40/. In fact, suppressed CO dissociation on MgO supported Rh catalyst was the lowest followed by SiO_2, Al_2O_3 and TiO_2 /16,17/.

The surface species obtained with H_2 + CO interaction by Erdöhelyi and Solymosi /16/ and Solymosi et al /17/ were the same with MgO as with previously described carriers. The species detected at hydrogenation reaction temperatures were linear and bridged CO species together with formate ion and surface carbon. In the presence of H_2 the stability of the formate species decreased appreciably and simultaneously CH_4 was formed. However, the results of Efstathiou /87,88/ on CO/H_2 reaction over 2,5 w-% Rh/MgO at 220 ... 300 °C confirmed, that the steps for methane formation passed through a large reservoir of surface CO and through a small reservoir of active carbon. The formate species on the support were presumably the active intermediates to make most of the CO_2 according to the following reaction: CO(m) + OH(s) ---> COOH(s) ---> CO_2 + ½H_2, where (s) refers to the support and (m) to the Rh metal. The lower activity of Rh/MgO than that of Rh/Al_2O_3, Rh/SiO_2 or Rh/TiO_2 seemed to result from a lower CO dissociation rate on the Rh/MgO than on the other mentioned catalysts.

The CO hydrogenation activity of highly dispersed 0,5 w-% loaded Rh/SiO_2, Rh/ZnO and Rh/MgO at atmospheric pressure and 200 °C with CO:H_2:He = 20:40:20 ml/min was studied by Kawai et al /40/. They obtained conversions of 1,3; 1,6 and 2,6 % respectively. The selectivities between the catalysts differed considerably: silica supported catalyst produced mainly methane (69 %), whilst the other two produced mainly methanol, 94 % and 88 % respectively. Consistent activity and selectivity results were reported also by Sachtler and Ichikawa /46/.

2.1.5 Rhodium on other carriers

The synthesis of oxygenated products over Rh is quite sensitive to support and promoter composition, as well as to metal dispersion. Since C_2-oxygenates are desirable products from an economic point of view, much attention has been paid to improve the catalyst activity and selectivity to C_2-oxygenates. In this respect V_2O_5,

La_2O_3, ThO_2, ZrO_2, Nd_2O_3 and Sm_2O_3 have been studied as Rh supports.

Bastein et al /67/ studied the influence of precursor and reduction temperature, 200 or 400 °C, on 4,5 w-% Rh/V_2O_3 at 1 bar with $CO:H_2$ ratio of 1:2 at 200 °C. Their results showed, that V_2O_3 supported Rh catalysts were highly selective in forming C_2-oxygenates from syngas provided that the Rh surface became partly covered by the support (i) by partial dissolution of the support resulting in a precipitate near or on the metal particles or (ii) by high temperature reduction. The coverage was found to be influenced by the choice of the rhodium precursor used, and it was related to the varying ability of the precursor solutions to dissolve a part of the support in the form of the vanadyl ion. The amount of $VOCl_2$ in the system was sympathetically correlated with both the acidity of the precursor solution and the selectivity to C_2-oxygenates. The most selective catalysts were obtained with an acidified rhodium chloride solution precursor together with reduction at 400 °C. When $Rh(NO_3)_3$ was used as a precursor, the vanadyl ion precipitated in the form of $VO(NO_3)_3$ yielding V_2O_5, which does not adhere well to the metallic surface. Consequently the catalyst reduced at 200 °C showed very high activity but zero selectivity. Kip et al /30/ characterized 1,5 w-% Rh/V_2O_3 prepared by the incipient wetness method using aqueous solution of $Rh(NO_3)_3$. This catalyst had a H:Rh ratio of 3,8 and an average particle size of 35 Å. Hence, hydrogen was adsorbed also on the support. However, vanadium oxide itself did not adsorb hydrogen. Presumably hydrogen bronzes like $H_{2x}V_2O_5$ were formed. The CO hydrogenation reaction was performed at 0,15 or 40 bar, 240 or 270 °C with H_2:CO ratio of 3 on Rh/V_2O_3 reduced *in situ* at 250, 450 and 550 °C. During HTR the rhodium particles became covered by V_2O_3. Consequently, the higher reduction temperature was found to decrease activity and increase oxoselectivity dramatically (from 13,6 to 70,3 and 80,3 % respectively). Thus Rh/V_2O_3 reduced at high temperature (> 450 °C) exhibited a relatively high oxoselectivity as reported also previously /55/, but a low activity and strong deactivation. Moreover, the structural properties of V_2O_3 i.e. low surface area, low pore volume and relatively high solubility in water made it an undesirable support.

Lanthana supported rhodium has been studied by Underwood and Bell /65,89/, Kieffer et al /39/ and Sachtler and Ichikawa /46/. Underwood and Bell /65/ characterized the 0,1 ... 8,0 w-% Rh/La_2O_3 catalyst. The IR spectra of CO adsorbed

at 40 °C showed that the linear CO species decreased as the rhodium loading increased. This observation was consistent with increasing LaO_x coverage of the Rh particles with increasing loading as a result of support dissolution during catalyst preparation. The IR spectra also indicated the presence of bidentate formate groups, which were formed by reaction of CO with OH groups on the surface of the La_2O_3 support. Hence, the measured CO uptakes could not be ascribed solely to chemisorption on Rh. The hydrogen uptake was found to increase with adsorption temperature for all catalysts, but the most significant effect was observed with the highest loading. The H:Rh ratios decreased monotonically with Rh loading, and they were unusually low for 3,5 and 8,0 w-% Rh/La_2O_3 catalysts due to partial blockage of Rh by lanthana. However, Rh particle size was concluded to increase with Rh loading. CO hydrogenation of the Rh/La_2O_3 was carried out at 257 °C with 4 bar of CO and 8 bar of H_2. The results indicated, that the specific influence of the LaO_x decoration was to increase the turnover frequencies for the formation of all products. For comparable dispersions, Rh/La_2O_3 exhibited a much higher methanol selectivity and a lower hydrocarbon selectivity than Rh/SiO_2 catalysts (see Figure 11). The increased activity and selectivity to oxygenates was believed to result from the creation of new catalytic sites along the perimeter of the LaO_x patches. Consistent results under similar reaction conditions with 0,5 w-% Rh supported SiO_2, La_2O_3, Nd_2O_3 and Sm_2O_3 were obtained by Underwood and Bell /89/. With $<0,1$ conversion the turnover frequencies were found to decrease in order $Nb_2O_3 > Sm_2O_3 > La_2O_3 > SiO_2$. Moreover, the selectivities of the REO-supported catalysts were very similar, but differed significantly from those of Rh/SiO_2. Methanol (appr. 50 %) was the dominant product formed over the REO-supported catalyst, whereas mainly methane (apr. 66 %) was formed on Rh/SiO_2. However, Sachtler and Ichikawa /46/ performed CO hydrogenation with P_{CO} 0,27 bar and P_{H2} 0,6 bar at 205 °C and 235 °C on 0,5 w-% Rh loaded on La_2O_3 and SiO_2. They obtained 3,0 % conversion on Rh/La_2O_3 with 38 % selectivity to methanol and 43 % to C_2-oxygenates, whereas Rh/SiO_2 produced 1,7 % conversion with 92 % methane selectivity. Moreover, Kieffer et al /39/ carried out the activity measurements at 320 °C and 70 bar with 1:1 ratio of CO and H_2. With a conversion of 23 % on 2,5 w-% Rh/La_2O_3 and of 11 % on 2,5 w-% Rh/SiO_2 they obtained a selectivity mainly to methane, 61 % and 78 % respectively. However, conversion to C_2-oxygenates was much higher on Rh/La_2O_3 than on Rh/SiO_2. Hence all studies indicated enhanced activity and oxygenate

selectivity with La_2O_3 support compared with SiO_2, but the product selectivities were strong functions of reaction conditions too.

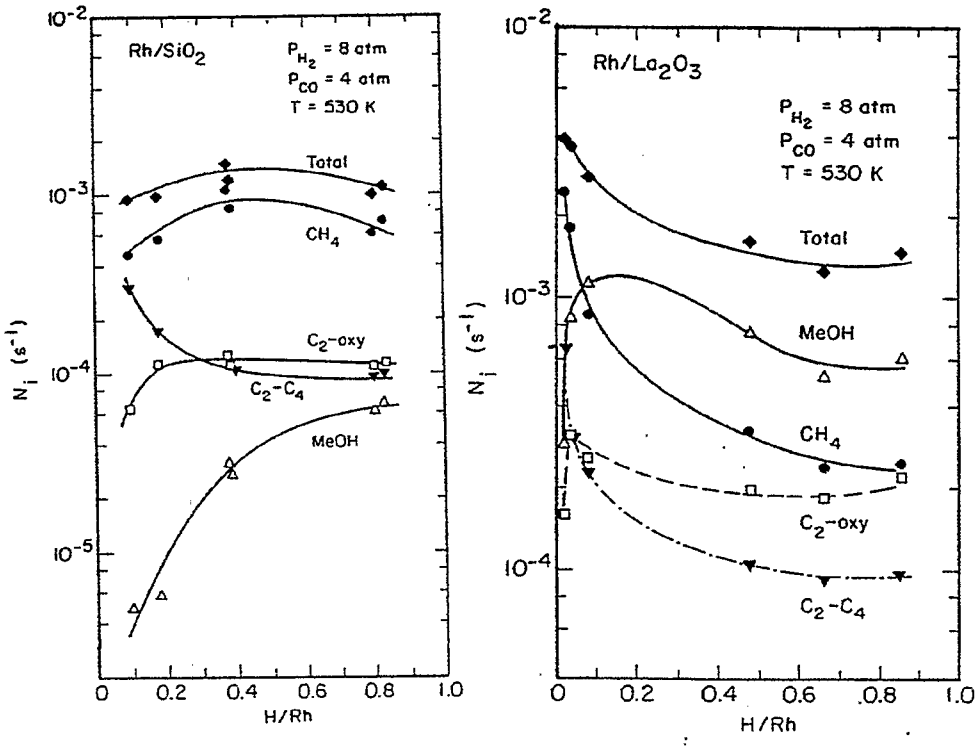

Figure 11. Dependence of product selectivity on H:Rh for Rh/SiO_2 on the left and Rh/La_2O_3 on the right /65/.

2.1.6 Supports in summary

By summing up the results of various authors with constant rhodium loading the activity in CO hydrogenation has been found to decrease in order TiO_2 > Al_2O_3 > La_2O_3 and other REO supports > SiO_2 > MgO. However, it has been noted, that with equal dispersions the orders might be of the same magnitude /36/. Moreover, the results were greatly influenced by the reaction conditions chosen. Particularly the selectivity of the Rh catalyst was closely related to the support. Hence, acidic oxides, such as SiO_2 and Al_2O_3 were reported to produce mainly non-oxygen containing hydrocarbons, whilst TiO_2, ZrO_2 or La_2O_3 produced methanol together with ethanol. The basic oxides, such as ZnO, MgO and CaO converted CO mainly to methanol /40/. An illustrative example of activities and selectivities under various supports is given in Table 4.

Table 4. Performance of catalysts prepared from $Rh_4(CO)_{12}$ impregnated on the different metal oxides catalyzed in an atmospheric CO-H_2 reaction [a] /46/

support MO_x	T, °C	CO conv, %/h	selectivity (CE,[b] %)		
			MeOH	C_2–O	HC
ZnO	220	1.6	94		4
MgO	220	2.6	88	2	7
CaO	230	0.8	92	1	2
La_2O_3	205	3.0	38	43	10
Nd_2O_3	210	3.8	24	47	21
ZrO_2	215	4.4	13	50	36
TiO_2	210	6.0	6	40	51
Nb_2O_5	195	5.8	7	39	51
MnO_2	205	1.2	4	25	63
SiO_2	235	1.7	tr[c]	6	92
γ-Al_2O_3	250	8.6	tr[c]	tr[c]	99

[a] Rh, 0.5 wt % loading from $Rh_4(CO)_{12}$; P_{CO} = 200 Torr, P_{H_2} = 450 Torr; a closed circulating reactor (volume: 400 mL STP) cited in ref 11. $Rh_4(CO)_{12}$ was impregnated from hexane solution at each oxide powder, followed by decomposing at 120–200 °C under vacuum. [b] CE = carbon efficiency; CE (%) = $100 n_j C_j (\sum_j n_j C_j)^{-1}$; n_j = number of carbon atoms in the jth molecule; C_j = concentration of the jth product. C_2–O, C_2–oxygenates, mostly consisting of EtOH. [c] tr = trace.

2.2 Cobalt catalysts

Cobalt follows nickel in the activity order of methanation catalysts. The catalytic properties of cobalt catalysts have been known to be affected by three factors - the support, the size of the cobalt particle and the extent of reduction - which have a decisive influence on the surface state of cobalt and of cobalt oxide species formed in cobalt-support interactions as well as on the course of these interactions /90,91/. Therefore a number of investigations have been devoted to the state of both unpromoted and promoted cobalt on various supports, such as alumina, silica, titania, magnesia, carbon and zeolite as reviewed in this literature survey.

2.2.1 Cobalt on alumina

The nature of the species formed on the surfaces of alumina supported cobalt catalysts has been a subject of numerous investigations carried out by a variety of experimental techniques. Qualitative identification of the surface metal species is an important step in catalyst characterization. Quantitation of these species provides an even better assessment of the effect of catalyst preparation conditions, and the effects of additives and promoters on catalyst activity. Ultimately the quantitative determination of the distribution of supported metal species aids in the prediction of catalyst activity and in tailoring of catalysts for specific chemical reactions.

The catalyst surfaces of Co/Al_2O_3 catalysts have been investigated by spectroscopic techniques in order to reveal the nature of the species formed as a result of metal support interactions. The observed interaction species have been found to arise from diffusion of Co^{2+} ions during calcination into lattice sites of the γ-Al_2O_3 where they occupied tetrahedral (Co-t) or octahedral (Co-o) sites /92,93/. At low metal concentrations, the cobalt was predominantly in Co-t sites of the support producing a Co "surface spinel" identical with $CoAl_2O_4$; the similarity was confirmed by spectroscopic, X-ray diffraction and magnetic measurements /93/. The amount of Co-t reached a maximum level at Co loadings between 1 and 2 w-% /94/. Formation of this species was favoured by high calcination temperatures. At higher cobalt concentrations an octahedrally coordinated interaction species, Co-o, was produced.

The amount of Co-o increased slightly with increasing Co-loading /94/. Eventually a bulk like Co_3O_4 phase segregated on the surface of the catalyst with further increases in metal loading. Co_3O_4 segregation occurred to a major extent on the surfaces of catalysts having Co concentrations higher than 10 w-%. Co_3O_4 had a normal spinel structure with Co^{2+} having tetrahedral symmetry and Co^{3+} having octahedral symmetry /92,93/. Under typical calcination conditions, the diffusion process was limited to the first few outer layers of the support.

The effects of starting cobalt salt upon the cobalt-alumina interactions was studied by Okamoto et al /95/. The precursors employed were $Co(NO_3)_2$, $Co(CH_3COO)_2$, $CoSO_4$, $CoCl_2$, $Co(HCOO)_2$, CoC_2O_4. Based on XPS results they concluded, that all the cobalt precursors, except for $Co(NO_3)_2$ provided well dispersed CoO/Al_2O_3 catalysts with high proportions of Co^{2+} species. Among the starting salts examined, only nitrate anions showed high oxidation ability. It was proposed, that Co^{3+} formation via oxidation of Co^{2+} during calcination promoted agglomeration of cobalt species resulting in poorly dispersed CoO/Al_2O_3.

Various additives have been used to modify the surface properties of Co/Al_2O_3. The modifying effect of these additives has been generally attributed to two processes: (i) coverage of the surface of the active phase by the additive resulting in a decrease in chemisorption capacity and the creation of new catalytic sites at the metal-additive interface, and/or (ii) the presence of partially reduced additive oxides which provide binding sites for the oxygen end of the CO molecule facilitating dissociation of the C-O bond /96/. Castner and Santilli /97/ studied the effect of potassium addition on 5 w-% Co/Al_2O_3 catalyst. Potassium addition was done prior to impregnating with Co. They observed, that the $Co/K\text{-}Al_2O_3$ catalyst had the same species present as those found on Co/Al_2O_3, but the Co-t phase concentration was lower and bulklike Co_3O_4 particles were present. Although the total amount of bulk cobalt reducible in H_2 at 480 °C had increased in $Co/K\text{-}Al_2O_3$ compared to that in Co/Al_2O_3, the amount of surface metallic cobalt present in the two systems was similar. No determination was made as to whether differencies between $Co/K\text{-}Al_2O_3$ and Co/Al_2O_3 were due to the presence of K, the higher support calcination temperature or the lower surface area of $K\text{-}Al_2O_3$. Ledford et al /96/ investigated the structure effect of La addition with La:Al atomic ratio of 0 ... 0,078 on 10 w-% Co/Al_2O_3. The ESCA data indicated

that lanthanum was highly dispersed over the alumina carrier. The catalysts prepared by reverse impregnation, i.e. by impregnating cobalt first and lanthanum thereafter, showed little evidence of Co-La interaction. However, lanthanum affected catalysts prepared by impregnating the alumina first by La followed by Co, i.e. Co-La/Al_2O_3. The low lanthanum content of up to La:Al 0,013 had little influence on the supported catalyst. With higher loadings (La:Al > 0,026) the Co_3O_4 cobalt phase was suppressed in favour of a more dispersed and less reducible amorphous La-Co mixture. Stranick et al /98/ studied the influence of TiO_2 on the speciation of 3 w-% Co/Al_2O_3 catalysts. The results indicated that with low Ti loadings (<4 w-% Ti) the Co phase was present primarily as Co_3O_4 with lesser amount of octahedral and tetrahedral cobalt (Co-o; Co-t). With high Ti contents, Co_3O_4 formation was suppressed with increasing Ti loadings in favour of a $CoTiO_3$-like surface phase, which accounted for the increase in Co-o with increasing titania loading. Thus two forms of Co-o were present on the surfaces of Co/Al_2O_3-TiO_2; Co-o-Al formed through interaction with alumina and Co-o-Ti formed by interaction with titania surface phase. The increase of Co-o inhibited agglomeration of cobalt during calcination and resulted in increased dispersion. Chin and Hercules /99/ studied the effect of 1 and 2 w-% additions of zinc on surface properties of impregnated 0 ... 20 w-% Co/Al_2O_3. The influence of zinc on the Co/Al_2O_3 catalyst appeared to be twofold. At low cobalt concentrations (0 ... 8 w-% Co) the presence Zn^{2+} enhanced the formation of the Co-t interaction species. Above 8 w-% Co, the dominant species on the surfaces of both catalysts was Co_3O_4, but dramatic differencies in dispersion were observed for doped and undoped catalysts as a result of stabilization of the Co oxide particles in the presence of zinc.

The reducibility of Co/Al_2O_3 catalysts has been found to depend strongly on the metal loading and calcination temperature. It has been established that the ability of the catalysts to undergo reduction is hindered by strong metal-support interaction. This has been attributed to the formation of the chemically inert Co-t species. Temperature-programmed reduction studies (TPR) carried out by Castner and Santilli /97/, Wang and Chen /100/ and Lapidus et al /101/ indicated that the surface spinel Co-t was resistant to reduction even at temperatures above 850 °C and it corresponded the structure of $CoAl_2O_4$. Hence, for conditions which favoured the formation of Co-t the percentage of reducible cobalt was suppressed. The influence

of the Co-t species on catalyst reducibility was especially prevalent for catalysts of low metal loadings and high calcination temperatures /93,100/. An increase in metal concentration favoured the formation of Co-o and Co_3O_4, which were readily reduced. Although the reducibility increased as a function of metal content, also dispersion affected it. Generally, dispersion decreased with increasing metal loading, and a decrease in dispersion resulted in lower reducibility. This was consistent with segregation of Co_3O_4 on the catalyst surfaces at concentrations of 12 w-% Co. As more of the cobalt on the catalyst surface was used to form Co_3O_4 crystallites, the cobalt dispersion decreased, along with a new decrease in reducibility /93/.

The reduction of Co_3O_4 takes place in two steps: Co_3O_4 ---> CoO ---> Co as indicated in TPR studies of Brown et al /102/. However, it should be noted, that the reduction temperatures for Co_3O_4 on alumina were higher than those of bulk Co_3O_4 /97,100/. This temperature effect was suggested to be due to (i) the smaller metal oxide particles present in CoO/Al_2O_3 rendering them more difficult to reduce than the larger particles of bulk Co_3O_4, (ii) some cobalt oxide-cobalt aluminate interaction resulting in difficulty in the reduction of cobalt oxide, (iii) some Co^{3+} species different from Co_3O_4 present on the support surface /100/. However, Castner et al /103/ suggested that high reduction temperature of supported cobalt was due to the presence of small pores in the catalyst causing H_2O buildup and carrier migration and not due to a cobalt oxide species that was inherently difficult to reduce, i.e. $CoAl_2O_4$. They observed that the Co_3O_4 to CoO step of the reduction was independent of particle size, morphology, and support properties, whereas the CoO to Co step was dependent on the particle size and support properties, with the ease of reduction decreasing with decreasing Co particle size.

Zowtiak et al /104/ and Zowtiak and Bartholomew /105/ applied the technique of temperature-programmed desorption (TPD) to the investigation of hydrogen adsorption and desorption from a series of cobalt catalysts. The results obtained quantitatively evidenced that adsorption of H_2 on cobalt was activated, i.e. the quantity of hydrogen adsorbed on cobalt increased with increasing temperature. The extent of activation was a function of support and metal loading. Reuel and Bartholomew /106/ and Fu and Bartholomew /107/ determined that H_2 adsorption uptake of a Co/Al_2O_3 catalyst increased and the activation factor, which is

the ratio of maximum H_2 uptake to room temperature uptake, decreased with increasing cobalt content. Hence, the degree of H_2 activation decreased with increasing cobalt loading. The results suggested, that the activation barrier for dissociative adsorption on cobalt increased with increasing degree of metal-support interaction.

The observation, that hydrogen adsorption on supported cobalt was strongly activated had important implications in regard to experimental practices for measuring hydrogen adsorption uptakes on cobalt catalysts. There are essentially two alternatives: (i) measurement of the total H_2 uptake at the temperature of maximum adsorption, determined separately for each cobalt catalyst or (ii) measurement of the total uptake at 25 °C after cooling in H_2 from the reduction temperature (e.g., 400 - 450 °C). In using either alternative it should be emphasized that total monolayer coverage is best obtained using the static adsorption technique, since flow technique measures only strongly held hydrogen and since a portion of the hydrogen monolayer on cobalt is reversibly adsorbed /105,106/.

Reuel and Bartholomew /106/ studied CO adsorption on cobalt/alumina catalysts to determine the effects of support, preparation and loading. The following apparent general trends important in result interpretation and comparison were obtained: the increase in cobalt loading lead to (i) increased percentage of reduction, (ii) decreased percentage of dispersion and (iii) increased crystallite diameter. Unlike hydrogen, carbon monoxide adsorption on cobalt catalysts did not increase at elevated temperatures, i.e. was apparently not activated. The data obtained evidenced of a wide variation in CO adsorption stoichiometry with cobalt dispersion, support, metal loading and preparation. The number of CO molecules per cobalt surface atom ($CO:Co_s$ ratio) generally decreased with increasing loading (i.e. increasing reduction). The $CO:Co_s$ ratio of impregnated Co/Al_2O_3 varied in the range 0,4 ... 1,1 with 1 ... 15 w-% Co loadings. The $CO:Co_s$ ratio of a precipitated 3 w-% Co/Al_2O_3 catalyst was significantly higher, 1,7. This variability of adsorption stoichiometry was probably due to the adsorption of CO in combinations of different configurations, i.e., bridged, linear and gem-dicarbonyl forms. The bridged species apparently predominated in poorly dispersed unsupported cobalt, whereas linear and gem-dicarbonyl species predominated in well dispersed supported cobalt catalysts. Lapidus et al /101/

determined the IR spectra of adsorbed carbon monoxide on freshly reduced 10 w-% Co/Al_2O_3 catalyst. Carbon monoxide was found to be adsorbed in four different states: on Co^{2+} ions and metallic centres with less marked electron donor properties ($Co^{\delta+}$ centres) in linear forms, and on metallic particles (Co^0) in linear and bridged forms. The amount of adsorbed carbon monoxide was found to increase as the degree of cobalt reduction decreased, which agreed with results of Reuel and Bartholomew /106/. Thus the increase in the pretreatment temperature led to a formation of new oxide phases $xCoO \cdot yAl_2O_3$, that contained carbon monoxide adsorption centres.

Reuel and Bartholomew /106/ and Lee et al /108/ determined the ratio of the number of CO molecules irreversibly adsorbed per hydrogen atoms irreversibly adsorbed on 1 ... 20 w-% Co/Al_2O_3 catalysts. They observed that the $(CO:H)_{irrev}$ ratio and catalyst dispersion decreased with increasing metal loading and extent of reduction. Lee et al /108/ carried out experiments with constant metal loading of 10 w-% together with only slightly varying particle size in order to define whether the changes in $(CO:H)_{irrev}$ with cobalt loading were due to the particle size or to the extent of reduction. The ratio was found not to be a function of the extent of reduction, but of dispersion only. On the other hand, the dispersion estimated from hydrogen uptake did not remain constant with reduction extent at constant loading. The values of $(CO:H)_{irrev}$ at low extents of reduction (7,9 ... 17,2 %) were very high (15,7 ... 6,0 respectively). Hence hydrogen chemisorption on poorly reduced cobalt particles was found to be highly suppressed resulting in underestimated dispersions calculated from hydrogen uptakes. Reuel and Bartholomew /106/ also observed that the catalysts prepared by pH controlled precipitation had larger $(CO:H)_{irrev}$ ratios than their impregnated counterparts /106/. The decreases in $(CO:H)_{irrev}$ ratios apparently resulted from a combination of changes in the $CO:Co_s$ adsorption stoichiometry and in the fraction of H_2 which was irreversibly adsorbed. The observed adsorption ratios were attributed to metal-support interactions.

Nakamura et al /109/ studied the reactivity and characteristics of the carbon deposited on Co/Al_2O_3 by disproportionation of CO. They classified the carbonaceous species into three types, highly reactive CH_x; CH and/or CH_2, which gave methane and ethane in the reaction with H_2, reactive carbidic carbon and less reactive graphitic carbon. The carbidic carbon was formed at low temperatures, whereas the reversible

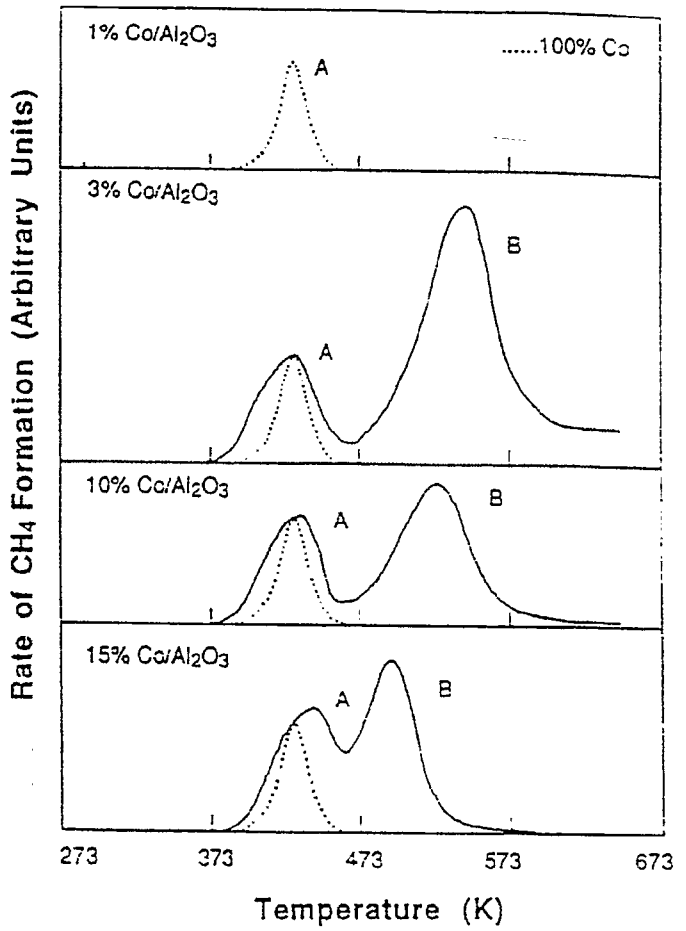

Figure 12. CH_4 TPSR spectra for unsupported cobalt (shown as the dotted line) and Co/Al_2O_3 catalysts of different metal loadings. Co/Al_2O_3 catalysts were reduced at 375 °C and CO was adsorbed at 25 °C in He /110/

formation of graphitic carbon was preferred temperatures higher than 300 °C. Lee and Bartholomew /110/ studied the temperature-programmed surface reaction (TPSR) of hydrogen with adsorbed CO on 1 ... 15 w-% Co/Al_2O_3 in order (i) to identify active sites and/or reaction states for CO hydrogenation on Co/Al_2O_3, (ii) to investigate the effects of metal loading and the pretreatment on distributions of these sites/states, and (iii) to shed light on the origin of the apparent structure sensitivity in

CO hydrogenation observed on Co/Al_2O_3 catalysts. The results of hydrogen TPSR with CO adsorbed on Co/Al_2O_3, shown in Figure 12, indicated two methane reaction states: A at 167 ± 7 °C, the position of which was relatively invariant with metal loading or reduction temperature, and B at 227 ... 700 °C, the position of which was highly dependent upon metal loading and reduction temperature as indicated in Table 5. The data of this study was consistent with the assignment of peaks A and B to two reaction states of differing rates. The A state for Co/Al_2O_3 accounted for hydrogenation of CO adsorbed on Co metal atoms bonded to other Co atoms, e.g., Co atoms in large, three-dimensional (3D) crystallites. Indeed only A state was observed on the completely reduced unsupported Co catalyst (see Fig. 12), which consisted entirely of large 3D Co metal crystallites. State B apparently took place on both large and fairly inaccessible small crystallites and it involved species created on sites in the presence of the support and having chemical properties distinct from those of the A sites. In fact, state B was assigned for decomposition of CH_xO-complex formed on the support as a result of spill over of the adsorbed CO and hydrogen from sites A to the Al_2O_3 support. The results were consistent with the analysis of Anderson and Jen /111/ on the mobility of OCH_3^- and H^+ and their reaction to form CH_4 on alumina using the atom superposition and electron delocalization molecular orbital (ASED-MO) theory. Theoretical evidence was given, that OCH_3^-, which is known to spill over from supported Ni and Pt to the alumina support, moves as an anion, OCH_3^-, from one Al^{3+} site to another, paired with a proton, which moves from one O^{2-} site to another. Hence two different methanation mechanisms occurred on Co/Al_2O_3: (1) hydrogenation of α-carbon (reaction A) and (2) decomposition of a CH_xO complex (reaction B) formed on the support. Both reactions occurred on metallic sites. The distribution of these reactions (states) was a function of metal loading and reduction temperature; the fraction of methane formed by reaction A increased with increasing metal loading and extent of reduction. In addition, the activity of the B state increases with increasing metal loading, further explaining the higher activity of high metal loading catalysts. Furthermore, at low reaction temperatures, reaction A predominated, whilst at high reaction temperatures reaction B predominated due to its higher activation energy.

Table 5. Methane peak temperatures, areas, and area ratios as functions of metal loading and reduction temperature /110/.

Catalysts and reduction temp. (K)	Peak temp. (K)		Peak area[b]		Peak area ratio[c] $A/(A+B)$
	A	B	A	B	
1% Co/Al_2O_3					
1023	447	757	1	1	0.42
3% Co/Al_2O_3					
648	432	543	1	1	0.23
773	432	553	2.17	1.57	0.29
873	432	581	3.31	2.26	0.30
973	432	613	4.79	2.46	0.37
10% Co/Al_2O_3					
648	432	526	1	1	0.34
773	432	543	2.06	2.12	0.33
873	432	548	3.12	2.61	0.38
15% Co/Al_2O_3					
648	440	494	1	1	0.41
773	434	509	1.22	1.19	0.38
873	434	517	1.47	1.29	0.40

[a] Based on the CH_4 TPSR for CO adsorbed at 298 K.
[b] Methane peak areas normalized with respect to those for 648 K reduction (except for 1% Co/Al_2O_3).
[c] Ratio of the area of Peak A to the sum of areas for Peaks A and B.

The previously presented study of Lee and Bartholomew /110/ therefore supported both of the previously suggested mechanisms of methanation and related them to reaction states A and B. Hence A corresponds to the mechanism known as "carbide" mechanism and B to enolic "complex" mechanism. Agrawal et al /112/ have summarized the previous results and represented the reaction sequence of the "carbide" mechanism as follows:

$$CO(g) + * \text{<--->} CO_{ad}$$
$$CO_{ad} + * \text{<--->} C_{ad} + O_{ad}$$
$$H_2 + 2* \text{<--->} 2H_{ad}$$
$$C_{ad} + H_{ad} \text{<--->} CH_{ad} + *$$
$$CH_{ad} + H_{ad} \text{<--->} CH_{2ad} + *$$
$$CH_{2ad} + H_{ad} \text{<--->} CH_{3ad} + *$$
$$CH_{3ad} + H_{ad} \text{<--->} CH_{4ad} + *$$
$$CH_{4ad} \text{<--->} CH_4(g) + *$$

where * represents a vacant surface site. The reaction sequence of the second mechanism referred as the "enolic complex" mechanism can be represented as

$CO(g) + * <---> CO_{ad}$

$H_2 + * <---> H_{2ad}$

$CO_{ad} + H_{2ad} <---> CHOH_{ad} + *$

$CHOH_{ad} + H_{2ad} <---> H_2O + CH_{2ad}$

and so on. A survey of the rate equations derived by considering the "carbide" and "enol complex" theory indicated, that the general form of the rate equations was the same in both mechanisms for similar rate-controlling steps. Using dissociative chemisorption of H_2 in the "enol complex" mechanism would have yield an identical dependence of the methanation rate on H_2 concentration in both cases. However, Auger electron spectroscopy suggested, that CO hydrogenation proceeded at least partially via a surface carbon intermediate. A good agreement between the experimental data on CO hydrogenation over Co/Al_2O_3 and the model was attained if the catalyst surface was assumed to consist of two types of sites active for methanation, with each type having different heats of adsorption for CO and H_2. The first type of surface sites had a high heat of CO adsorption and yielded a maximum rate of methanation at very low CO concentrations; the second type of sites had a lower heat of adsorption which shifted the CO concentration required to achieve the maximum rate of methanation to a much higher value. The results of Agrawal et al /112/ were consistent with reaction states A and B, since the adsorption of CO on Al_2O_3 was weak, nondissociative and small relative to that on the CO under the conditions of TPSR experiment /110/. Lapidus et al /113/ extended the multiple reaction route mechanism further by supposing that the weaker adsorption sites that adsorb carbon monoxide in a non-dissociated linear form, were responsible for the formation of liquid hydrocarbons on Co/Al_2O_3 catalysts.

In summary, the following apparent general trends of Co/Al_2O_3 were obtained /106,107,108,110/: the increase in cobalt loading led to (i) increased percentage of reduction, (ii) decreased percentage of dispersion and (iii) increased crystallite diameter. The CO adsorption and hydrogenation on alumina-supported cobalt took place by two mechanisms: (state A) CO dissociation followed by hydrogenation and (state B) spillover of CO and H to the support forming CH_xO-complex, which subsequently decomposed on the metal. At low reaction temperatures state A predominated and determined the overall rate, whilst at high reaction temperatures

state B dominated the reaction rate due to its higher activation energy. Catalysts of higher metal loading and extent of reduction involved a higher fraction of the state A together with increasing activity of the state B, and were more active in CO hydrogenation /110/. In fact, a 10 ... 20 fold increase of Co/Al_2O_3 catalyst activity was found by Fu and Bartholomew /107/, Lee et al /108/ and Reuel and Bartholomew /114/ as metal loading increased within range 2 ... 25 w-%.

Lapidus et al /113/ extended the multiple reaction route mechanism further to describe hydrocarbon formation from carbon monoxide and hydrogen. They supposed that the weaker adsorption sites that adsorbed carbon monoxide in a non-dissociated linear form, were responsible for the formation of liquid hydrocarbons on Co/Al_2O_3 catalysts. Hence, high reaction temperature and low metal loading together with low extent of reduction should increase the fraction of state B, and enhance the selectivity of liquid hydrocarbon formation. However, the selectivity results obtained at 1 bar and 225 °C by Reuel and Bartholomew /114/ showed that in the Co/Al_2O_3 system, activity and selectivity for high molecular weight hydrocarbons increased dramatically with increasing cobalt loading. The 15 w-% cobalt catalyst was found to be 20 times more active than 3 w-% catalyst and moreover, 86 % of its hydrocarbon fraction was in the C_5 ... C_{12} (gasoline) range compared with 18 w-% respectively (Figure 13).

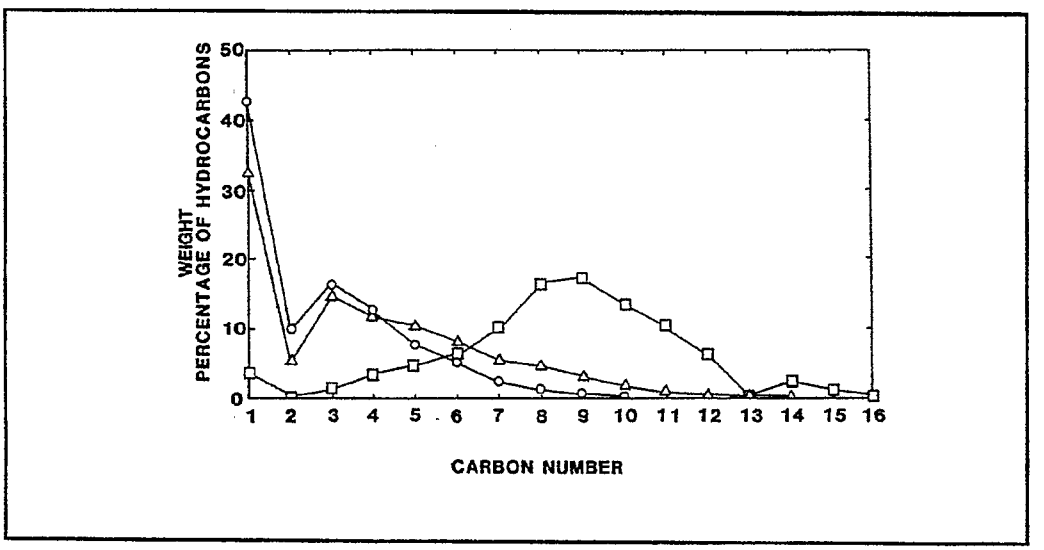

Figure 13. Hydrocarbon product selectivity for impregnated Co/Al_2O_3 at atmospheric pressure. ○, 3 % Co/Al_2O_3 at 225 °C; △, 10 % Co/Al_2O_3 at 225 °C; □, 15 % Co/Al_2O_3 /114/.

Similar observation was made by Wang and Chen /100/ and Lee et al /108/. They explained the increasing production of higher hydrocarbons with increasing cobalt content by changes in the adsorption strength of carbon containing intermediates. The increasing strength might have resulted in longer residence times of carbon containing reaction intermediates on the surface, and the intermediates probably propagated more easily to higher hydrocarbons. The decrease in alkene fraction with the increase in cobalt loading was possibly due to the stronger competition of hydrogen against carbon monoxide for active sites. The selectivity of alcohols on Co/Al_2O_3 /114/, however, increased with decreasing metal loading and decreasing reduction. Hence, state B appeared to enhance formation of oxygen containing products rather than the hydrocarbon chain growth. Nevertheless, Anderson and Jen /111/ calculated the $CH_4(g)$ formation on the support as more stabilizing than $CH_3OH(g)$ formation. Since the spilled over heterolytic pair was so stable, methanol generation from it was considered a high temperature process.

The effect of promoters on CO hydrogenation activity of Co/Al_2O_3 has been investigated by various authors. Castner and Santilli /97/ performed CO hydrogenation at 260 °C and 10 bar with H_2:CO ratio of 3:1 on 5 w-% Co/Al_2O_3. They observed, odd enough, a large fall of conversion from 17 to < 5 % with Co/Al_2O_3 catalyst compared to the $Co/K\text{-}Al_2O_3$ catalyst, despite of the same amount of reduced cobalt present in both. Hence the effect of potassium could have originated from direct interaction with adsorbed CO or hydrogen. However, consistent results have been obtained with potassium addition on Rh as described in section 2.1. Ledford et al /96/ studied CO hydrogenation activity of 10 w-% Co/Al_2O_3 catalysts at 1 bar and 185 °C with La:Al atomic ratio of 0 ... 0,078. The results were consistent with the observed structural changes imposed by the promotor, described previously. Hence, the low lanthanum content of up to La:Al 0,013 had little influence on the activity and selectivity of the reduced catalyst in CO hydrogenation. With higher loadings (La:Al > 0,026) the turnover frequencies for CO hydrogenation decreased and the selectivity to higher hydrocarbons and olefins increased dramatically for high La loadings. This selectivity increase was attributed to the formation of lanthanum-promoted sites on the catalyst. Stranick et al /98/ studied the influence of TiO_2 on CO hydrogenation activity over Co/Al_2O_3 under differential conditions with CO:H_2 of 1:3 at 185 °C. They found that the CO

hydrogenation rates and turnover frequencies decreased sharply with increasing TiO_2 loadings. For low Ti loadings the decrease was attributed to a site-blocking mechanism resulting from a migration of reduced TiO_2 species. Particle size changes and variation in the extent of Co reduction might have contributed to the decrease at high Ti loadings. Dent and Lin /115/ studied the addition of various amounts of manganese on Co/Al_2O_3. The CO hydrogenation carried out using 10 % CO, 30 % H_2 and 60 % He feed at 7,8 bar at 227 °C showed, that Mn doped catalyst produced more C_2 ... C_4 olefins. An alkali (K_2O) addition to Mn containing cobalt catalyst improved the olefin selectivity further. The effect of 5 ... 30 w-% copper addition on $CoAl_2O_4$ on the catalyst structure, activity and selectivity at 40 bar pressure and 270 °C temperature was studied by Baker et al /116/. They observed that an addition of copper to the cobalt spinel resulted in a sharp increase in the amount of cobalt reduced, and this was reflected by the large increase of overall activity which had a maximum. The activity for the formation of methanol and other oxygenates also passed through a maximum, hence their formation was not directly related to the amount of Cu-Co bimetallic phase.

The deactivation process of the Co/Al_2O_3 was clarified by kinetic studies of the initial catalytic activity and of each of the pseudo steady state activity regions. Agrawal et al /112,117,118/ studied CO hydrogenation over alumina supported cobalt under sulphur-free and sulphur poisoning conditions at atmospheric pressure at temperatures of 200 ... 400 °C. Under sulphur free conditions two steady-states were observed: (i) an upper pseudo steady state and (ii) lower pseudo steady state. A third steady state was observed for sulphur poisoned Co catalyst. Under sulphur free conditions the catalytic activity decreased only slowly (apr. 30 % per 24-h period) over a period whose duration was shorter at higher temperatures or higher CO concentrations; this period was referred to as the upper pseudo steady state. At the end of the upper pseudo steady state period, the rate of catalyst deactivation accelerated and the activity drops almost 50-fold before approaching the lower pseudo steady state, as shown in Figure 14 /117/. The rate of deactivation in the lower steady state was about the same as in the upper pseudo steady state. The AES examination of the catalyst removed from the reactor while it was still in the upper pseudo steady state showed mainly Co on the surface with very small amounts of carbon, less than 10 ... 20 % of a monolayer. Hence the CO hydrogenation activity

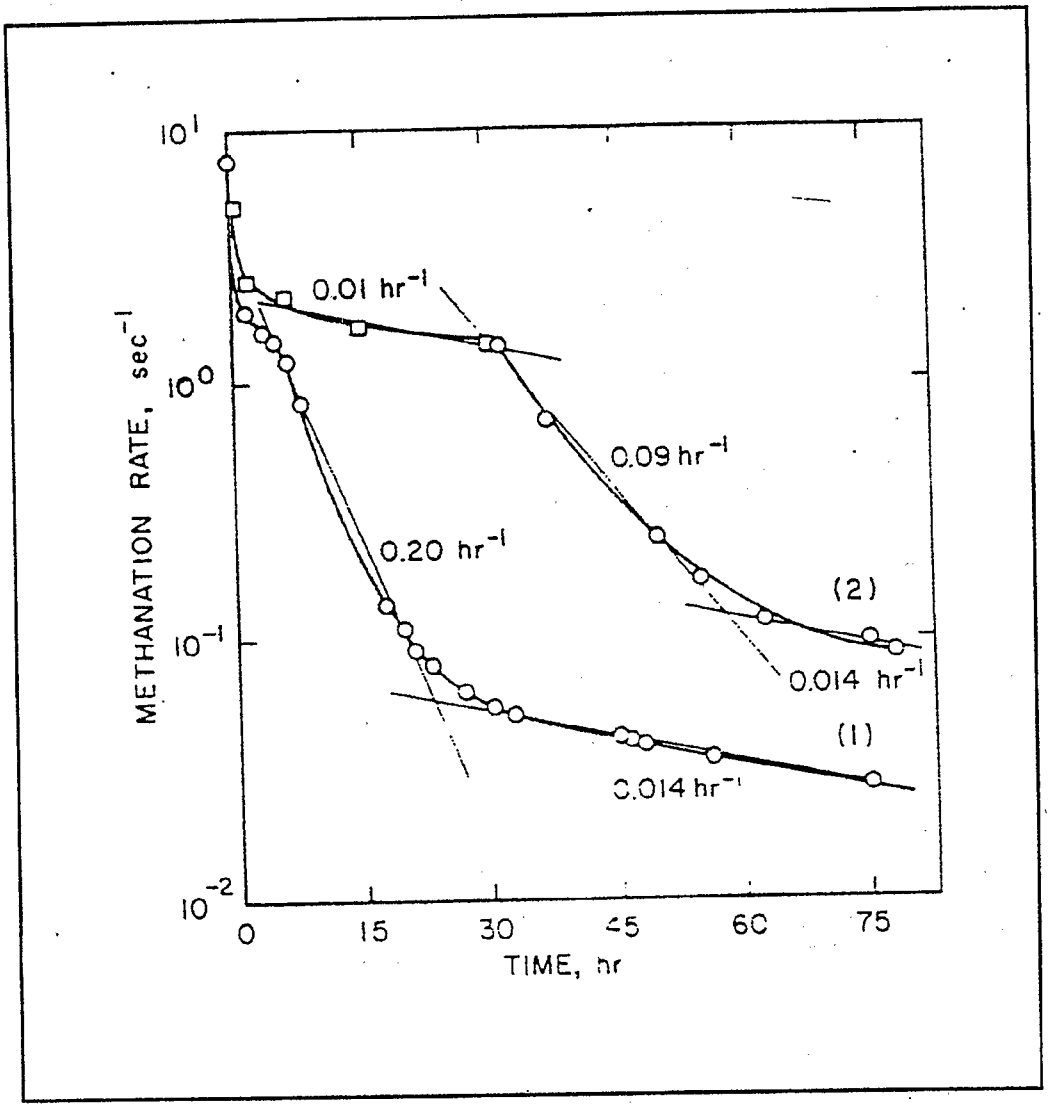

Figure 14. Effect of CO concentration on deactivation of Co/Al_2O_3. Reaction conditions: (1) ○ 0-4 % CO in H_2 at 400 °C; (2) □ 0,5 % CO in H_2 at 400 °C, ○ 0-4 % CO in H_2 at 400 °C /117/.

in the upper pseudo steady state was that of metallic Co. For Co catalysts deactivated to the lower pseudo steady state, AES showed an almost complete absence of Co on the surface with as little as 1 % present in some. Hence, extensive coverage of graphitic carbon and bulk carburization to a depth of several hundred ångströms existed. Therefore the CO hydrogenation activity was that of a deactivated, carburized Co; about 10^2-fold lower than that in the upper pseudo steady state, but the selectivity to higher hydrocarbons was unchanged. This implied that there was no change in the mechanism or in the rate-limiting step of the reaction in transition from

the upper to lower steady state. However, the extent of deactivation influenced the regenerability by H_2 at 400 °C considerably: Co surfaces containing a fractional monolayer were fully regenerated, whereas Co surfaces containing multilayer graphitic deposits were not regenerable, and showed no CO intensity increase. A third steady state was observed for sulphur poisoned Co catalyst. In the presence of 13 ppb of H_2S the steady-state methanation activity with 1 % CO in H_2 on Co/Al_2O_3 was reduced by almost four orders of magnitude. The poisoning resulted from the formation of a two-dimensional, saturated sulphide layer corresponding to one sulphur atom per two surface Co atoms. In the sulphur poisoning of Co/Al_2O_3 carbon did not play any significant role; sulphur absolutely dominated /112,118/.

2.2.2 Cobalt on silica

Silica has been used as a support to Co catalysts to minimize the metal-support interaction and to isolate the effect of particle size from effects of other variables. Calcined Co/SiO_2 catalysts have been characterized as a function of catalyst preparation and pretreatment by Castner et al /119/ and Ho et al /120/. Castner et al /119/ impregnated 10 w-% of Co on precalcined (500 °C) supports, and recalcined the dried catalysts at 250 °C for 1 h and at 450 °C for 2 h. Ho et al /120/ prepared two catalyst series on precalcined support (pore volume 1,0 cm^3/g) 400 °C, 8 h): (i) with 1 ... 10 w-% Co impregnation followed by drying and calcining at 100 °C for 300 h, and (ii) with constant 3 w-% Co impregnation followed by drying and heating in vacuo at 200 ... 400 °C. The results of several characterization techniques utilized in these studies, i.e. XAS, XPS, AEM, XRD, ESCA and H_2 chemisorption, showed that Co_3O_4 was the major, and probably only, cobalt species present in the calcined catalysts /97,101,119,120/. The data of Castner et al /119/ indicated that for bulk Co_3O_4 the particles were octahedrally shaped and 1 - 5 μm in size. 10 w-% Co on small pore size silica (mean pore size 143 Å) resulted in Co_3O_4 particles 100 ... 300 Å in size, clustered together in 0,1 - 1 μm aggregates. When 10 w-% Co was loaded on large pore size silica (mean pore size 33 Å) the particles were less than 60 Å in size /119/. Ho et al /120/ observed, that cobalt dispersion decreased with increasing calcination and that cobalt phase was better dispersed in vacuo calcined than air calcined catalysts.

The hydrogen reduction properties of Co/SiO_2 catalysts described above /119,120/ have been examined by Castner et al /103/ and Ho et al /120/ and respectively of Co/KG (KG stands for kieselguhr) catalysts by Sexton et al /121/ and Viswanathan and Gopolakrishnan /122/. Castner et al /103/ identified spectroscopically that the reduction process proceeded as Co_3O_4 ---> CoO ---> Co. The first step of the reduction occurred near 300 °C for all Co/SiO_2 catalysts. Similar results were obtained for Co/KG catalysts /121,122/. Thus the Co_3O_4 to CoO step in the reduction process was virtually unaffected by the differencies in particle size, morphology, pore size and surface area of the catalysts. In contrast, the second step showed significant differencies among the samples as shown in Figure 15, and complete reduction was obtained above 600 °C. A likely explanation to the observed differencies in CoO to Co reduction step was the $H_2O:H_2$ ratio in the immediate vicinity of the cobalt oxide particles. One molecule of H_2O was produced for each Co^{2+} reduced to a Co^0 atom. The H_2O molecules had to be removed in order to drive the reduction reaction to completion and this removal was relatively easy for the bulk Co_3O_4 and large pore Co/SiO_2 catalyst on contrary to small pore size Co/SiO_2.

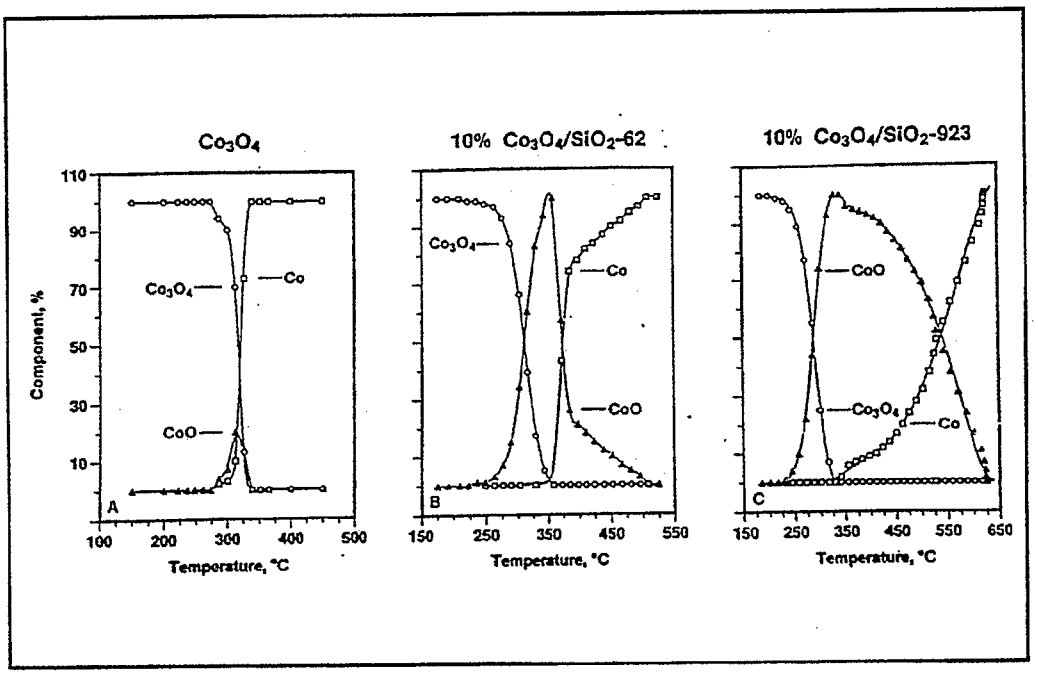

Figure 15. XAS/TPR results showing changes in Co_3O_4, CoO and Co concentrations with temperature for (A) Co_3O_4, (B) small pore Co/SiO_2 and (C) large pore Co/SiO_2. The reduction was carried out at 1 bar of flowing H_2 with a temperature ramp of 5 °C/min /103/.

Furthermore, the H_2O present in the pores can also lead to silica migration resulting in encapsulation or reaction with the Co particles. Reduction resulted in Co metal particles 30 ... 50 % smaller in size than the Co_3O_4 particles. The Co particles of small pore Co/SiO_2 were 90 Å in size, grouped together in 0,1 ... 1 μm aggregates. The Co particles of large pore Co/SiO_2 were 35 Å in size. Ho et al /120/ observed an increase in cobalt particle size from 10 to 18 nm with increasing cobalt loading. A particle size increase from 5 to 9 nm was found with 3 w-% vacuo calcinated cobalt catalysts with increasing decomposition temperature. However, no particle size effect on CO hydrogenation turnover frequency for Co/SiO_2 was found in the cobalt dispersion range of 6 ... 20 %. Rosynek and Polansky /123/ investigated the effect of identity of the cobalt salt employed in the surface reduction properties of silica-supported cobalt catalysts. They observed that reduction of $Co(NO_3)_2/SiO_2$ involved an initial reductive decomposition to form CoO_x-SiO_2 surface species that were difficult to reduce completely to metallic cobalt. By contrast, reduction of the supported chloride salt occurred in a single step that was unaffected by the presence of the silica support and that resulted in almost complete reduction to zero-valent cobalt. Calcination at 500 °C prior to reduction treatment produced Co_3O_4/SiO_2 from the nitrate and chloride precursors, whilst a Co_3O_4 phase was not observed with the calcined acetate precursor. Precalcination enhanced the extent of subsequent bulk reduction in hydrogen for all three of the silica supported cobalt salts.

The effects of modifications on the characteristics of Co/SiO_2 catalysts has been studied by various authors. Takeuchi et al /124/ studied the effect of alkaline earth metals on silica-supported cobalt catalysts prepared from dicobalt octacarbonyl. The high pressure *in situ* FT-IR studies showed, that both linear and bridged species were present on the Co(CO)-Ba/SiO_2, whereas linear species predominated on both $Co(CO)/SiO_2$ and Co(CO)-Mg/SiO_2. The presence of bridged species was related to the formation of alcohols. Sexton et al /121/ and Viswanathan and Gopalakrishnan /122/ studied the effect of ThO_2 and MgO, on 3 ... 50 w-% cobalt supported on kieselguhr. Sexton et al /121/ observed very little, if any, interaction between the Co_3O_4 phase and promotors, whereas the promoters appeared to retard the reduction of CoO. The relative rates of reduction at 400 °C were higher for non-magnesia-containing catalysts than magnesia-containing ones. It was proposed that CoO formed a solid solution with MgO at 400 °C and this new phase was more resistant to

reduction. The nature of ThO_2 was less clear; presumably a mixed ThO_2-CoO phase of unknown structure was formed resulting in a higher kinetic or thermodynamic barrier to reduction. In contrast to these results, Viswanathan and Gopalakrishnan /122/ observed that the presence of ThO_2 increased the extent of reduction by hindering the migration of kieselguhr over the active phase. Takeuchi et al /125/ studied silica supported cobalt catalysts promoted with ruthenium and alkaline earths. The XPS analysis indicated that the cobalt in Co/SiO_2 catalyst remained in the divalent state even after treatment in a stream of hydrogen at 450 °C, and was tightly bound with high dispersion on the surface of SiO_2 through S-O-Co^{2+} bonds. The coordination structure of the cobalt atom in this catalyst was similar to that of cobalt(II)acetate. Divalent cobalt atoms were readily reduced in a stream of hydrogen to a zerovalent state by the modification with ruthenium chloride. Furthermore, the ruthenium and cobalt metals in the Co-Ru(CO) catalyst systems were highly dispersed on silica, whereas the cobalt metal in the Co-Ru(Cl) system was much larger than that in the Co-Ru(CO) catalyst system. The alkaline earth additives were found to depress the reduction of cobalt.

Zowtiak et al /104/, Zowtiak and Bartholomew /105/ and Reuel and Bartholomew /106/ investigated the hydrogen and CO adsorption/desorption of Co/SiO_2 catalysts as described in detail in section 2.2.1. Wiswanathan and Gopalakrishnan /122/ determined hydrogen and CO adsorption of 3, 10, 15, 20 and 25 w-% cobalt supported on prepurified kieselguhr and reduced at 327 °C for 48 h. These studies showed that adsorption of H_2 on cobalt supported on silica was less activated than on alumina. Nevertheless, the H_2 adsorption uptake of Co/SiO_2 and Co/KG catalyst increased and the activation factor decreased; for example with Co/SiO_2 from 1,3 to 1,0 when cobalt content increased /104,105,106,122/. Unlike hydrogen, CO adsorption on cobalt catalysts was not activated. The CO:Co_s ratio of impregnated Co/SiO_2 decreased from 1,3 to 0,7 with an increase in cobalt loading from 3 to 10 w-% /106/ but that of Co/KG increased from 0,1 to 0,8 with an increase in cobalt loading from 3 to 33,3 w-% /122/. However, in the case of Co/KG the percentage of reduction did not increase as metal loading increased, rather vice versa /122/. The CO/Co_s ratio of a precipitated 3 w-% Co/SiO_2 catalyst was 1,2 /106/. Lapidus et al /101/ found the uptake of CO at 1 bar and 20 °C of 10 w-% Co/SiO_2 catalyst to increase, while both the degree of reduction and percentage of dispersion decreased.

Moreover, this increase was markedly higher than with respective Co/Al_2O_3 catalyst. According to Reuel and Bartholomew /106/ the $(CO:H)_{irrev}$ ratio of impregnated Co/SiO_2 decreased from 2,5 to 0,8 with an increase of metal loading from 3 to 10 w-%; an apparent consequence from a combination of decreasing $CO:Co_s$ and increasing fraction of irreversibly adsorbed H_2 as metal loading increased. However, the $(CO:H)_{irrev}$ ratio was exceptionally high, 14, with precipitated 3 w-% Co/SiO_2.

Catalytic activity and selectivity studies have shown Co/SiO_2 to be an effective CO hydrogenation catalyst. Castner and Santilli /97/ carried out CO hydrogenation by $3H_2$:CO mixture at 10 bar at 260 °C and found Co/SiO_2 more active than Co/Al_2O_3. The higher CO conversion with the same amount of catalyst was presumably due to better reducibility. The selectivities, however, did not differ significantly. Reuel and Bartholomew /114/ studied the specific activity and selectivity of Co/SiO_2 at low conversions, 1 bar and 175 ... 350 °C. For catalysts containing 3 w-% Co the specific CO hydrogenation activity of Co/SiO_2 was higher than that of Co/Al_2O_3. The specific activity as well as the production of heavier hydrocarbons increased with increasing cobalt content, as shown in Figure 16 /114/. With a constant loading of 10 w-% cobalt, Lipidus et al /113/ observed that the increasing calcination temperature of Co/SiO_2 resulted in (i) decreasing reducibility, (ii) increasing turnover frequencies of carbon monoxide conversion, (iii) markedly decreasing total hydrocarbon yield and (iv) slightly increasing average carbon number of the products. Rosynek and Polanski /123/ studied the effect of the identity of cobalt salt used in Co/SiO_2. They observed, that the activity of nitrate-derived catalyst decreased after precalcination, while both the chloride- and acetate-based catalysts exhibited higher activities. Nevertheless, with one exception (uncalcined reduced $CoCl_2/SiO_2$) all of the reduced precursors exhibited comparable catalytic activities for carbon monoxide hydrogenation at 250 °C and 1 bar, and their selectivities at comparable levels of conversion were virtually identical. Takeuchi et al /124,125/ also investigated the effect of cobalt precursor on 5 w-% Co/SiO_2 on the CO hydrogenation activity. The reactions were carried out at 21 bar and 220 ... 250 °C with $CO:H_2:Ar$ of 3:6:1. They observed, that the catalyst prepared from $Co_2(CO)_8$ was considerably more active than catalysts prepared from cobalt(II)nitrate, acetate and chloride listed in the decreasing order of activity. This $Co(CO)/SiO_2$ catalyst gave over 20 % oxygenate selectivity with 80 % formation of hydrocarbons in the syngas reaction. The catalysts prepared from other precursors

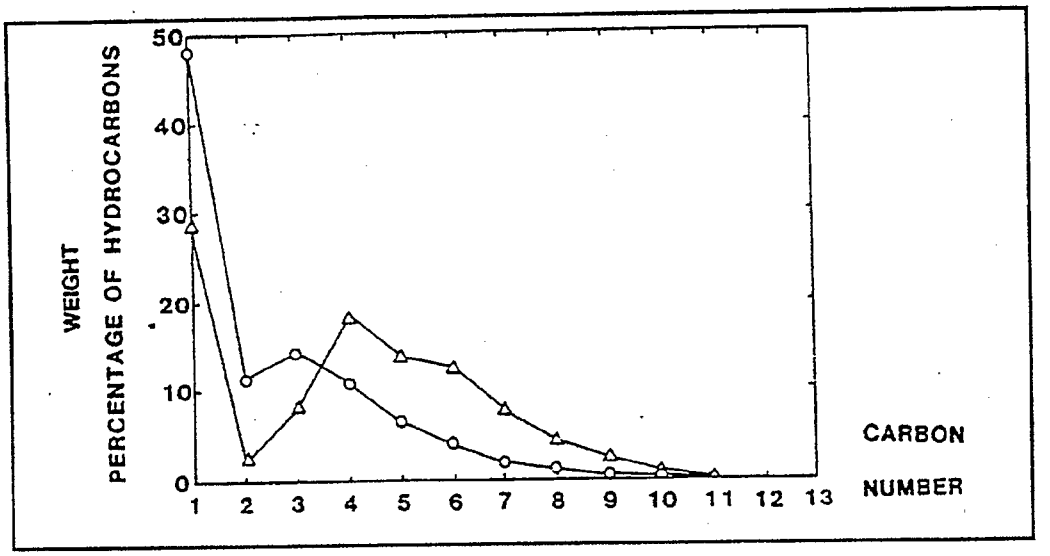

Figure 16. Hydrocarbon product selectivity for impregnated Co/SiO_2 at 225 °C and atmospheric pressure. ○, 3 % Co/SiO_2 ; △, 10 % Co/SiO_2 /114/.

were virtually inactive with respect to oxygenate formation. The results were considered as a first example of the formation of oxygenates by a cobalt catalyst in the absence of a promotor.

Takeuchi et al /124/ and Matsuzaki et al /126/ studied the effect of modification of highly dispersed Co/SiO_2 with alkali earth or alkali cations. Typical reaction conditions were $CO:H_2:Ar$ with 3:6:1 molar ratio, 21 bar, 300 ... 380 °C and GHSV 2000/h. They observed, that alkali earth and alkali modification decreased the overall reaction rate whereas it increased the selectivity to oxygenates. The results indicated that alkali cations were more effective as modifiers for C_2-oxygenates than alkaline earth cations. Moreover alkali metals enhanced the production of acetaldehyde and acetic acid, whereas ethanol comprised almost all of the C_2-oxygenated compounds in case of alkaline earth promotion. Selectivities to C_2-oxygenates were found to decrease in order of Ba>Sr>Ca>Mg for alkaline earth and K>Na>Li for alkali metals. The catalytic activity order was reversed. Fujimoto and Oba /127/ studied synthesis gas conversion over 5-(0...35)-(0...3)/100 w/w $Co-Mo-K_2O/SiO_2$ under 50 bar, 250 °C and $H_2:CO$ of 2:1. They observed, that alcohols with a distribution from

C_1 to C_7 were formed with fairly high selectivity; the total yields on carbon base were 3,8 % alcohols, 3,4 % hydrocarbons and 7,0 % CO_2. Cobalt was found essential for the catalyst activity and carbon-carbon bond formation whereas molybdenum and potassium were effective for promoting the alcohol formation. Molybdenum shifted the molecular weight of product alcohols downwards, whilst potassium was essential for the production of higher alcohols. Madon and Taylor /128/ studied CO hydrogenation over a precipitated, alkalized 100-16-2/93 in weight proportion Co-ThO_2-K/KG catalyst at pressures of 6 ... 11 bar and at 197 °C. The conversions during all experiments were high; the total (H_2 + CO) conversion of unsulphided catalysts was over 80 %, sulphided catalysts gave conversions 20 ... 30 % below those obtained for unsulphided catalysts. The selectivity to C_{5+}-hydrocarbons was consistently high, apr. 75 ... 85 %, indicating that less than 25 % of the CO was used to make gaseous hydrocarbons and CO_2. Ekstrom and Lapszewicz /129/ carried out CO hydrogenation in the integral mode at 208 °C with $H_2/H_2O/CO$ mixture over Co/MgO/ThO_2/KG catalyst. They found that the total conversion and the conversion to C_{2+} hydrocarbons increased linearly with increasing H_2:CO feed ratio, whereas the conversion of CO to CO_2 was independent of it. However, the methane yield decreased sharply with decreasing H_2:CO ratio, both absolutely and as a fraction of the total CO converted. Takeuchi /125,130/ carried out the conversion of syngas at 21 bar and 220 ... 250 °C with CO:H_2:Ar ratio of 3:6:1 over ruthenium or rhenium, and alkaline earth modified 5 w-% Co/SiO_2 prepared from acetate precursor. They observed, that the activity of cobalt catalysts was effectively enhanced and oxygenate selectivity slightly increased by ruthenium or rhenium modification although each metal component had little activity for these components. Addition of strontium to Co-Ru/SiO_2 or Co-Re/SiO_2 improved the C_2-oxygenate selectivity, but decreased the catalytic activity. The addition of alkaline earths to the Co-Ru(CO)/SiO_2 also depressed the catalytic activities and enhanced the formation of C_2-oxygenates. The C_2-oxygenate selectivity was found to increase in the order none< <Mg<Ca<Ba<Sr whereas the catalytic activity decreased in the order none> >Mg> >Ca>Sr>Ba. It was proposed, that CO hydrogenation proceeded on a cobalt site, ruthenium and rhenium promoted cobalt reduction and supplied activated hydrogen to cobalt size, and alkaline earths controlled the electronic state of cobalt metal and stabilized the oxygenated intermediates. Dent and Lin /115/ studied the addition of varying amounts of zirconia, copper, chromium and

manganese on cobalt impregnated on kieselguhr. The CO hydrogenation carried out using 10 % CO, 30 % H_2 and 60 % He feed at 7,8 bar at 227 °C showed, that the activities of the chromium- and zirconium doped catalysts were substantially higher than manganese or copper doped ones. These Cr and ZrO_2 containing catalysts were highly selective towards methanation, whereas Cu and Mn produced more C_2 ... C_4 olefins.

2.2.3 Cobalt on titania

TiO_2 provides a high surface area for the catalyzing metal, and moreover, through metal support interaction it strongly influences the catalytic behaviour of the metal as reviewed in section 2.1.3 over Rh/TiO_2. The Co/TiO_2 catalysts have, however, attracted considerably less attention.

Castner and Santilli /97/ found two cobalt oxide species, Co_3O_4 and Co^{2+}, present on the calcined Co/TiO_2 catalyst. After H_2 reduction at 480 °C, 85 % of the cobalt was metallic, with the remainder Co^{2+}. During the reduction also the total amount of Co detected by XPS decreased by a factor of two. This was possibly a consequence of either the cobalt particles sintering, cobalt diffusing into the TiO_2 support, or Ti oxide species diffusing onto the cobalt particles. Reuel and Bartholomew /106/ and Vannice /131/ observed that a less than a monolayer coverage of H_2 occurred on Co/TiO_2. This effect was presumably due to a strong interaction between cobalt and TiO_2 similar to the SMSI reported earlier for Group VIII metals on TiO_2. Vannice /131/ reported very low uptakes of both H_2 and CO gases on 1,5 w-% Co/TiO_2. The uptake results were, however, consistent with the ones observed by Reuel and Bartholomew /106/. They reported increasing H_2 uptake with increasing cobalt loading, and obtained the H_2 adsorption activation factor of 1 for 3 ... 10 w-% impregnated Co/SiO_2. The adsorption of CO was not activated as described earlier. The CO uptake increased with increasing Co loading and the $Co:Co_s$ ratio for impregnated Co/TiO_2 decreased slightly from 0,9 to 0,8 when loading was increased from 3 to 10 w-%. Again, a considerably higher value of 1,4 was obtained by precipitated 3 w-% catalyst. Moreover, the ratio $(CO:H)_{irrev}$ decreased with increasing metal loading, and it was higher for the precipitated catalyst, as a result of respective variations in

irreversible CO adsorption.

Reuel and Bartholomew /114/ reported that the specific activity (H_2:CO = 2, 1 bar, 225 °C) of 3 w-% impregnated Co/TiO_2 was higher than that of its precipitated counterpart, and moreover it was comparable to respective Co/SiO_2 and higher than 3 w-% Co/Al_2O_3. Moreover, Co/TiO_2 had a zero selectivity towards CO_2 production, and its fraction of heavier hydrocarbons increased with increasing metal loading, increasing extent of reduction and decreasing dispersion. Also Vannice /131/ observed comparable turnover frequencies of Co/TiO_2 and Co/Al_2O_3. In contrast, Castner and Santilli /97/ found that at 260 °C, 10 bar and $3H_2$:CO ratio the Co/TiO_2 had similar activity with Co/Al_2O_3, and a noticeably lower activity than Co/SiO_2 as a result of a large difference of cobalt reduction properties. Moreover, Co/TiO_2 catalyst produced less methane and more C_{5+} hydrocarbons.

2.2.4 Cobalt on magnesia, manganese oxide or carbon

Cobalt has also been supported by MgO and carbon. Reuel and Bartholomew /106/ stated that the trends of H_2 and CO adsorption on Co/MgO and Co/C catalysts were consistent with Co/Al_2O_3, Co/SiO_2 and Co/TiO_2. It was evident, that H_2 adsorption on Co/Al_2O_3 and Co/MgO was more highly activated than on Co/SiO_2, Co/C and Co/TiO_2. Moreover, the unexpectedly high dispersion of 36 - 86 % observed for the Co/C catalysts was perhaps a result of a fortuitous combination of preparation technique and the presence of active sites on the carbon ideal for binding with cobalt nitrate precursor.

Rao et al /132/ studied the surface properties of cobalt obtained from gas-phase deposition of $Co_2(CO)_8$ on fully dehydroxylated MgO. In addition to linear CO species they obtained evidence for the nucleophilic attack of basic surface O^{2-} ions on CO chemisorbed on cobalt atoms located at the periphery of the cobalt particles with the formation of $Co(CO)_4^-$ and CO_3^{2-} species according to Scheme presented in Figure 17. The CO hydrogenation activity of cobalt supported on magnesia was studied by Reuel and Bartholomew /114/ at 1 bar and 225 ... 400 °C with H_2/CO of 2. They obtained poor dispersion of the cobalt-magnesia system. The apparently low

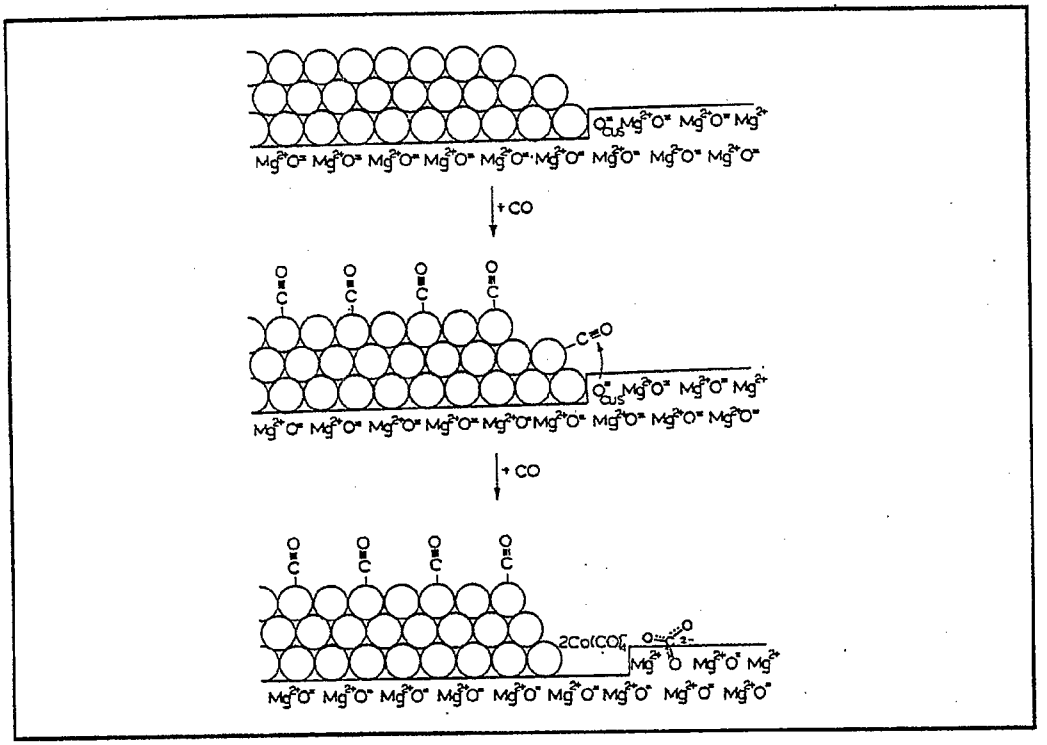

Figure 17. Schematic presentation over the interactions of CO adsorption on Co/MgO /132/.

dispersion of Co/MgO resulted presumably from (i) suppression of H_2 adsorption or (ii) formation of a stable $CoMgO_2$ surface spinel. Furthermore 3 w-% Co/MgO was found inactive up to 400 °C, and a low specific activity was obtained with 10 w-% Co/MgO. Hence, magnesia was found undesirable as a support for cobalt in CO hydrogenation, at least at low metal loadings.

Reuel and Bartholomew /114/ found that under the conditions described above the specific activity of 3 w-% loaded Co/C was higher than that of Co/MgO, but lower than that of Co/SiO_2, Co/Al_2O_3 or Co/TiO_2. The low activity of the cobalt-carbon system was compensated for by its high dispersions and large activation energies, which resulted in high rates of hydrocarbon production at elevated temperatures (250 ... 275 °C). Barrault et al /133/ investigated hydrogenation of CO on 6,6 w-% Co/C, 6,7-2,7 w-% Co-La/C and 6,5-2,5 w-% Co-Ce/C catalysts at atmospheric pressure at 250 °C using H_2:CO ratio of 1. The catalysts were prepared by

coimpregnation, and reduced *in situ* with hydrogen at 250 °C or 400 °C. They observed, that the addition of lanthanum or cerium to cobalt considerably reduced the adsorption of carbon monoxide and, even more, that of hydrogen. With increasing reduction temperature the chemisorption of CO and particularly that of H_2 increased. The promotor addition led to a significant increase of activity per gram of cobalt, and the activity increased further with increasing reduction temperature. Moreover, a significant shift in selectivity was observed: lanthanum and cerium enhanced the production of higher hydrocarbons containing mainly olefins.

Recently also precipitated Co/MnO catalysts have been studied as CO hydrogenation catalysts /134/. The characterization of these catalysts has shown, that the calcined catalysts consisted of mixed Co-Mn oxide spinels identified as $(Co,Mn)(Co,Mn)_2O_4$ and $CoMnO_3$, which were subsequently reduced to a solid solution of Co(fcc) + MnO. After extended period of synthesis (apr. 120 h), the Co(fcc) has transformed into a body centered cubic form [Co(bcc)], which was believed to be its true active phase for CO hydrogenation. Hence the catalyst required a stabilization period or bedding in period of 120 h at 200 °C and 5 bar with GHSV of 250 h^{-1} for maximum stable activity and selectivity to be attained. These Co/MnO catalysts have gained interest due to their hydrocarbon synthesis activity, and particularly due to their ability to enhance the C_2 and C_3 olefin content. Colley et al /134/ studied also the effect of potassium promotor on the CO hydrogenation reaction over precipitated cobalt-manganese oxide catalyst with atomic ratio Co:(Co+Mn) of 0,5 at 220 °C, 5,4 bar and $CO:H_2$ ratio 1:1. Alkali addition was found not to affect the bulk structure of the catalyst or the length of the stabilization period. The maximum activity was obtained at low potassium level and a small decrease in CO conversion was observed at the optimum potassium loadings of between 0,1 and 0,2 w-% potassium. The alkali metal was observed to decrease the hydrogenation ability of the catalysts as indicated by a decrease in methane selectivity and an increase in product (C_2 and C_3) olefinity. There was also an observed shift to higher-molecular weight hydrocarbons with potassium promotion. The results obtained are displayed in Table 6 for illustrative purposes.

Table 6. Activities and selectivities of CO-hydrogenation using K-promoted Co/MnO catalysts /134/.

% K promotion	0.0	0.01	0.05	0.1	0.25	0.5	1.0
Reaction time/h	170	103	170	144	170	144	144
GHSV/h^{-1}	268	236	253	254	267	251	251
CO conversion (%)	44.1	43.0	38.8	39.0	37.5	28.7	21.1
α^b	0.79	0.84	0.84	0.86	0.86	0.85	—
			Hydrocarbon selectivity (% m/m)				
CH_4	8.3	6.9	5.8	4.2	4.7	6.0	14.5
C_2H_4	2.3	2.3	2.7	1.9	2.7	3.1	8.3
C_2H_6	3.5	3.0	1.4	1.4	0.6	0.6	1.5
C_3H_6	13.6	13.8	12.2	10.1	9.9	8.6	15.3
C_3H_8	3.7	3.4	2.7	2.2	1.8	1.8	3.4
C_4	9.3	9.3	9.5	7.4	7.9	7.7	13.1
C_5^+	38.2	39.3	40.1	47.2	47.8	48.5	36.9
Total C_3 hydrocarbon	17.3	17.2	14.9	12.3	11.7	10.4	18.7
C_2–C_4 fraction	32.4	31.6	28.5	23.0	21.9	21.8	41.8
			Alcohol selectivity (% m/m)				
CH_3OH	0.6	0.5	0.6	0.6	0.3	0.2	—
C_2H_5OH	2.0	1.8	1.3	1.4	0.8	0.4	—
1-C_3H_7OH	3.9	3.7	3.6	3.5	3.8	2.0	—
1-C_4H_9OH	1.0	1.4	1.7	1.6	1.3	0.9	—
C_5OH^+	8.3	9.1	11.9	11.5	14.1	16.6	—

[a] Pressure 540 ± 40 kPa and temperature 220°C.
[b] Anderson–Schulz–Flory chain growth probability factor.

2.2.5 Cobalt on other carriers

Cobalt supported on lanthana, ceria or zirconia has been studied by Barrault et al /135/ and Bruce et al /136/. Barrault et al /135/ characterized the 8,7 w-% Co/La_2O_3 and 9,4 w-% Co/CeO_2 catalysts by XRD before and after catalytic reaction. They observed only oxidized cobalt species (Co_3O_4 and CoO) and the rare earth oxides for the catalysts calcined at 500 °C. After catalytic reaction these oxidized species were no longer visible. For Co/La_2O_3 only metallic cobalt and lanthanum sesquioxide (La_2O_3) or oxycarbonate ($La_2O_2CO_3$) were observed. For Co/CeO_2 only the CeO_2 support was evident. The CO hydrogenation of these catalysts and 7,2 w-% Co either on Al_2O_3 or SiO_2 was carried out at 350 °C and 1 bar with H_2/CO ratio of 1. The results indicated, that the activity based on turnover frequencies decreased in the order Co/SiO_2 > Co/Al_2O_3 > Co/La_2O_3 > Co/CeO_2. Co/La_2O_3 had a higher

CO_2 selectivity (36 %) and lower C_{2+}-selectivity (16 %) than Co/SiO_2 (17 % and 32 %) or Co/Al_2O_3 (17 % and 47 %). Co/CeO_2 produced mainly CO_2. Bruce et al /136/ studied the activity of cobalt-zirconia and cobalt-nickel-zirconia preparations at 1 bar and 100 °C keeping the conversion of CO to hydrocarbons below 8 %. The results indicated that impregnation of cobalt on pure zirconia gave very inactive catalysts. Impregnation of 2,7 w-% cobalt with 8,0 w-% nickel on pure zirconia resulted in a more active catalyst with 33 % selectivity to methane, 22 % C_3 and 18 % C_{5+}-hydrocarbons. Coprecipitation of 2,8 w-% cobalt with zirconia also gave very inactive catalysts, whereas 9,8 w-% cobalt resulted in a catalyst with considerably higher activity accompanied by 30 % selectivity to methane and 32 % to C_{5+}-hydrocarbons. However, impregnation of cobalt and nickel on a 3,1 w-% nickel-zirconia co-precipitated base produced 7,0-2,9 w-% $Co\text{-}Ni/ZrO_2$ and 7,8-4,7 w-% $Co\text{-}Ni/ZrO_2$ catalysts of the highest activities and selectivities in excess of 60 w-% to C_{5+}-hydrocarbons.

Physical and chemical properties as well as activity and selectivity of bifunctional catalysts, combinations of cobalt and zeolites, have been studied for conversion of synthesis gas. The use of zeolite supports offers high metal dispersion, strong metal-zeolite interaction and shape-selectivity.

Stencel /137/ used spectroscopic techniques to investigate cobalt speciation in impregnated Co/ZSM-5 catalysts containing 1,4 ... 9,5 w-% cobalt. Two major cobalt species were shown to exist in the Co/ZSM-5 catalysts. Interior to the ZSM-5 were the highly dispersed, ion-exchanged Co^{2+} species, which did not reduce to cobalt metal at 450 °C. On the external surface of the ZSM-5 crystallites were large 34,5 nm sized cobalt oxide crystallites, Co_3O_4, that reduced to cobalt metal and CoO at 350 °C. Calleja et al /138/ made XPS studies on calcined and reduced catalyst with 9 w-% Co/ZSM-5 prepared by incipient wetness impregnation. The results showed that after calcining in air at 350 °C for 12 h, the phase present was Co_3O_4 with a particle size of 450 ... 500 Å. The X-ray diffraction pattern of the reduced catalyst (350 °C, 24 h) showed the existence of cubic metal, but no evidence of an oxidic phase. The mean particle size of metallic cobalt was about 400 Å. Hence most of the cobalt particles were on the exterior surface of the zeolite.

The Co/ZSM-5 catalyst activity was evaluated by Stencel et al /137/ and Calleja et al /138/ at 280 °C and 21 bar using 1:1 ratio of H_2:CO. The data obtained by Stencel et al /137/ indicated, that 1,4 w-% cobalt in the interior of ZSM-5 produced negligible conversion, whilst the catalysts containing the 1,6 w-% cobalt physically admixed with ZSM-5 produced significant conversion - 19,9 % based on Co and 32,4 % based on H_2. The catalysts containing both interior and exterior cobalt with a loading of 7,3 w-% had reasonable conversion, 56,5 % and 85,8 % based on CO and H_2 respectively. In this case the physical admixture containing 8,5 % cobalt gave the corresponding values of 55,0 % and 66,5 %, i.e. lower conversions. Furthermore, the admixed catalyst produced considerably less olefins and C_{5+}-hydrocarbons and clearly more aromatics. Calleja et al /138/ carried out comparative experiments varying the cobalt percentage in the catalyst from 0 ... 12 w-%. They found that cobalt loadings higher than 5 w-% led to catalysts whose activity was independent of cobalt loading. This was probably related to the anomalous basal growth in cobalt oxide particles on the external zeolite surface. It was supposed that with constant contact surface, the catalytic activity would not change significantly. Calleja et al /138/ and Rao et al /139/ added 0 ... 3 w-% thoria on 9 w-% Co/ZSM-5. The analysis of calcined 1,5 w-% thorium containing catalysts by Calleja et al /138/ suggested the formation of solid solutions of thorium and cobalt oxides that improved metal dispersion. Moreover, Rao et al /139/ observed a considerable reduction in cobalt particle diameter with thoria addition. Both investigations showed that the catalytic activity was increased with a content of thorium as low as 0,4 w-%, with the maximum at 1,5 w-% loading. The most significant increase corresponded to the non-aromatic C_{6+}-fraction.

Gormley et al /140/ examined the mechanism of synthesis gas conversion over precipitated and impregnated Co/SiO_2 and Co-Cu/SiO_2 admixed with ZSM-5 catalysts in 1:1 weight ratio to gasoline range hydrocarbons. The reactions were carried out at 21 bar and 280 °C using H_2:CO ratio of 1. Some experiments were performed in two stages in one reactor tube; the first stage consisted of the metal catalyst alone. It was separated by a layer of glass wool from the second bed, which consisted of ZSM-5 alone. The addition of ZSM-5 to precipitated 14,4 w-% Co/SiO_2 in two stage operation increased the conversion of both CO and H_2 slightly, and resulted in noticeable increase in the yield of C_3- and C_4-alkanes, while methane production was

unchanged. In one stage operation the corresponding addition produced slightly decreased CO conversion and slightly increased H_2 conversion resulting in increased methane production. The selectivity to aromatics was, however, nearly the same as that in the two-stage experiment, suggesting that hydrogenolysis was occurring over cobalt as secondary reaction. The addition of ZSM-5 component to impregnated cobalt catalyst either in a two-stage reaction or in a single stage considerably increased the gasoline yield from 47,2 w-% to 67,6 or 66,1 respectively. In the case of the single stage operation the percentage of methane produced was considerably higher, presumably as a result of hydrogenolysis or thermal effects. The bifunctional Co-Cu/SiO_2 + ZSM-5 catalyst also produced more methane.

Hydrogenation of carbon monoxide over cobalt containing zeolite catalysts, NaY and NaX, has been studied by Lee and Ihm /141/ and Wang and Chen /90/. Lee and Ihm /141/ compared the CO hydrogenation activity, selectivity and kinetics of cobalt containing NaY zeolite catalysts at 230 - 310 °C, 1 bar and H_2:CO ratio of 1. The catalysts were prepared by three methods - excess-water, ion exchange and carbonyl complex impregnation techniques. A negative reaction order of methanation on CO partial pressure was observed with excess water technique catalysts and no dependence with ion exchanged and carbonyl complex impregnated catalysts. The excess water technique catalysts were most active, whilst the carbonyl complex impregnated catalysts were most selective to higher hydrocarbons and olefins. Wang and Chen /90/ investigated the synthesis of hydrocarbons from catalytic hydrogenation of carbon monoxide by Co/NaX catalysts at 1 bar, 220 ... 260 °C and H_2:CO ratio of 2. They observed a negligible amount of hydrogen adsorption attributed to the high cobalt dispersion. Moreover, cobalt seemed to be located within zeolite pores and to be of a size less than that of faujasite supercages (1,3 nm). The low reducibility of Co/NaX was readily referred to its high overall Brönsted acidity. Characteristic to highly dispersed, non-reduced catalysts, the activity of Co/NaX was low, and it produced α-alkenes and normal alkenes. Trace amounts of methanol and formaldehyde were also detected. Hence, they hypothesized that mechanism B, suggested by Lee and Bartholomew /110/ in context with Co/Al_2O_3, dominates the reaction on Co/NaX.

Rathousky et al /91/ studied hydrocarbon synthesis from carbon monoxide and hydrogen on impregnated 10 w-% cobalt/silica-alumina catalyst. Catalytic measurements were performed in a continuous flow, fixed bed reactor under atmospheric pressure at 200 ... 210 °C with $CO:H_2$ inlet ratio of ½. They observed that $Co/SiO_2 \cdot Al_2O_3$ catalysts were more similar to Co/SiO_2 than to Co/Al_2O_3. Thus, an increase of calcination temperature from 20 to 400 °C decreased both cobalt reduction and the activity of hydrocarbon synthesis. The total yield of gaseous products remained constant, whilst that of liquid products decreased 1,8-fold. The liquid hydrocarbon yields were, however, 1,3 ... 1,5 times greater than with Co/SiO_2. Furthermore, on $Co/SiO_2 \cdot Al_2O_3$ catalysts, a much greater proportion of i-alkanes was formed than over both Co/SiO_2 and Co/Al_2O_3. This was explained by a greater extent of isomerization reactions, resulting from the higher acidity of the $SiO_2 \cdot Al_2O_3$ support. These results were interpreted to confirm the hypothesis of participation of weakly bonded adsorption centres in the production of liquid hydrocarbons.

2.2.6 Supports in summary

The specific activity and selectivity of cobalt varies with support, dispersion, metal loading and preparation method. The order of decreasing CO hydrogenation activity of cobalt is Co/TiO_2, Co/SiO_2, Co/Al_2O_3, Co/C and Co/MgO. The specific activity of cobalt decreases significantly with increasing dispersion. Product selectivity is best correlated with dispersion and extent of reduction, i.e. the molecular weight of hydrocarbon products is lower and the $CO_2:H_2O$ ratio is higher for catalysts having higher dispersions and lower extents of reduction. An illustrative example of CO hydrogenation reaction on conventional carriers is shown in Table 7. The main aim of bifunctional catalysts, namely cobalt supported on or mixed with zeolites, has been to increase the liquid product, and in particular gasoline, selectivity of cobalt catalysts.

Table 7. Hydrocarbon and carbon dioxide:water product distributions for supported and unsupported cobalt catalysts /114/.

Catalyst	Temp. (°C)	Weight percentage CO_2 selectivity[a,b]	Weight percentage hydrocarbon group selectivities[a,c]					Average carbon number[d]
			C_1	C_2–C_4	C_5–C_{12}	C_{13+}	Alcohols	
100% Co	225	0	29	42	28	0	1.1	3.4
Co/SiO_2								
3%	225	41	47	34	15	0	3.9	2.5
10	225	0	29	27	42	0.2	1.3	4.0
3[e]	325	33	99	1.1	0	0	0	1.0
Co/Al_2O_3								
1%	[g]	[g]	[g]	[g]	[g]	[g]	[g]	[g]
3	225	71	41	36	18	0	4.0	3.1
10	225	18	32	31	35	0.7	1.3	3.8
15	215	0	3.8	5.5	86	4.4	0	9.5
3[e]	225	18	27	31	39	0	2.7	4.0
Co/TiO_2								
3%	225	0	31	35	31	0	3.5	3.5
10	225	0	16	30	52	1.7	1.1	5.0
3[e]	225	0	22	39	37	0	2.1	4.2
Co/MgO								
3%	[g]	[g]	[g]	[g]	[g]	[g]	[g]	[g]
10	300	36	55	39	6.2	0	0.6	1.9
Co/C (Type UU)								
3%[f]	275	84	30	54	16	0	0	2.7
10[f]	225	44	53	31	16	0	0	2.3
Co/C (Spheron)								
3%[f]	250	24	85	8.1	7.0	0	0	1.5
10[f]	225	8	66	23	11	0	0	2.1

[a] Measured at temperature shown above at $H_2/CO = 2$, and 1 atm.
[b] Weight percentage of CO_2 in oxygen-containing, nonhydrocarbon products: $CO_2(10^2)/(CO_2 + H_2O)$.
[c] Weight percentage of hydrocarbon groups based on total hydrocarbons in the product.
[d] Weight averaged carbon number.
[e] Controlled-pH precipitation.
[f] Evaporative deposition.
[g] Inactive up to 400°C.

3. REFERENCES

1. Seglin, L., Methanation of synthesis gas, Am. Chem. Soc. Adv. Chem. Ser., 146, Washington, 1975, p. 177

2. Sheldon, R.A., Chemicals from synthesis gas, catalytic reactions of CO and H_2, Reidel Publishing Company, Dordrecht, 1983, p. 216

3. Twigg, M.V. (ed.), Catalyst Handbook, 2nd ed., Wolfe Publishing Ltd., London, 1989, p. 608

4. Heinemann, H. (ed.), Catalysis Reviews, 8 (2), Marcel Dekker, New York, 1973, 159-316

5. Keiski, R., Keski-Korsu, A. and Veijola, V., Metanoinnin termodynamiikka, kinetiikka ja reaktorimitoitus, Report 96, University of Oulu, Oulu, 1984, p. 53

6. Fahey, D.R. (ed.), Industrial chemicals via C_1 processes, Am. Chem. Soc. Symp. Ser., 328, p. 249

7. Vannice, M.A., The catalytic synthesis of hydrocarbons from H_2/CO mixtures over the group VIII metals. I. The specific activities and product distributions of supported metals, J. Catal., 37, 449-461

8. Chuang, S.C., Goodwin, J.G.Jr. and Wender, I., The effect of alkali promotion on CO hydrogenation over Rh/TiO_2, J. Catal., 95, 435-446

9. Watson, P.R., and Somorjai, G.A., The hydrogenation of carbon monoxide over rhodium oxide surfaces, J. Catal., 72, 347-363

10. Van't Blik, H.F.J., van Zon, J.B.A.D., Koningsberger, D.C. and Prins, R., An extended X-ray absorption fine structure spectroscopic study of a highly dispersed Rh/Al_2O_3 catalyst: The influence of CO chemisorption on the topology of rhodium, J. Phys. Chem., 87 (13), 2264-2267

11. Solymosi, F. and Pasztor, M., An infrared study of the influence of CO chemisorption on the topology of supported rhodium, J. Phys. Chem., 89 (22), 4789-4793

12. Dai, C.H. and Worley, S.D., Effects of potassium on carbon monoxide methanation over supported rhodium films, J. Phys. Chem., 90 (18), 4219-4221

13. Cavanagh, R.R. and Yates, J.T.Jr., Site distribution of Rh supported on Al_2O_3 - An infrared study of chemisorbed CO, J. Chem. Phys., 74 (7), 4150-4154

14. Miessner, H., Gutschick, D., Ewald, H. and Müller, H., The influence of support on the geminal dicarbonyl species $Rh^{I}(CO)_2$ on supported rhodium catalysts: an IR spectroscopic study. J. Mol. Catal., 36, 359-373

15. Solymosi, F. and Erdöhelyi, A., Dissociation of CO on supported Rh, Surf. Sci., 110, L630-633

16. Erdöhelyi, A. and Solymosi, F., Effects of support on the adsorption and dissociation of CO and on the reactivity of surface carbon on Rh catalysts, J. Catal., 84, 446-460

17. Solymosi, F., Tombacz, I. and Kocsis, M., Hydrogenation of CO on supported Rh catalysts, J. Catal., 75, 78-93

18. Yin-Sheng, X. and Xiao-Le, H., EHMO calculations for CO dissociation on supported metal catalysts, J. Mol. Catal., 33, 179-188

19. Efstathiou, A.M. and Bennett, C.O., The CO/H_2 reaction on Rh/Al_2O_3 I. Steady-state and transient kinetics, J. Catal., 120, 118-136

20. Efstathiou, A.M. and Bennett, C.O., The CO/H_2 reaction on Rh/Al_2O_3 II. Kinetic study by transient isotopic methods, J. Catal., 120, 137-156

21. Mochida, I., Ikeyama, N., Ishibashi, H. and Fujitsu, H., A kinetic study on the effects of support on the catalytic performances of Rh/SiO_2, Rh/Al_2O_3, and Rh/TiO_2 in a $CO-H_2$ reaction, J. Catal., 110, 159-170

22. Duprez, D., Barrault, J. and Geron, C., Effect of partial reduction on the formation of oxygenated compounds in the hydrogenation of carbon monoxide on rhodium/alumina, Appl. Catal., 37, 105-114

23. Worley, S.D., Rice, C.A., Mattson, G.A., Curtis, C.W., Guin, J.A. and Tarrer, A.R., The effect of rhodium precursor on Rh/Al_2O_3 catalysts, J. Chem. Phys., 76 (1), 20-25

24. Vis, J.C., Van't Blik, H.F.J., Huizinga, T., van Grondelle, J. and Prins, R., The morphology of rhodium supported on TiO_2 and Al_2O_3 as studied by temperature-programmed reduction-oxidation and transmission electron microscopy, J. Catal., 95, 333-345

25. Solymosi, F., Pasztor, M. and Rakhely, G., Infrared studies of the effects of promoters on CO-induced structural changes in Rh, J. Catal., 110, 413-415

26. Blackmond, D.G., Williams, J.A., Kesraoui, S. and Blazewick, D.S., The effects of Cs promotion on Rh/Al_2O_3 catalysts, J. Catal., 101, 496-504

27. Dictor, R. and Roberts, S., Influence of ceria on alumina-supported rhodium: Observations of rhodium morphology made using FTIR spectroscopy, J. Phys. Chem., 93 (15), 5846-5850

28. DeCanio, E.C. and Storm, D.A., Carbon monoxide adsorption by K/Co/Rh/Mo/Al_2O_3 higher alcohols catalyst, J. Catal., 132, 357-387

29. Foley, H.C., Hong, A.J., Brinen, J.S., Allard, L.F. and Garratt-Reed, A.J., Bimetallic catalysts comprised of dissimilar metals for the reduction of carbon monoxide with hydrogen, Appl. Catal., 61, 351-375

30. Kip, B.J., Smeets, P.A.T., van Wolput, J.H.M.C., Zandbergen, H.W., van Grondelle, J. and Prins, R., Preparation and characterization of vanadium oxide promoted rhodium catalysts, Appl. Catal., 33, 157-180

31. Kraus, L., Zaki, M.I. and Knözinger, H., Support and additive effects on the state of rhodium catalysts, J. Mol. Catal., 55, 55-69

32. Crucq, A., Degols, L., Frennet, A. and Lienard, G., Fast, slow and strong adsorption of H_2 on Rh/Al_2O_3 catalysts: effects of chlorine, J. Mol. Catal., 59, 257-266

33. Kip, B.J., Dirne, F.W.A., van Grondelle, J. and Prins, R., The effect of chlorine in the hydrogenation of carbon monoxide to oxygenated products at elevated pressure on Rh and Ir on SiO_2 and Al_2O_3, Appl. Catal., 25, 43-50

34. Kip, B.J., Smeets, P.A.T., van Grondelle, J. and Prins, R., Hydrogenation of carbon monoxide over vanadium oxide-promoted rhodium catalysts, Appl. Catal., 33, 181-208

35. Gopal, P.G., Schneider, R.L. and Wetters, K.L., Evidence for production of surface formate upon direct reaction of CO with alumina and magnesia, J. Catal., 105, 366-372

36. Van't Blik, H.F.J., Vis, J.C., Huizinga, T. and Prins, R., The catalytic behaviour of rhodium supported on Al_2O_3 and TiO_2 in synthesis gas reactions, Appl. Catal., 19, 405-415

37. Gilhooley, K., Jackson, S.D. and Rigby, S., Steady-state effects in the medium pressure hydrogenation of carbon monoxide over rhodium catalysts, Appl. Catal., 21, 349-357

38. Mori, Y., Mori, T., Hattori, T. and Murakami, Y., Selectivities in carbon monoxide hydrogenation on rhodium catalysts as a function of surface reaction rate constants, Appl. Catal., 66, 59-72

39. Kieffer, R., Kiennemann, A., Rodriguez, M., Bernal, S. and Rodriguez-Izquierdo, J.M., Promoting effect of lanthana in the hydrogenation of carbon monoxide over supported rhodium catalysts, Appl. Catal., 42, 77-89

40. Kawai, M., Uda, M. and Ichikawa, M., The electronic state of supported Rh catalysts and the selectivity for the hydrogenation of carbon monoxide, J. Phys. Chem., 89 (9), 1654-1656

41. Kesraoui, S., Oukaci, R. and Blackmond, D., Adsorption and reaction of CO and H_2 on K-promoted Rh/SiO_2 catalysts, J. Catal., 105, 432-444

42. Underwood, R.P. and Bell, A.T., Lanthana-promoted Rh/SiO_2. I Studies of CO and H_2 adsorption and desorption, J. Catal., 109, 61-75

43. Krause, K.R., Schabes-Retchkiman, P. and Schmidt, L.D., Microstructure of Rh-Ce particles on silica: Interactions between Ce and SiO_2, J. Catal., 134, 204-219

44. Kip, B.J., Hermans, E.G.F., van Wolput, J.H.M.C., Hermans, N.M.A., van Grondelle, J. and Prins, R., Hydrogenation of carbon monoxide over rhodium/silica catalysts promoted with molybdenum oxide and thorium oxide, Appl. Catal., 35, 109-139

45. Ichikawa, M. and Fukushima, T., Infrared studies of metal additive effects on CO chemisorption modes on SiO_2 supported Rh-Mn, -Ti, and -Fe catalysts, J. Phys. Chem., 89 (9), 1564-1567

46. Sachtler, W.M.H. and Ichikawa, M., Catalytic site requirements for elementary steps in syngas conversion to oxygenates over promoted rhodium, J. Phys. Chem., 90 (20), 4752-4758

47. Orita, H., Naito, S. and Tamaru, K., Mechanism of formation of C_2-oxygenated compounds from CO + H_2 reaction over SiO_2 supported Rh catalysts, J. Catal., 90, 183-193

48. Wilson, T.P., Kasai, P.H. and Ellgren, P.C., The state of manganese promotor in rhodium-silica gel catalysts, J. Catal., 69, 193-201

49. Lisitsyn, A.S., Stevenson, S.A. and Knözinger, H., Carbon monoxide hydrogenation on supported Rh-Mn catalysts, J. Mol. Catal., 63, 201-211

50. de Jong, K.P., Glezer, J.H.E., Kuipers, H.P.C.E., Knoester, A. and Emeis, C.A., Highly dispersed Rh/SiO_2 and $Rh/Mn/SiO_2$ catalysts, J. Catal., 124, 520-529

51. van den Berg, F.G.A., Glezer, J.H.E. and Sachtler, W.M.H., The role of promoters in CO/H_2 reactions: Effects of MnO and MoO_2 in silica-supported rhodium catalysts, J. Catal., 93, 340-352

52. Trunschke, A., Ewald, H., Gutschick, D., Miessner, H., Skupin, M., Walther, B. and Böttcher, H-C., New bimetallic Rh-Mo and Rh-W clusters as precursors for selective heterogeneous CO hydrogenation, J. Mol. Catal., 56, 95-106

53. Hu, Z., Wakasugi, T., Maeda, A., Kunimori, K. and Uchijima, T., A comparison of niobia- and vanadia-promoted Rh catalysts: The behaviours of $RhMO_4$ (M = Nb, V) on SiO_2 during calcination and reduction treatments, J. Catal., 127, 276-286

54. Koerts, T., Welters, W.J.J. and van Santen, R.A., Reactivity of CO on vanadium-promoted rhodium catalysts as studied with transient techniques, J. Catal., 134, 1-12

55. Kowalski, K., van der Lee, G. and Ponec, V., Vanadium oxide as a support and promoter of rhodium in synthesis gas reactions, Appl. Catal., 19, 423-426

56. Hu, Z., Nakamura, H., Kunimori, K., Yokoyama, Y., Asano, H., Soma, M. and Uchijima, T., Structural transformation in Nb_2O_5-promoted Rh catalysts during calcination and reduction treatments, J. Catal., 119, 33-46

57. Jen, H.W., Zheng, Y., Shriver, D.F. and Sachtler, W.M.H., Characterization of Zn-promoted Rh/SiO_2 catalysts by chemisorption, infrared spectroscopy, and temperature-programmed desorption, J. Catal., 116, 361-372

58. Chuang, S.S.C., Pien, S-I. and Narayanan, R., C_2 oxygenate synthesis from CO hydrogenation on $AgRh/SiO_2$, Appl. Catal., 57, 241-251

59. Underwood, R.P. and Bell, A.T., Lanthana promoted Rh/SiO_2. II: Studies of CO hydrogenation, J. Catal., 111, 325-335

60. Fukushima, T., Arakawa, H. and Ichikawa, M., In situ high pressure FT-IR studies on the surface species formed in CO hydrogenation on SiO_2-supported Rh-Fe catalysts, J. Phys. Chem., 89 (21), 4440-4443

61. van der Lee, G. and Ponec, V., The formation of C_2-oxygenates from synthesis gas over oxide supported rhodium, J. Catal., 99, 511-512

62. Orita, H., Naito, S. and Tamaru, K., Mechanism of formation of C_2 oxygenated compounds from CO + H_2 reaction over SiO_2-supported Rh catalysts, J. Catal., 90, 183-193

63. Jackson, S.D., Brandreth, B.J., and Winstanley, D., A mechanistic study of carbon monoxide hydrogenation over rhodium catalysts using isotopic tracers, J. Catal., 106, 464-470

64. Koerts, T. and van Santen, R.A., Transient response study of CO insertion into CH_x surface intermediates on a vanadium-promoted rhodium catalyst, J. Catal., 134, 13-23

65. Underwood, R.P. and Bell, A.T., Influence of particle size on carbon monoxide hydrogenation over silica- and lanthana-supported rhodium, Appl. Catal., 34, 289-310

66. Ellgren, P.C., Bartley, W.J., Bhasin, M.M. and Wilson, T.P., Rhodium-based catalysts for the conversion of synthesis gas to two-carbon chemicals, Am. Chem. Soc. Adv. Chem. Ser., 178, 147-157

67. Bastein, A.G.T.M., van der Boogert, W.J., van der Lee, G., Luo, H., Schuller, B. and Ponec, V., Selectivity of Rh catalysts in the syngas reactions. The role of supports and promotors, Appl. Catal., 29, 243-260

68. Henrion, A., Ewald, H., Miessner, H. and Zimmermann, T., Application of chemometric tools in catalysis, carbon monoxide hydrogenation on a multipromoted Rh/SiO_2, Appl. Catal., 62, 23-34

69. Ehwald, H., Ewald, H., Gutschick, D., Hermann, M., Miessner, H., Öhlmann, G. and Schierhorn, E., A bicomponent catalyst for the selective formation of ethanol from synthesis gas, Appl. Catal., 76, 153-169

70. Fuentes, S., Vazquez, A., Peres, J.G. and Yacaman, M.J., About the structure of small metal Rh particles on TiO_2: TEM study, J. Catal., 99, 492-497

71. Meriaudeau, P., Ellestad, O.H., Dufaux, M. and Naccache, C., Metal-support interaction. Catalytic properties of TiO_2-supported platinum, iridium and rhodium, J. Catal., 75, 243-250

72. Anderson, J.B.F., Burch, R. and Cairns, J.A., The reversibility of strong metal support interactions. A comparison of Pt/TiO_2 and Rh/TiO_2, Appl. Catal., 25, 173-180

73. Taniguchi, S., Mori, T., Mori, Y., Hattori, T. and Murakami, Y., Effect of strong metal-support interaction on the rate of hydrogenation of adsorbed carbon monoxide over titania-supported noble metal catalysts as revealed by pulse surface reaction rate analysis, J. Catal., 116, 108-118

74. Anderson, J.B.F., Burch, R. and Cairns, J.A., The reversibility of the strong metal-support interaction under reaction conditions, Appl. Catal., 21, 179-185

75. Sadeghi, H.R., and Henrich, V.E., SMSI in Rh/TiO_2 model catalysts: Evidence for oxide migration, J. Catal., 87, 279-282

76. Singh, A.K., Pande, N.K. and Bell, A.T., Electron microscopy study of the interactions of rhodium with titania, J. Catal., 94, 422-435

77. Demmin, R.A., Ko, C.S. and Gorte, R.J., Support effects studied on model supported catalysts, Am. Chem. Soc. Symp. Ser., 298, 48-53

78. Resasco, D.E. and Haller, G.L., A model for metal-oxide support interaction for Rh on TiO_2, J. Catal., 82, 279-288

79. Sadeghi, H.R. and Henrich, V.E., Electronic interactions in the rhodium/TiO_2 system, J. Catal., 109, 1-11

80. Levin, M.E., Salmeron, M., Bell, A.T. and Somorjai, G.A., The enhancement of CO hydrogenation on rhodium by TiO_x overlayers, J. Catal., 106, 401-409

81. Buchanan, D.A., Hernandez, M.E., Solymosi, F. and White, J.M., CO-induced structural changes of Rh on TiO_2 support, J. Catal., 125, 456-466

82. Orita, H., Naito, S. and Tamaru, K., Infrared spectroscopic study of $CO + H_2$ reaction over TiO_2-supported Rh catalysts, J. Catal., 112, 176-182

83. Chuang, S.C., Goodwin, J.G.Jr. and Wender, I., The effect of alkali promotion on CO hydrogenation over Rh/TiO_2, J. Catal., 95, 435-446

84. Orita, H., Naito, S. and Tamaru, K., Improvement of selectivity for C_2oxygenated compounds in $CO-H_2$ reaction over TiO_2 supported Rh catalysts by doping alkali metal cations, Chem. Lett., 1983, 1161-1164

85. Inoue, T., Iizuka, T. and Tanabe, K., Hydrogenation of carbon dioxide and carbon monoxide over supported rhodium catalysts under 10 bar pressure, Appl. Catal., 46, 1-9

86. Bond, G.C. and Richards, D.G., Lanthanum oxide promoted rhodium/titania and rhodium-platinum/titania catalysts for alcohol formation from synthesis gas, Appl. Catal., 28, 303-319

87. Efstathiou, A.M., The CO/H_2 reaction on Rh/MgO studied by transient isotopic methods, J. Mol. Catal., 67, 229-249

88. Efstathiou, A.M., Temperature-programmed desorption (TPD), reaction (TPR) and oxidation (TPO) of species formed on Rh/MgO after interaction with H_2 and CO, J. Mol. Catal., 69, 41-60

89. Underwood, R.P. and Bell, A.T., CO hydrogenation over rhodium supported on SiO_2, La_2O_3, Nd_2O_3 and Sm_2O_3, Appl. Catal., 21, 157-168

90. Wang, W-J. and Chen, Y-W., Carbon monoxide hydrogenation on cobalt/alumina and cobalt/NaX catalysts, Appl. Catal., 77, 21-36

91. Rathousky, J., Zukal, A., Lapidus, A. and Krylova, A., Hydrocarbon synthesis from carbon monoxide+hydrogen on impregnated cobalt catalysts. Part III. Cobalt (10%)/silica-alumina catalysts, Appl. Catal., 79, 167-180

92. Greegor, R.B., Lytle, F.W., Chin, R.L. and Hercules, D.M., Investigation of supported cobalt and nickel catalysts by X-ray absorption spectroscopy, J. Phys. Chem., 85 (9), 1232-1235

93. Chin, R.L., and Hercules, D.M., Surface spectroscopic characterization of cobalt-alumina catalysts, J. Phys. Chem., 86 (3), 360-367

94. Stranick, M.A., Houalla, M. and Hercules, D.M., Determination of the distribution of species in supported metal catalysts by X-ray photoelectron spectroscopy, J. Catal., 103, 151-159

95. Okamoto, Y., Adachi, T., Nagata, K., Odawara, M. and Imanaka, T., Effects of starting cobalt salt upon the cobalt-alumina interactions and hydrodesulfurization activity of CoO/Al_2O_3, Appl. Catal., 73, 249-265

96. Ledford, J.S., Houalla, M., Proctor, A., Hercules, D.M. and Petrakis, L., Influence of lanthanum on the surface structure and CO hydrogenation activity of supported cobalt catalysts, J. Phys. Chem., 93 (18), 6770-6777

97. Castner, D.G. and Santilli, D.S., X-ray photoelectron spectroscopy of cobalt catalysts, Am. Chem. Soc. Symp. Ser., 248, 39-56

98. Stranick, M.A., Houalla, M. and Hercules, D.M., The influence of TiO_2 on the speciation and hydrogenation activity of Co/Al_2O_3, J. Catal., 125, 214-226

99. Chin, R.L. and Hercules, D.M., The influence of zinc on the surface properties of cobalt-alumina catalysts, J. Catal., 74, 121-128

100. Wang, W-J. and Chen, Y-W., Influence of metal loading on the reducibility and hydrogenation activity of cobalt/alumina catalysts, Appl. Catal., 77, 223-233

101. Lapidus, A., Krylova, A., Kazanskii, V., Borovkov, V., Zaitsev, A., Rathousky, J., Zukal, A. and Jancalkova, M., Hydrocarbon synthesis from carbon monoxide and hydrogen on impregnated cobalt catalysts. Part I. Physico-chemical properties of 10 % cobalt/alumina and 10 % cobalt/silica, Appl. Catal., 73, 65-82

102. Brown, R., Cooper, M.E. and Whan, D.A., Temperature programmed reduction of alumina-supported iron, cobalt and nickel bimetallic catalysts, Appl. Catal., 3, 177-186

103. Castner, D.G., Watson, P.R. and Chan, I.Y., X-ray absorption spectroscopy, X-ray photoelectron spectroscopy, and analytical electron microscopy studies of cobalt catalysts. 2. Hydrogen reduction properties., J. Phys. Chem., 94 (2), 819-828

104. Zowtiak, J.M., Weatherbee, G.D. and Bartholomew, C.H., Activated adsorption of H_2 on cobalt and effects of support thereon, J. Catal., 82, 230-235

105. Zowtiak, J.M. and Bartholomew, C.H., The kinetics of H_2 adsorption on and desorption from cobalt and the effects of support thereon, J. Catal., 83, 107-120

106. Reuel, R.C. and Bartholomew, C.H., The stoichiometries of H_2 and CO adsorptions on cobalt: Effects of support and preparation, J. Catal., 85, 63-77

107. Fu, L. and Bartholomew, C.H., Structure sensitivity and its effects on product distribution in CO hydrogenation on cobalt/alumina, J. Catal., 92, 376-387

108. Lee, J-H., Lee, D-K. and Ihm, S-K., Independent effect of particle size and reduction extent on CO hydrogenation over alumina-supported cobalt catalyst, J. Catal., 113, 544-548

109. Nakamura, J., Tanaka, K-I. and Toyoshima, I., Reactivity of deposited carbon on $Co\text{-}Al_2O_3$ catalyst, J. Catal., 108, 55-62

110. Lee, W.H., and Bartholomew, C.H., Multiple reaction states in CO hydrogenation on alumina-supported cobalt catalysts, J. Catal., 120, 256-271

111. Anderson, A.B. and Jen, S-F., Methoxy mobility and methane formation on the alumina support, J. Phys. Chem., 95 (20), 7792-7795

112. Agrawal, P.K., Katzer, J.R. and Manogue, W.H., Methanation over transition metal catalysts. 4. Co/Al_2O_3. Rate behaviour and kinetic modeling, Ind. Eng. Chem. Fundam., 21, 385-390

113. Lapidus, A., Krylova, A., Rathousky, J., Zukal, A. and Jancalkova, M., Hydrocarbon synthesis from carbon monoxide and hydrogen on impregnated cobalt catalysts, Appl. Catal., 80, 1-11

114. Reuel, R.C. and Bartholomew, C.H., Effects of support and dispersion on the CO hydrogenation activity/selectivity properties of cobalt, J. Catal., 85, 78-88

115. Dent, A.L. and Lin, M., Cobalt-based catalysts for the production of C_2-C_4 hydrocarbons from syngas, Am. Chem. Soc. Adv. Chem. Ser., 178, 47-63

116. Baker, J.E., Burch, R. and Yugin, N., Investigation of $CoAl_2O_4$, $Cu/CoAl_2O_4$ and $Co/CoAl_2O_4$ catalysts for the formation of oxygenates from a carbon monoxide - carbon dioxide - hydrogen mixture, Appl. Catal., 75, 135-152

117. Agrawal, P.K., Katzer, J.R. and Manogue, W.H., Methanation over transition metal catalysts. II. Carbon deactivation of Co/Al_2O_3 in sulfur free studies, J. Catal., 69, 312-326

118. Agrawal, P.K., Katzer, J.R. and Manogue, W.H., Methanation over transition metal catalysts. III. Co/Al_2O_3 in sulfur-poisoning studies, J. Catal., 69, 327-344

119. Castner, D.G., Watson, P.R. and Chan, I.Y., X-ray absorption spectroscopy, X-ray photoelectron spectroscopy, and analytical electron microscopy studies of cobalt catalysts. 1. Characterization of calcined catalysts, J. Phys. Chem., 93 (8), 3188-3194

120. Ho, S-W., Houalla, M. and Hercules, D.M., Effect of particle size on CO hydrogenation activity of silica supported cobalt catalysts, J. Phys. Chem., 94 (16), 6396-6399

121. Sexton, B.A., Hughes, A.E. and Turney, T.W., An XPS and TPR study of the reduction of promoted cobalt-kieselguhr Fischer-Tropsch catalysts, J. Catal., 97, 390-406

122. Viswanathan, B. and Gopolakrishnan, R., Effect of support and promoter in Fischer-Tropsch cobalt catalysts, J. Catal., 99, 342-348

123. Rosynek, M.P. and Polansky, C.A., Effect of cobalt source on the reduction properties of silica-supported cobalt catalysts, Appl. Catal., 73, 97-112

124. Takeuchi, K., Matsuzaki, T., Hanaoka, T., Arakawa, H., Sugi, Y. and Wei, K., Alcohol synthesis from syngas over cobalt catalysts prepared from $Co_2(CO)_8$, J. Mol. Catal., 55, 361-370

125. Takeuchi, K., Matsuzaki, T., Arakawa, H., Hanaoka, T. and Sugi, Y., Synthesis of C_2-oxygenates from syngas over cobalt catalysts promoted by ruthenium and alkaline earths, Appl. Catal., 48, 149-157

126. Matsuzaki, T., Hanaoka, T., Takeuchi, K., Sugi, Y. and Reinikainen, M., Effects of modification of highly dispersed cobalt catalysts with alkali cations on the hydrogenation of carbon monoxide, Cat. Lett., 10, 193-200

127. Fujimoto, K. and Oba, T., Synthesis of C_1 - C_7 alcohols from synthesis gas with supported cobalt catalysts, Appl. Catal., 13, 289-293

128. Madon, R.J. and Taylor, W.F., Effect of sulphur on the Fischer-Tropsch synthesis, Am. Chem. Soc. Adv. Chem. Ser., 178, 93-111

129. Ekstrom, A. and Lapszewicz, J., The direct conversion of synthesis gas of low H_2/CO ratio to liquid hydrocarbons, Appl. Catal., 21, 111-117

130. Takeuchi, K., Matsuzaki, T., Arakawa, H. and Sugi, Y., Synthesis of ethanol from syngas over Co-Re-Sr/SiO_2, Appl. Catal., 18, 325-334

131. Vannice, M.A., Titania-supported metals as CO hydrogenation catalysts, J. Catal., 74, 199-202

132. Rao, K.M., Spoto, G. and Zecchina, A., IR investigation of CO adsorbed on Co particles obtained via $Co_2(CO)_8$ adsorbed on MgO and SiO_2, J. Catal., 113, 466-474

133. Barrault, J., Guilleminot, A., Achard, J.C., Paul-Boncour, V. and Percheron-Guegan, A., Hydrogenation of carbon monoxide on carbon-supported cobalt rare earth catalysts, Appl. Catal., 21, 307-312

134. Colley, S.E., Betts, M.J., Copperthwaite, R.G., Hutchings, G.J. and Coville, N.J., Carbon monoxide hydrogenation using cobalt-manganese oxide catalysts: the influence of potassium as a promotor, J. Catal., 134, 186-203

135. Barrault, J., Guilleminot, A., Achard, J.C., Paul-Boncour, V., Percheron-Guegan, A., Hilaire, L. and Coulon, M., Syngas reaction over lanthanum-cobalt intermetallic catalysts, Appl. Catal., 22, 273-287

136. Bruce, L.A., Hope, G.J. and Mathews, J.F., The activity of cobalt zirconia and cobalt-nickel-zirconia preparations in the Fischer-Tropsch reaction, Appl. Catal., 8, 349-358

137. Stencel, J.M., Rao, V.U.S., Rhee, K.H., Dhere, A.G. and DeAngelis, R.J., Dual cobalt speciation in Co/ZSM-5 catalysts, J. Catal., 84, 109-118

138. Calleja, G., De Lucas, A. and van Grieken, R., Cobalt/HZSM-5 zeolite catalyst for the conversion of syngas to hydrocarbons, Appl. Catal., 68, 11-29

139. Rao, V.U.S., Gormley, R.J., Shamsi, A., Petrick, T.R., Stencel, J.M., Schlehl, R.R., Chi, R.D.H. and Obermayer, R.T., Promotion and characterization of zeolitic catalysts used in the synthesis of hydrocarbons from syngas, J. Mol. Catal., 29, 271-283

140. Gormley, R.J., Rao, V.U.S., Anderson, R.R., Schlehl, R.R. and Chi, R.D.H., Secondary reactions on metal-zeolite catalysts used in synthesis gas conversion, J. Catal., 113, 193-205

141. Lee, D-K. and Ihm, S-K., Hydrogenation of carbon monoxide over cobalt containing zeolite catalysts, Appl. Catal., 32, 85-102

U.S. DEPARTMENT OF COMMERCE
Technology Administration
National Technical Information Service
Springfield, VA 22161 (703) 605-6000